NOVEL GUAR CROSSLINKERS FOR IMPROVED OPHTHALMIC SOLUTIONS

NOVEL GUAR CROSSLINKERS FOR IMPROVED OPHTHALMIC SOLUTIONS

By ROOZBEH MAFI, B.SC., M.SC.

A Thesis

Submitted to the School of Graduate Studies

in Partial Fulfillment of the Requirements

for the Degree

Doctor of Philosophy

McMaster University

DOCTOR OF PHILOSOPHY (2015) McMaster University

(Chemical Engineering) Hamilton, Ontario

TITLE: Novel Guar Crosslinkers for Improved Ophthalmic Solutions

AUTHOR: Roozbeh Mafi, B.Eng. (Amirkabir University of Technology), M.Sc. (Amirkabir University of Technology)

SUPERVISOR: Professor R. H. Pelton

NUMBER OF PAGES: xv, 120

ABSTRACT

In-situ chain extension of polymers used in the formulation of artificial tears and mild gelation are techniques to increase the residence time of eye drops on cornea. *In-situ* chain extension also helps to control the stability of ophthalmic emulsions both in the bottle and in the tear film. In this work, the interaction of hydrophobically modified guar and tear proteins as a method of polymer chain extension and mild gelation has been evaluated. Guar and its derivatives have been found to be very effective for ophthalmic applications. The ideal guar gelation agent is the one that turns on the gelation upon introduction onto the eye and that gelation chemistry is biocompatible and biodegradable. Controllable gelation is desirable to have relatively low viscosity eye drops for easy application and the drops form weak gels in the eye.

One recent strategy to cure dry eye disease is to include emulsions in lubricant eye drops. The idea is to supplement the natural lipid layer on the exterior surface of the tear film. Formulating artificial tear emulsions is relatively complicated and must satisfy conflicting criteria. Emulsion droplets should be stable over the period of their shelf life without creaming or aggregate formation. On the other hand, in the tear film the emulsion droplets must cream fast enough and deposit onto the water/lipid film interface on the exterior surface of the tear film. Thus, the emulsion must be stable but not too stable. Initially, science-based design rules were proposed for the development of future generations of lubricant eye drops. The effect of guar molecular weight and concentration on emulsion stability was evaluated. According to the concentration-molecular weight plot, polymer solutions can be divided into stable and unstable regions. They are defined based on the

critical flocculation concentration (CFC) and critical viscosity concentration (C*). Inverted QCM-D has been proposed as a simple and fast method to define the stability of oil in water emulsion systems. This technique is a promising alternative for time consuming conventional creaming experiments.

Low molecular weight guar can be optimized to out-perform high molecular weight guars without the complications of formulating eye drops with high molecular weight polymers. Hydroxypropyl guar samples were oxidized and modified with linear alkyl amines to give a series of hydrophobically modified guars (MGuars). Lysozyme and human serum albumin (HSA), natural tear proteins, are able to extend the effective chain length of MGuar through polymer/protein complex formation. Hydrophobic modifications on guar enable efficient interaction with proteins, through their mutual hydrophobic characteristics. The interaction of proteins with various alkyl chain lengths, degrees of substitution and a range of molecular weights were examined. Binding and rheological measurements were employed to evaluate the interactions efficiency. Our results suggest that higher degrees of substitution and longer alkyl chain length give higher viscosity values. Lowering molecular weight allows for higher concentration, while keeping the initial viscosity constant. Higher viscosity was achieved as the chain extension occurred. The influence of hydrophobic modification and molecular weight variation on lubrication behavior of MGuars has also been determined. Hydrophobic modification enhanced the lubrication between hydrophobic surfaces. However, saturation of hydrophobes with protein abolished the lubricity.

ACKNOWLEDGMENTS

I wish to express my sincere appreciation to those who have contributed to this thesis and supported me during all steps of my project.

First of all, this thesis reflects unwavering help and guidance from Professor Dr. Robert Pelton. He encouraged me during every single steps of my research, patiently supervised me during the thesis, taught me skills of writing papers and went through several drafts of my thesis.

I also would like to thank my supervisory committee members; Professor Michael Brook and Professor Todd Hoare for their brilliant suggestions on my research work that helped me make the necessary improvements according to their comments.

I wish to thank Alcon Laboratories, specifically Dr. Howard Ketelson and Dr. James Davis of Alcon Laboratories for their support and Natural Sciences and Engineering Research Council of Canada (NSERC) and Alcon Laboratories for their financial support of my research work.

I would like to thank all interfacial engineering group at chemical engineering department of McMaster university especially laboratory manager, Mr. Doug Keller for all kind of support and assistance, Ms. Sally Watson for all helps in administration and Alcon project group members, Dr. Yuguo Cui, Allen Yu and Minrui Chen for their useful discussions and suggestions.

In particular, I would like to thank my summer students: Amin Tiss, Hu Han and especially Cameron Gray and Wing Yan Lam. They all did great job throughout the project. I am also thankful to all my friends at McMaster University for their helps and

supports. In particular I would like to thank Dr. Zuohe Wang, Justin Hu, Vida Rahmani, Erlita Mastan, Sahar Mokhtari, Hajir Mokhtari, Rabia Mateen, Xiaofei Dong, Teruaki Sato, Monique Tardif and Behnam Naderi Zand.

Many thanks are to be given to Professor Shiping Zhu for helping me to understand the value of modeling and Dr. Monsur Ali for useful discussion and helps within the early stages of my project. I would also like to acknowledge Dr. Nicholas A. Burke for his help in GPC measurements, Professor Richard Epand and Professor Raquel Epand for the access to ITC instrument, Professor Shiping Zhu for access to rheometer instrument, Professor Boxin Zhao and Wei Zhang for their help and support in tribology experiments, Dr. Steve Kornic and Dr. Bob Berno for their help in NMR, FT-IR measurements.

I am grateful to the entire Department of Chemical Engineering staffs, Ms Kathy Goodram, Ms Lynn Falkiner, Ms Cathie Roberts, Ms. Kristina Trollip, Mrs. Nanci Cole, Ms. Melissa Vasi for their administrative assistance, and Mr. Paul Gatt, Mrs Justyna Derkach and Mr. Dan Wright for their technical assistance.

Finally, I owe special gratitude to my parents, Mahvash Movasssagh and Abbas Mafi and my brother Behrang Mafi who all guided and supported me my entire life. Most importantly, I must thank my wife Azadeh for her enduring patience, understanding and love.

TABLE OF CONTENTS

LIST OF FIGURES AND TABLES

LIST OF Figures

Chapter 1

Chapter 3

Chapter 6

LIST OF TABLES

Chapter 3

Chapter 5

LIST OF SI Figures

Chapter 2

Chapter 5

LIST OF ABBREVIATIONS

BCA	Bicinchoninic Acid
BSA	Bovine Serum Albumin
CFC	Critical Flocculation Concentration
CVC	Critical Viscosity Concentration
D	Dissipation
DLS	Dynamic Light Scattering
DS	Degree of Substitution
EDC	N-(3-dimethylaminopropyl)-N'-ethylcarbodiimide hydrochloride
F	Frequency
FTIR	Fourier Transform Infrared Spectroscopy
GPC	Gel Permeation Chromatography
HEPES	4-(2-hydroxyethyl)-1-piperazineethanesulfonic acid
HMP	Hydrophobically Modified Polymer
HPG	Hydroxypropyl Guar
HSA	Human Serum Albumin
MGuar	Modified Guar
MW	Molecular Weight
MWD	Molecular Weight Distribution
NMR	Nuclear Magnetic Resonance
PDMS	Polydimethylsiloxane
PS	Polystyrene
QCM-D	Quartz Crystal Microbalance with Dissipation
SEM	Scanning Electron Microscope
TEMPO	2,2,6,6-tetramethyl-1-piperidinyloxy

DECLARATION OF ACADEMIC ACHIEVEMENT

The majority of the work described in this thesis was conceived, conducted, interpreted, and written by the author of this thesis, with the following exceptions:

- In Chapter 2, Guar hydrolysis and GPC measurements were conducted with the help of my summer student, Cameron Gray. Dr. Pelton revised the versions I wrote, helped to analyze data and re-wrote the final version.

- In Chapter 3, my summer student, Wing Yan Lam helped with making emulsions for the inverted QCM-D experiments.

- In Chapter 4, Modification of Guar has been done based on the method has been previously developed in our lab by Dr. Yuguo Cui. Protein binding experiments were conducted with the help of my summer student, Wing Yan (Joyce) Lam. Dr. Pelton revised the versions I wrote, helped to analyze data and organized the final version.

- In Chapter 5, friction tests were done with the help of Wei Zhang. He helped to make the tip and substrate of friction pairs.

Chapter 1 Introduction and Literature Review

1.1 Introduction

Dry eye syndrome (DES) is an increasing problem in today's society. Between 15 and 30% of people suffer from DES, and the numbers increase to 52% for contact lens wearers (*1*). Other than aging, the main cause for DES is due to the consequences of recent technology advances, such as prolonged usage of computers, wearing contact lenses, and as a side effect of ocular surgeries. The increasing number of patients suffering from DES led to the development of various treatments. One of the most popular options in treating DES is by using artificial tears. Artificial tears relieve discomfort, lower visual disturbances, and reduce the instability of tear film, which are some of the common symptoms of DES. This allows prevention of damage on the ocular surface. However, there are obvious limitations for reproducing tear film functions and maintaining its integrity due to the complexity of natural tear structure. Attempts have been made to rebuild the tear film structure through the use of emulsions containing *in-situ* hydrogel forming polymers.

A promising polymer that has been recently used in the formulation of artificial tears is Hydroxypropyl guar (HPG), a linear polysaccharide. Guar is able to increase viscosity even at very low concentration. Therefore, high concentration of guar is not necessary, nor it is desirable, as it lowers the stability of emulsion eye drops during their shelf life. Moreover, uniform spreading of a drop with high viscosity is not achievable on the cornea surface. This problem could be remedied through *in-situ* gelation *(2)*, which allows optimum spreading and residence time on the outer surface of the eye. However, hydrogel formation of guar derivatives and production of weak gels in the eye are challenging mainly due to physiological limitations of the environment. Modifications on guar backbone, such as conjugating hydrophobic groups, enable modified guar to interact with specific natural tear proteins with hydrophobic patches. These proteins act as connectors to form polymer/protein complexes.

1.2 Natural Tear

Eye, the most important sensory organ, has a transparent front part, cornea. Cornea is the most refractive medium in the eye and has a hydrophobic characteristic (Figure 1).

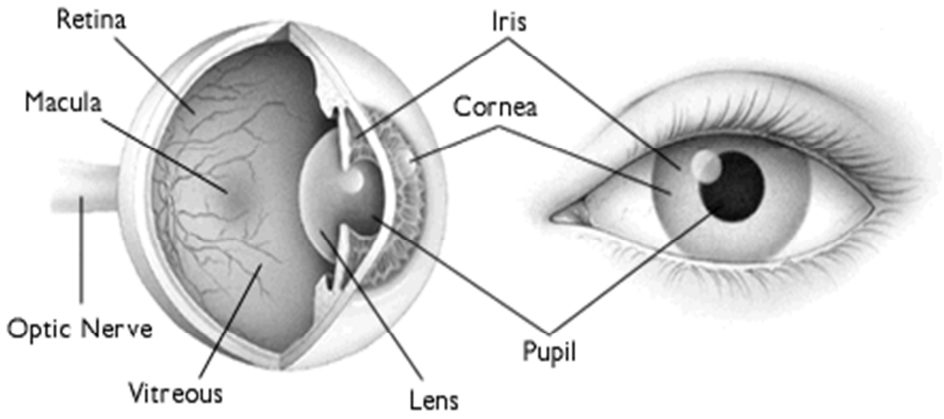

Figure 1: Basic eye anatomy. Adapted from www.eyesightresearch.org.

Cornea is covered with a thin fluid film, which is called tear film (Figure 2). Tear film maintains a smooth surface for light refraction, reduces friction by acting as lubricant between the eyelids and between the conjunctiva and the cornea. Tear film supplies the cornea with nutrients and helps metabolism of the corneal surface. It also aids in removing irritating foreign materials from the cornea and conjunctiva. Moreover, tear film prevents the ocular surface from bacteria attacks(*3*).

1.2.1 Tear Film Components

Tear film is comprised of three layers, as shown in Figure 3. The outer-most surface layer is lipid layer, which is in direct exposure with the external environment. The average reported thickness of lipid layer is less than 100 nm, making it the thinnest layer in comparison with the other two layers. It stabilizes the tear film through reduction of the evaporation rate of aqueous layer beneath it(*4*). Lipid layer also plays a key role in prevention of bacteria attack on the cornea and attachment of foreign particles to the ocular surface.

The second layer, aqueous layer, helps decreasing friction coefficient through both boundary and hydrodynamic lubrications. This middle layer of tear washes away the external particles. Soluble mucin is controlling the viscosity of tear film(*3*). Aqueous layer contains proteins with a total concentration of 6-20 g/L, including: lysozyme, albumin, lactoferrin, caeruloplasmin, transferrin and various types of immunoglobulins such as immunoglobulin A (IgA), immunoglobulin G (IgG) and immunoglobulin E (IgE)(*5*). Lipocalins, a family of lipid binding proteins, found in the tears mainly as tear lipocalin (lcn-1) (*6*) and in smaller amounts as Apo lipoprotein-D. Both are inducible lacrimal proteins. This layer also contains detectable levels of amino acids, bicarbonate, calcium, urea and magnesium.

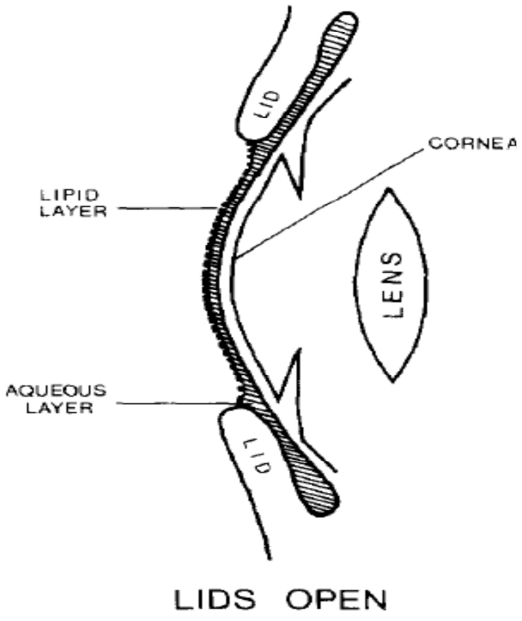

Figure 2: Structure of cornea surface covered by tear film. Adapted from reference (*7*)

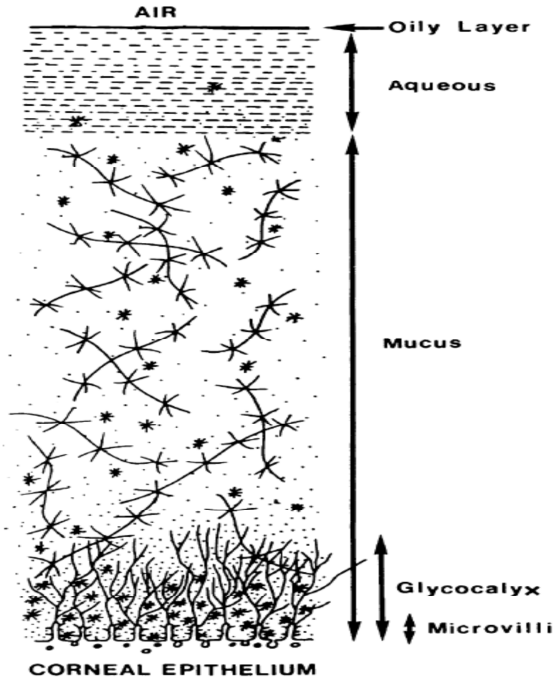

Figure 3: Schematic representation of the tear film. Adapted from reference (*8*)

The ocular mucus layer with a hydrophobic character helps the aqueous layer to spread more easily and evenly over the hydrophobic corneal epithelium surface. Mucus layer is attached to the glycocalyx but not adhered tightly to the epithelial layer, allowing it to move freely across the cornea both vertically and horizontally. This allows a better coverage of cells and it prevents damage caused by blinking to the epithelium cornea by damping the tension (*9*). Mucins are glycoproteins consisting of sugar and protein with molecular weight of around 1MDa. Mucins are categorized as membrane bound or secretory types. Tear film and ocular epithelium contain both types of mucins. Secretory mucins are categorized further as gel-forming or soluble. Membrane bound mucins with the thickness of 200-500 nm mainly act as a protection layer against bacterial attack. A generally accepted model of the tear film was proposed by Holly. The theory postulates goblet cell mucin to be present as a gel at the bottom of the film, while soluble mucin exists in the overlying aqueous layer (*10*).

1.3 Dry Eye

Constant production of healthy tear and tear film stability are essential for the integrity of corneal epithelium (*11*). Dry eye syndrome or dysfunctional tear syndrome, is a

multifactorial chronic disease of the tear film and involves inflammation of the ocular surface. It is caused by tear film instability, which is caused by a deficiency in tear production or evaporative dry eyes during the open-eye state (*12*). Diminished moistening of the ocular surface with tear fluid, leads to ocular surface damage and increases the risk of sight-threatening corneal infection (*13*). Symptoms worsen in windy or air-conditioned environments, as day progresses, after prolonged reading and working on computers(*14*). This syndrome is also age related, with higher frequency of occurrence in population over 65 years old (*15, 16*). Wearing low quality or insufficiently cleaned contact lenses is also a major cause of ocular surface inflammation(*17*). Irritation, redness, burning, stinging, itchy eyes, sandy-gritty feeling, blurred vision, tearing, increased frequency of blinking, pain, and in severe cases visual disability or blindness are common symptoms of DES(*18*). Common treatment options are tear substitutes through using artificial tear solutions, moisture-chamber glasses/goggles and punctal plugs. However, due to the multifactorial nature of dry eye, deep understanding of dry eye disease classification and management is necessary to find an effective treatment.

1.3.1 Consequences of Dry Eye Syndrome

Patients with DES experience variation in their tear flow rate. As a consequence, protein secretion varies(*19*). The resulting change in protein concentration depends on the type of DES. In most cases, the concentration of secretory proteins, such as lysozyme, lactoferrin, sIgA, and lipocalin, declines(*20*). However, during the chronical inflammation and due to the leakage of inflamed surface capillaries, the concentration of serum derived proteins, such as HSA(Human serum albumin) (*21*), IgG, and ceruloplasmin, increases(*20*).

The failure of tear to produce a uniform film results in dry spots. Due to the lack of lubricating tear, eyelids encounter excessive friction during blinking process. On average, blinking occurs approximately fifteen times per minute under normal conditions(*22*). The excessive friction during blinking may even lead to punctate wear of the corneal epithelium(*23*). Such a painful condition can result in severe erosion due to invasions by pathogens. There are different sources for dry eye syndrome and various definitions have been proposed(*24*). It may be caused by lid abnormalities or deficiencies by a combination of any of the tear film layers i.e. aqueous, lipid and/or mucin. Inability of tear to produce a weak gel makes the tear film unstable and leads to DES. Depending on deficiency of lipid or aqueous layer, the DES symptoms experienced could be more intense in the morning or evening. Commonly associated clinical signs include, low tear meniscus height, conjunctival hyperaemia, corneal staining and reduced time of tear break-up(*25*).

Currently, replacing tear by an artificial tear solution is the most important and widely used therapy for dry eye syndrome. The main results of using ophthalmic solutions are lubrication improvement, increase in humidity of ocular surface and smoothing the corneal surface, which improves vision. Although using artificial tear solutions is helpful,

they fail to exactly mimic the complex composition of natural tear and its three-layered structure.

1.4 Artificial Tears

Artificial tear solutions usually contain 97-99% water. In order to maintain osmotic pressure and to improve the biological function of these solutions in corneal epithelium metabolism, saline solutions are employed. The saline solutions may contain glycerol, monosaccharides and disaccharides, gelatines which can act as surfactant, lipids with the ability to provide additional evaporation retention and biological fluids.

Here, we only focus on three functions of eye drops: extending the residence time, lubrication and rebuilding the lipid layer on top of the natural tear.

1.4.1 Extending the Residence Time

A fundamental problem in applying liquid eye drop is the rapid and extensive precorneal loss after application. The residence time of a topically applied ophthalmic solution refers to the duration of its contact with the ocular surface. Extended ocular residence time would be desirable to prolong the enhancement of tear film stability. A concept that is of particular interest in formulating artificial tear solutions with increased residence time is by using polymers and hydrogels (*26*).

1.4.1.1 Polymers in Artificial Tears

Recently, a number of different polymers have been employed for artificial tear formulations to extend its residence time. This is achieved by increasing viscosity through hydrogel formation or via synergistic interaction between incorporated polymers(*27*). Using single polymers or even combinations of them without synergistic effect does not show enough usefulness for artificial tear formulations. On the other hand, incorporating polymers with hydrogel formation ability has been shown to be more promising with wider application. Hydrogels are three dimensional polymeric networks capable of adsorbing and retaining large amounts of water. Crosslinks in the polymer network prevent dissolution of polymer chains containing hydrophilic groups or domains(*28*). Moreover, there is also a rheological advantage for employing hydrogels in artificial tears. Low concentration hydrophilic polymers show Newtonian behaviour in the absence of chain entanglement and crosslinks. Crosslinking between polymer chains produces a network with a shear thinning behaviour, which is a desirable property for ophthalmic solutions.

Two important groups of polymers have been used in ophthalmic solutions formulations. First group is polysaccharides, such as cellulose, guar gums, dextran, and

hyaluronate. Second group is synthetic polymers, which could be further categorized into two major groups: vinyl derivatives such as polyvinyl alcohol and ethylene glycol derivatives.

Among polysaccharides employed in the formulation of artificial tear solutions, guar and its derivatives, such as hydroxyl propyl guar, have been found to be very effective for ophthalmic applications *(29)*. The structures of these chemicals are shown in Figure 4. Guar is a water-soluble polysaccharide, which consists of a linear backbone of α-1, 4 linked mannose units with β-1, 6-galactose pendent groups. The high molecular weight of guar gum, gives it a high viscosity in solution even at very low concentrations. Guar, with a non-uniform molecular structure along the chain, is soluble in cold water and hydrates quickly to produce viscous, shear-thinning solutions.

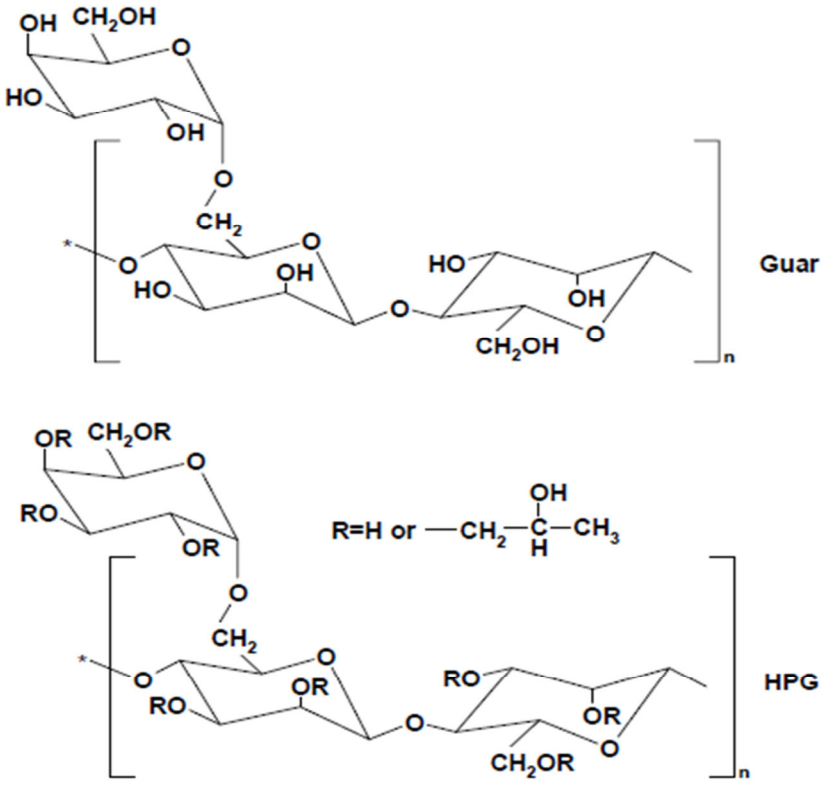

Figure 4: Schematic structure of Guar and Hydroxypropyl Guar(*29*)

1.4.2 Lubricating Behavior of Tear

Reducing the friction between eye lid and surface of cornea is one of the major functions of artificial tear solutions. Friction can be ascribed to the interactions between bodies' material zones that are in contact or moving relative to one another; it counteracts relative motion. Lubrication is a method that partially or completely separates friction bodies by introducing an interfacial medium called lubricant, which is usually a fluid, to

minimize friction and wear. There are different ways to achieve complete separation of the frictional surfaces by liquid lubricating film including hydrodynamic, boundary, or mixed lubrication(*30*).

To produce hydrodynamic lubrication, a viscous lubricant must move between the two body surfaces of a friction couple(*31*). In this method of lubrication, the friction body surfaces are converging and the converging gap is filled with the lubricant. The entraining velocity, which is different from relative velocity, is crucial for friction(*32*). This entraining velocity depends on the velocity at which the lubricant is dragged into the contact area. In boundary lubrication, the friction bodies are not separated by a lubricant and there are extensive asperity contacts. Lubricant's viscosity effect is negligible. The physical and chemical properties of thin surface film control the lubricating mechanisms in the contact(*33*). The boundary layers are formed by physical adsorption, chemisorption, and/or tribochemical reaction(*34*). When the fluid film breaks down, there may be direct contact between the sliding surfaces. In such conditions both the friction and wear may increase(*35*).

Two lubrication methods may be applicable for normal ophthalmologic conditions: "Mixed film lubrication" combines characteristics of both hydrodynamic and boundary lubrication; and "Squeeze film lubrication" that results from fluid expressing. Ehlers(*36*) suggested boundary lubrication for tear. Later, Holly and Holly(*37*) proposed hydrodynamic lubrication. They proposed that when the thickness of the lubricant is higher than the surface roughness, lubrication would be hydrodynamic.

1.4.3 Rebuilding the Lipid Layer

Tear film lipid layer contains meibomian oil, which provides tear film stability and helps preventing evaporation (*8*). Lipid layer consists of polar and non-polar phases as shown in Figure 5. The relatively thick nonpolar phase is believed to play the main role to retard evaporation of the tear film(*38*). Although the thickness of non-polar layer determines the prevention of water evaporation, the underlying polar layer defines its functional integrity. The polar layer act as a surfactant to produce a uniform interface with aqueous layer(*39*). In patients exhibiting symptoms of DES, the thickness of tear film lipid layer is thinner than the lipid layer of healthy patients (*40*). Rebuilding the lipid layer has been recently considered in formulation of artificial tear solutions. Scaffidi et al. compared two commercial eye drops and their effects on lipid layer formation. Although both eye drops contained emulsions, their ability on increasing the thickness of lipid layer was different(*41*).

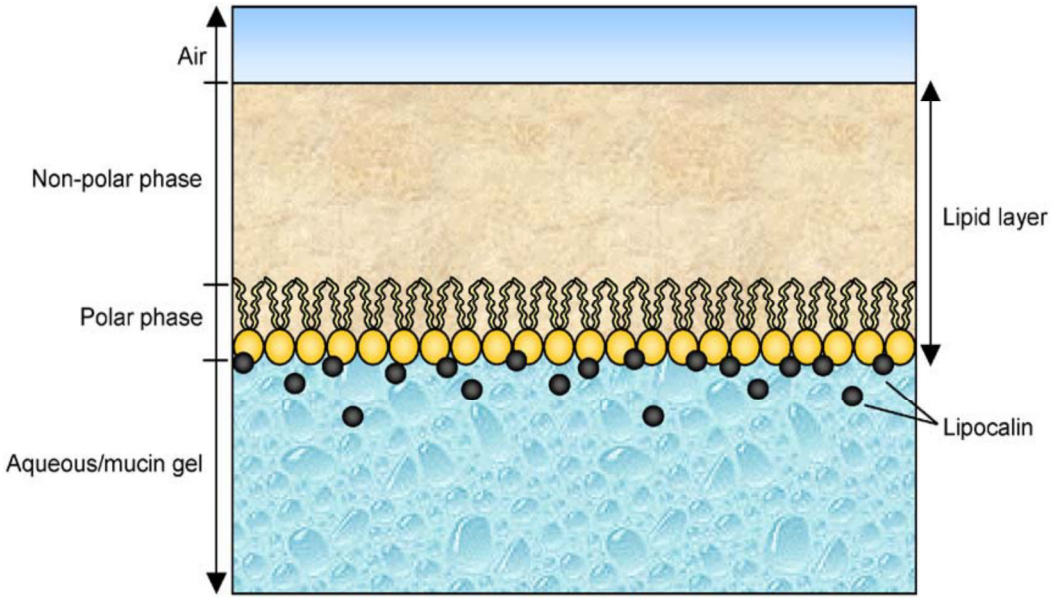

Figure 5: Structure of tear film lipid layer. Adapted from reference (*19*).

1.4.3.1 Emulsions in Artificial Tear Formulation

Recently, oil in water emulsions have been employed in the formulation of eye drops aiming at restoring the lipid tear film (*38, 40*). It has been reported that these emulsions effectively reduce the rate of tear evaporation (*42*). The main concern in the formulation of ophthalmic emulsions is to keep them stable in the bottle, while they have to be unstable and form larger droplets soon after their topical administration on the eye and prior to their drainage.

1.4.3.2 Stability of Emulsions in the Bottle and in the Eye

Water soluble polysaccharides are usually employed to improve the stability of emulsions through viscosity enhancement of the continuous phase(*43*). Influence of polysaccharides on creaming and stability is complicated and highly dependent on the polymer-emulsion system properties. Non-adsorbing polysaccharides are capable of inducing depletion flocculation in emulsions at a certain concentration, referred to as the critical flocculation concentration (CFC). The depletion flocculation leads to creaming instability(*44, 45*) through an increase in the size of emulsion droplets and promotes creaming(*46*). According to Stoke's law(*47*), the larger droplets have a faster upward movement than the smaller ones. However, extensive flocculation causes a negative effect and results in the formation of a network of particles that lowers the rate of creaming. On the other hand, polysaccharides are able to retard the emulsion droplets to move upward at a relatively high polymer concentration by trapping them in an entangled

network of polymer chains(*48*). These phenomena must be taken into account when designing the amount of polysaccharides added. To understand and to obtain the optimum concentration of polysaccharides, the behavior of the emulsion droplets is further discussed in this section as a function of polysaccharides concentration. Strategy to obtain different emulsion behavior during storage and during application is also discussed based on these phenomena.

In dilute regime, unflocculated emulsion droplets behave like individual particles with no significant interaction occurs between them. Large droplets rise faster than the small ones as there is no major resistance from polymer chains. Increasing the polymer concentration over the critical viscosity concentration (CVC) causes the polymer chains to overlap. At CVC, as the polymer concentration in the solution increases, polymer chains overlap and a change in the slope of the viscosity-concentration curves occurs while a double logarithmic plot of viscosity against concentration is presented(*49*). Continuing the increase of polymer concentration results in more polymer interactions and reptation as single polymer chains occupy less volume of space. At this point, the second slope change in the viscosity-concentration curves occurs and is called the CVC*. This has been considered as the transition from the semi-dilute regime to the concentrated regime(*50, 51*).

The CVC is inversely proportional to the volume occupied by the isolated macromolecule coils (50) as given by(*52*)

$$CVC = \frac{3M_w}{4\pi N_A {R_g}^3} \qquad (1)$$

where M_w is the molecular weight of polymer chain, N_A being the Avogadro's number and R_g is the radius of gyration. A transition from dilute to semi-dilute regime occurs at this point(*53*). This transition is believed to be a crossover region between the two regimes instead of being a sharp point(*54*). At semi-dilute regime, the solution behavior is more complicated due to interpenetration and reptation of polymer chains. Additionally, the density of polymeric network increases with increasing polymer concentration. The rate of upward movement of droplets highly depends on the size of openings between polymer chains, which decreases over the CVC(*55*). Therefore, the polymeric network mesh size, ξ, defines the pathway through which the emulsion droplets diffuse. Over the CVC and in the semi-dilute regime, the mesh size, ξ, decreases rapidly with increasing polymer concentration, *C*, by(*56*)

$$\xi = R_g\left(\frac{CVC}{C}\right)^{\frac{3}{4}} \qquad \text{for } C > CVC \qquad (2)$$

Rheological behavior and complex viscosity of the continuous phase can be used to predict the creaming process (*57*).

Based on the explanations of critical concentrations and their effect on the stability of the emulsions, as illustrated by Figure 6, the polymer concentration should be lower than

the CFC to avoid creaming in eye drop bottle over the shelf life period. Delivery of higher polymer concentration below the CFC is desirable to improve the emulsion stability (*43, 57*). Therefore, the starting point should be somewhere below the CFC line. While the artificial tear solution introduces into the eye, through the crosslinking or chain extension reaction, extended chains of polymer will form. These reactions promote polymers to behave as higher molecular weight polymers, where the CFC happens at lower concentrations. Crossing the CFC line causes the formation of larger droplets or flocs with faster upwards movement. Meanwhile, staying at concentrations lower than the CVC allows the easy upwards movement of droplets. Crossing the CVC line towards higher concentrations is not desirable as the polymeric network mesh size decreases rapidly, which increases the possibility of trapping the droplets in the polymer network. As can be seen in Figure 6, the CVC and the CFC appear to vary with molecular weight (MW).

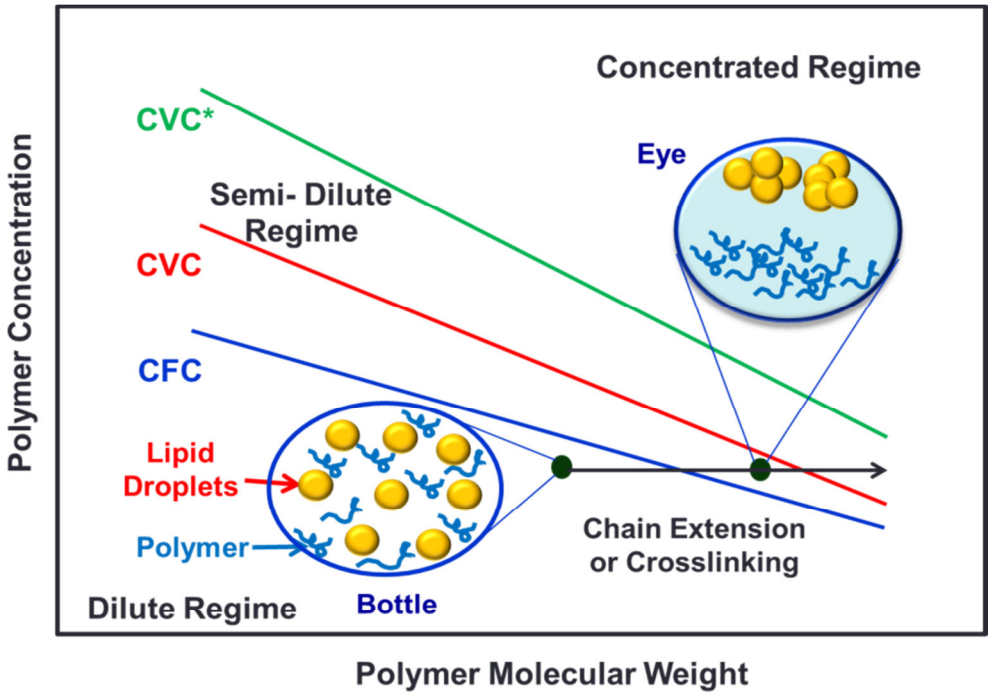

Figure 6: Artificial tear emulsion stability as function of polymer concentration and MW.

1.5 *In-situ* Mild Gelation

Increasing the residence time is of particular interest for topically applied eye drops in order to enhance their therapeutic behavior. Mild gelation through formation of reversible *in-situ* crosslinking is a method to prevent extensive drainage immediately after application. Most of crosslinking reagents are toxic species(*58*). Similar to other

biological applications, a crosslinker for hydrogel formation on the eye must be non-toxic and biocompatible. Unreacted agents should not cause side effects or react with natural tear species. Moreover, crosslinking reaction should occur in physiological environment (at temperature 37°C and pH=7.4) and its rate has to be slower than the diffusion rate of crosslinker (*59*), particularly for high molecular weight crosslinkers. This allows proper mixing of polymer and crosslinker and leads to a more uniform crosslinked network. On the other hand, crosslinking should occur fast enough to form hydrogel prior to drainage from eye. Physiologically responsive crosslinkers form hydrogels through different methods such as hydrogen bonding or by temporary physical entanglements, which are either crosslinked polymeric networks or polymer complexes. Concentration of dissolved polymer and amount of crosslinker affects the network properties. Utilizing low molecular weight crosslinkers having two or more reactive groups is the most common chemical hydrogel preparation technique, which crosslinks the pendant functional groups of a hydrophilic polymer (*60*).

Several methods of stimuli-responsive hydrogel formation have been reported, which responds to temperature(*61-63*), pH(*64, 65*), light(*66*), solvent(*67*), ionic composition(*68, 69*), electric and magnetic fields(*70*), and biochemical (*71*). Borate, a popular crosslinker for guar, has the drawback of requiring high pH conditions in order to form hydrogel. This limits its application in physiological condition. A number of other guar crosslinkers have been investigated; most of them require harsh experimental conditions. Gliko-Kabir *et al*.(*72*), Cunha(*73*) and Sandolo (*74*) prepared guar hydrogels using glutaraldehyde as the crosslinker at pH=2. Glutaraldehyde is a toxic reagent even at low concentrations. It acts as a crosslinker for water soluble polymers containing hydroxyl groups in rather drastic conditions such as low pH or high temperature.

Recently, the use of biological molecules in environmental responsive hybrid hydrogels with novel mechanisms of crosslinking has been reported. These hybrid hydrogels generally consist of two components interconnected either covalently or non-covalently: a hydrophilic polymeric backbone, and a biological origin molecule that functions as a chemical or physical crosslinker. Biological crosslinkers include oligopeptide sequences, which can be recognized by specific proteases(*75*), full-length native proteins and their ligands(*76, 77*), antibody-antigen bindings(*78, 79*) single strands of oligodeoxyribonucleotides with complementary sections(*80, 81*), stereospecific oligo(glycolic acid)s with complementary D/L conformations(*82*) and recombinant protein domains(*83*). In all examples of the biological crosslinkers, biological component determines the stimuli response of the hybrid hydrogels. Studying the structural and physicochemical criteria for the formation of reproducible and reversible hydrogels with precisely defined three-dimensional networks is of great importance(*84*). There are four major interactions that play essential role in biological molecules to determine the hydrogel structure and their specific functions as crosslinker: hydrogen bonding, van der Waals forces, hydrophobic and ionic interactions (*85*).

1.5.1 Reversible Gelation Through Interaction With Proteins

There are numerous studies on the application of amphiphilic water soluble polymers in biological and pharmaceutical fields(*86, 87*). Hydrophobic sections can be incorporated into a polymer through various methods, including chemical grafting (*88*) or copolymerization(*89*). Biopolymers and charged or non-ionic synthetic polymers have been previously used as the hydrophilic backbone to prepare hydrophobically modified polymers. Even minor hydrophobic modification of water soluble polymers will drastically change the properties of the solution and eventually its rheological properties(*90*).

Hydrophobically modified polymers (HMPs) are well recognized for their reversible self-association behavior. Self-association usually leads to thickening and formation of reversible gels(*91*). To enhance the hydrophobic association between polymers, molecules or particles, such as surfactants, micelles, vesicles or proteins, are reversibly bound to the hydrophobic side chains of HMPs(*86, 92, 93*). Proteins such as lysosome and albumin can act as connectors for the HMPs with long enough hydrophobic alkyl pendant chains. The interaction between the net charge of proteins and the charge of polymer backbone is not significant and can be neglected at high ionic strength(*94*). Proteins are able to form crosslinks or extend the chain length of HMPs through hydrophobic interaction with dangling alkyl chains of hydrophobic polymer.

Addition of proteins with increasing concentration ratio of protein to HMP would initially increase the degree of crosslinking and consequently raise the viscosity of HMP solutions to a maximum value. However, as more and more proteins are added, the hydrophobic chains of HMPs would get saturated, and the proteins would not be shared by different polymer chains any longer(*86, 95*). Therefore, at a relatively high protein concentration, proteins would fail to effectively crosslink side chains of different HMPs and their thickening effect would be lost(*94*). Finding the optimum protein and polymer concentration is highly crucial for effective hydrophobic interaction, thickening effect and controlling the gelation of HMP solutions. A summary of crosslinking and de-crosslinking mechanisms are shown in Figure 7.

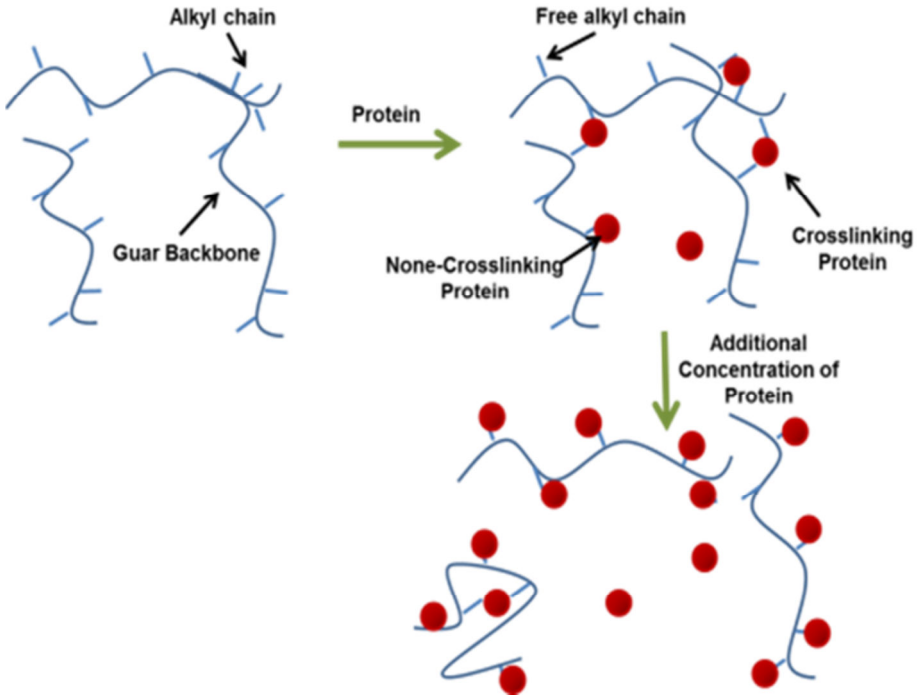

Figure 7: Association mechanism between HMG and protein molecules: a) HMG in the absence of protein, b) presence of proteins and the association of their hydrophobic patches with hydrophobic pendant groups of modified guar leading to the crosslinking of the polymer chains below critical concentration of protein, c) Further addition of protein leads to de-crosslinking, the connectivity of the system is lost. Modified from (*86*)

Among water soluble polymers with hydrophilic backbone, various types of polysaccharides have been used extensively to form amphiphilic polymers(*95*) for various applications (*87, 93, 97, 98*). Hydrophobically modified guar has already been produced through different methods and found applications as associative thickener for rheological modifier additives (*99*). Modified guars, such as hydroxypropyl guar (HPG) and hydroxybutyl guar (HBG), have been shown to have better thickening efficiency in comparison to native guar(*96*). Hydrophobically modified guar (HMG) derivatives can be achieved whether by introducing single alkyl chains or through other methods such as graft copolymerization(*100, 101*). Using the latter, different hydrophobic monomers can be introduced to guar backbone as hydrophobic regions(*102, 103*).

1.6 Objectives

The research conducted was aimed to develop novel approaches to *in-situ* chain extension and mild gelation for artificial tear solutions. The two main goals of this project were to increase the residence time of eye drops and to control the stability of ophthalmic emulsions both in the eye drop bottle and in the tear film. More specific objectives are listed below:

1. To determine the factors controlling the physical stability of ophthalmic emulsions, typical of those used to treat dry eye symptoms.

2. To evaluate the possibility of modified guars interaction with human serum albumin (HSA) and lysozyme to produce weak gels through formation of polymer/protein complexes.

3. To define the proper hydrophobic pendant group and degree of substitution for modified guars that enables effective interaction with HSA and lysozyme in their actual concentration range in tear films.

4. To clarify the effect of molecular weight variation on the interaction of modified guars with HSA and lysozyme.

5. To understand the influence of hydrophobic modification and molecular weight variation on lubrication behavior of guar.

6. To determine the effect of modified guar interaction with proteins on the size of emulsion droplets and the rate of creaming.

7. Demonstrating inverted QCM-D cell without flow as a method that gives insight into the gravity-induced build-up of a concentrated emulsion layer (consolidation layer) near the sensor surface.

1.7 Thesis Outline

Chapter 1. ***Introduction and literature review.*** This chapter presents the background of this project, including natural tear film composition, dry eye syndrome and its influence on tear film components, artificial tear properties, including residence time, lubrication and lipid layer restoration. *In-situ* gelation through interaction of hydrophobically modified polymers and proteins is also explained. The objective of the thesis, and the thesis outline, are provided.

Chapter 2. ***On formulating ophthalmic emulsions***. Formulating ophthalmic emulsions is relatively complicated. They should be stable over the period of their shelf

life but should cream fast enough in tear film to help rebuilding the structure of lipid layer. Most of them contain polymers, which are used in the formulation of eye drops to help lubrication of eye drops and to improve the residence time. This is in conflict with emulsion stability. Exceeding the critical flocculation concentration (CFC) leads to depletion flocculation and aggregation of emulsified droplets. Polymer molecular weight and concentration are two important parameters to control the emulsion stability. The purpose is to define a simple approach to predict CFC for ophthalmic emulsions containing polymers with various molecular weights. A wide range of guar molecular weight has been achieved through acid hydrolysis. The CFC and critical viscosity concentrations (CVC and CVC*) were determined using dynamic light scattering and rheology experiments. Visual creaming experiments were also employed to determine the stability of emulsions in the presence of various guars. The results showed that increasing the concentration of guar over the CFC produced an increase in creaming rate due to depletion flocculation. The CFC for higher molecular weight polymers occurs at lower concentrations. Additional amount of guar concentration over CVC and towards CVC*, stabilized the emulsion because of the formation of a dense polymeric network as a continuous phase. Trough defining critical concentrations and using Mark-Houwink parameters, polymer properties for designing desired stability for ophthalmic emulsions can be achieved. This chapter has been published in *Colloids and Surfaces B: Biointerfaces.*

Chapter 3. ***Inverted QCM-D: A Method to Evaluate the Emulsion Stability.*** The interactions of oil-in-water emulsions with solid surfaces were determined with Quartz Crystal Microbalance (QCM-D) measurements. Conventional measurements, in flow, gave adsorption information whereas quiescent measurements with inverted QCM-D sensors probed the initial stages of consolidated (cream) layer formation next to the surface. Some emulsions only show deposition with no evidence of a consolidation layer – these tend to be dilute, small and colloidally stable. By contrast, larger and less stable emulsions display rich behaviours in both frequency shifts and dissipation over the period of hours as consolidation layers build up next to the QCM-D sensor surface. Voigt-based viscoelastic modelling fits to inverted QCM-D data gives insight into the evolution of the properties of the consolidation layers with time.

Chapter 4. ***Hydrophobic Guar Mild Gelation by Albumin in Simulated Human Tear Solutions.*** Albumin leakage from inflamed surface capillaries and conjunctiva blood vessels in some types of dry eye syndrome elevates albumin concentration in natural tear. The increased concentration approaches a value that may interact effectively with hydrophobically modified polymers to raise the viscosity of artificial tear solution. This interaction and mild gelation helps elevating the residence time of therapeutic eye drops. In this chapter, the preparation and characterization methods of Modified guar (MGuar) with various alkyl chains and degrees of substitution is explained. The ability of MGuars to form a connected structure through hydrophobic interaction with albumin has been revealed through rheological measurements. Immediate interaction of albumin with MGuars has been observed and the interaction of MGuars with proteins studied in this work was found to be a strong function of alkyl chain length, degree of alkylation,

polymer and protein concentration. By controlling these parameters, degree of chain extension and as a result, level of increase in viscosity will be adjusted for a proper range, which can be applied in the mild gelation mechanism of artificial tear solutions in tear environment. This chapter has been published in *Biomacromolecules.*

Chapter 5. ***In-Situ Chain Extension through Interaction of Modified Guars with Tear Proteins.*** Broadening the range of application of increased eye drop residence time through interaction of MGuars and proteins is the main objective of this chapter. Lysozyme, one of the most abundant natural tear proteins, is a potential candidate. A series of hydrophobically modified guar polymers (MGuar) were prepared. Methods employed to elevate lysozyme tendency to bind to MGuar are explained. As a method to improve the extent of chain extension and polymer/protein complex formation, lower molecular weight guars were examined. Acid hydrolysis has been used to prepare a range of molecular weights. Binding and rheological measurements were employed to evaluate MGuar interactions with lysozyme. Our results revealed the ability of low molecular weight MGuar to improve the efficiency of viscosity enhancement. Modifications on guar affected the lubrication behavior of MGuars, as has been experienced by using PDMS surfaces in a friction test. Hydrophobic modification enhances the lubrication between hydrophobic surfaces, while saturation of hydrophobes with lysozyme diminishes the lubricity. This chapter is being prepared for publication.

Chapter 6. ***Concluding remarks*****.** This chapter presents the conclusions, major contributions and future work.

1.8 References

1. Nichols, J. J., Ziegler, C., Mitchell, G. L., and Nichols, K. K. (2005) Self-reported dry eye disease across refractive modalities, Investigative ophthalmology & visual science 46, 1911-1914.
2. Cohen, S., Lobel, E., Trevgoda, A., and Peled, Y. (1997) A novel in situ-forming ophthalmic drug delivery system from alginates undergoing gelation in the eye, Journal of Controlled Release 44, 201-208.
3. Davidson, H. J., and Kuonen, V. J. (2004) The tear film and ocular mucins, Veterinary Ophthalmology 7, 71-77.
4. Foulks, G. N. The Correlation Between the Tear Film Lipid Layer and Dry Eye Disease, Survey of Ophthalmology 52, 369-374.
5. Fullard, R. J., and Snyder, C. (1990) Protein levels in nonstimulated and stimulated tears of normal human subjects, Investigative Ophthalmology & Visual Science 31, 1119-1126.
6. Redl, B. (2000) Human tear lipocalin, Biochimica et Biophysica Acta (BBA) - Protein Structure and Molecular Enzymology 1482, 241-248.
7. Holly, F. J. (1974) Surface chemistry of tear film component analogs, Journal of Colloid and Interface Science 49, 221-231.
8. Bron, A. J., Tiffany, J. M., Gouveia, S. M., Yokoi, N., and Voon, L. W. (2004) Functional aspects of the tear film lipid layer, Experimental Eye Research 78, 347-360.
9. Dilly, P. N. (1985) On the nature and the role of the subsurface vesicles in the outer epithelial cells of the conjunctiva, British Journal of Ophthalmology 69, 477-481.
10. Holly, F. J. (1973) Formation and rupture of the tear film, Experimental Eye Research 15, 515-525.
11. Schrage, N., Wuestemeyer, H., and Langefeld, S. (2004) Do different osmolar solutions change the epithelial surface of the healthy rabbit cornea?, Graefe's Archive for Clinical and Experimental Ophthalmology 242, 668-673.
12. Schrader, S., Mircheff, A., and Geerling, G. (2008) Animal models of dry eye.
13. Virtanen, T., Konttinen, Y. T., Honkanen, N., Härkönen, M., and Tervo, T. (1997) Tear fluid plasmin activity of dry eye patients with Sjögren's syndrome, Acta Ophthalmologica Scandinavica 75, 137-141.
14. Wolkoff, P., and Kjærgaard, S. K. (2007) The dichotomy of relative humidity on indoor air quality, Environment International 33, 850-857.
15. Schein, O. D., Munoz, B., Tielsch, J. M., Bandeen-Roche, K., and West, S. (1997) Prevalence of dry eye among the elderly, American journal of ophthalmology 124, 723-728.
16. Begley, C. G., Caffery, B., Chalmers, R. L., Mitchell, G. L., and Group, D. E. I. S. (2002) Use of the Dry Eye Questionnaire to Measure Symptoms of Ocular Irritation in Patients With Aqueous Tear Deficient Dry Eye, Cornea 21, 664-670.
17. Choy, M. H., Stapleton, F., Willcox, M. D., and Zhu, H. (2008) Comparison of virulence factors in Pseudomonas aeruginosa strains isolated from contact lens-and non-contact lens-related keratitis, Journal of medical microbiology 57, 1539-1546.

18. Terry, M. A. (2001) Dry eye in the elderly, Drugs & aging 18, 101-107.
19. Johnson, M. E., and Murphy, P. J. (2004) Changes in the tear film and ocular surface from dry eye syndrome, Progress in retinal and eye research 23, 449-474.
20. Mackie, I., and Seal, D. (1984) Diagnostic implications of tear protein profiles, British journal of ophthalmology 68, 321-324.
21. Bron, A., and Mengher, L. (1989) The ocular surface in keratoconjunctivitis sicca, Eye 3, 428-437.
22. Holly, F. J. (1987) Tear Film Physiology, International Ophthalmology Clinics 27, 2-6.
23. Bernal, D. L., and Ubels, J. L. (1993) Artificial Tear Composition and Promotion of Recovery of the Damaged Corneal Epithelium, Cornea 12, 115-120.
24. Begley, C. G., Chalmers, R. L., Mitchell, G. L., Nichols, K. K., Caffery, B., Simpson, T., DuToit, R., Portello, J., and Davis, L. (2001) Characterization of Ocular Surface Symptoms From Optometric Practices in North America, Cornea 20, 610-618.
25. Begley, C. G., Chalmers, R. L., Abetz, L., Venkataraman, K., Mertzanis, P., Caffery, B. A., Snyder, C., Edrington, T., Nelson, D., and Simpson, T. (2003) The Relationship between Habitual Patient-Reported Symptoms and Clinical Signs among Patients with Dry Eye of Varying Severity, Investigative Ophthalmology & Visual Science 44, 4753-4761.
26. Snibson, G. R., Greaves, J. L., Soper, N. D. W., Tiffany, J. M., Wilson, C. G., and Bron, A. J. (1992) Ocular Surface Residence Times of Artificial Tear Solutions, Cornea 11, 288-293.
27. Hoichman, D., Gromova, L., and Sela, J. (2007) Synergistic gel formation in aqueous solutions of guar-gellan composition, Pharmaceutical Chemistry Journal 41, 274-277.
28. Hennink, W. E., and van Nostrum, C. F. (2002) Novel crosslinking methods to design hydrogels, Advanced Drug Delivery Reviews 54, 13-36.
29. Cui, Y. (2010) CHARACTERIZING HYDROXYPROPYL GUAR- BORATE INTERACTIONS WITH MODEL TEAR FILM COMPONENTS.
30. Bhushan, B., and Gupta, B. K. (1991) Handbook of Tribology: Materials, coatings, and surface treatments.
31. Meyer, A. E., Baier, R. E., Chen, H., and Chowhan, M. (2007) Differential tissue-on-tissue lubrication by ophthalmic formulations, Journal of Biomedical Materials Research Part B: Applied Biomaterials 82B, 74-88.
32. Bhushan, B., Author, Ko, P. L., and Reviewer. (2003) Introduction to Tribology, Applied Mechanics Reviews 56, B6-B7.
33. Suh, N. P., and Saka, N. (1980) Fundamentals of tribology.
34. Weißbach, W. (2007) Tribologische Beanspruchung und werkstofftechnische Maßnahmen, In Werkstoffkunde, pp 347-366, Vieweg.
35. Caravia, L., Dowson, D., Fisher, J., Corkhill, P. H., and Tighe, B. J. (1993) A comparison of friction in hydrogel and polyurethane materials for cushion-form joints, Journal of Materials Science: Materials in Medicine 4, 515-520.

36. Ehlers, N. (1965) THE PRECORNEAL FILM. BIOMICROSCOPICAL, HISTOLOGICAL AND CHEMICAL INVESTIGATIONS, Acta ophthalmologica. Supplementum, SUPPL 81: 81.
37. Holly, F. J., and Holly, T. F. (1994) Advances in ocular tribology, In Lacrimal Gland, Tear Film, and Dry Eye Syndromes, pp 275-283, Springer.
38. Scaffidi, R. C., and Korb, D. R. (2007) Comparison of the efficacy of two lipid emulsion eyedrops in increasing tear film lipid layer thickness, Eye & contact lens 33, 38-44.
39. McCulley, J., and Shine, W. (1997) A compositional based model for the tear film lipid layer, Transactions of the American Ophthalmological Society 95, 79.
40. Di Pascuale, M. A., Goto, E., and Tseng, S. C. (2004) Sequential changes of lipid tear film after the instillation of a single drop of a new emulsion eye drop in dry eye patients, Ophthalmology 111, 783-791.
41. Korb, D. R., Scaffidi, R. C., Greiner, J. V., Kenyon, K. R., Herman, J. P., Blackie, C. A., Glonek, T., Case, C. L., Finnemore, V. M., and Douglass, T. (2005) The effect of two novel lubricant eye drops on tear film lipid layer thickness in subjects with dry eye symptoms, Optometry & Vision Science 82, 594-601.
42. Khanal, S., Tomlinson, A., Pearce, E. I., and Simmons, P. A. (2007) Effect of an oil-in-water emulsion on the tear physiology of patients with mild to moderate dry eye, Cornea 26, 175-181.
43. Parker, A., Gunning, P. A., Ng, K., and Robins, M. M. (1995) How does xanthan stabilise salad dressing?, Food Hydrocolloids 9, 333-342.
44. McClements, D. (2000) Comments on viscosity enhancement and depletion flocculation by polysaccharides, Food Hydrocolloids 14, 173-177.
45. Gunning, P. A., Hennock, M. S., Howe, A. M., Mackie, A. R., Richmond, P., and Robins, M. M. (1986) Stability of oil-in-water emulsions. The effect of dispersed phase and polysaccharide on creaming, Colloids and surfaces 20, 65-80.
46. Basaran, T., Demetriades, K., and McClements, D. (1998) Ultrasonic imaging of gravitational separation in emulsions, Colloids and Surfaces A: Physicochemical and Engineering Aspects 136, 169-181.
47. Manoj, P., Fillery-Travis, A. J., Watson, A. D., Hibberd, D. J., and Robins, M. M. (1998) I. Creaming Behavior, Journal of colloid and interface science 207, 283-293.
48. Cao, Y., Dickinson, E., and Wedlock, D. J. (1990) Creaming and flocculation in emulsions containing polysaccharide, Food Hydrocolloids 4, 185-195.
49. Robinson, G., Ross-Murphy, S. B., and Morris, E. R. (1982) Viscosity-molecular weight relationships, intrinsic chain flexibility, and dynamic solution properties of guar galactomannan, Carbohydrate Research 107, 17-32.
50. Ying, Q., and Chu, B. (1987) Overlap concentration of macromolecules in solution, Macromolecules 20, 362-366.
51. Graessley, W. W. (1980) Polymer chain dimensions and the dependence of viscoelastic properties on concentration, molecular weight and solvent power, Polymer 21, 258-262.
52. Sperling, L. H. (2005) Introduction to physical polymer science, John Wiley & Sons.

53. Milas, M., Rinaudo, M., and Tinland, B. (1985) The viscosity dependence on concentration, molecular weight and shear rate of xanthan solutions, Polymer Bulletin 14, 157-164.
54. De Gennes, P.-G. (1979) Scaling concepts in polymer physics, Cornell university press.
55. Langevin, D., and Rondelez, F. (1978) Sedimentation of large colloidal particles through semidilute polymer solutions, Polymer 19, 875-882.
56. Moates, G. K., Watson, A. D., and Robins, M. M. (2001) Creaming and oscillation rheology of weakly flocculated concentrated emulsions, Colloids and Surfaces A: Physicochemical and Engineering Aspects 190, 167-178.
57. Buscall, R., Goodwin, J., Ottewill, R., and Tadros, T. F. (1982) The settling of particles through Newtonian and non-Newtonian media, Journal of colloid and interface science 85, 78-86.
58. Hermanson, G. T., (Ed.) (1996) Bioconjugate Techniques Academic Press, San Diego.
59. Ossipov, D. A., and Hilborn, J. (2006) Poly(vinyl alcohol)-Based Hydrogels Formed by "Click Chemistry", Macromolecules 39, 1709-1718.
60. Hoffman, A. S. (2002) Hydrogels for biomedical applications, Advanced Drug Delivery Reviews 54, 3-12.
61. Fitzsimons, S., Mulvihill, D., and Morris, E. (2008) Large enhancements in thermogelation of whey protein isolate by incorporation of very low concentrations of guar gum, Food Hydrocolloids 22, 576-586.
62. Geever, L., Devine, D., Nugent, M., Kennedy, J., Lyons, J., Hanley, A., and Higginbotham, C. (2006) Lower critical solution temperature control and swelling behaviour of physically crosslinked thermosensitive copolymers based on N-isopropylacrylamide, European Polymer Journal 42, 2540-2548.
63. Li, X., Wu, W., and Liu, W. (2008) Synthesis and properties of thermo-responsive guar gum/poly(N-isopropylacrylamide) interpenetrating polymer network hydrogels, Carbohydrate Polymers 71, 394-402.
64. Chen, G., Imanishi, Y., and Ito, Y. (1998) pH-Sensitive Thin Hydrogel Microfabricated by Photolithography, Langmuir 14, 6610-6612.
65. Huang, Y., Yu, H., and Xiao, C. (2007) pH-sensitive cationic guar gum/poly (acrylic acid) polyelectrolyte hydrogels: Swelling and in vitro drug release, Carbohydrate Polymers 69, 774-783.
66. Beines, P. W., Klosterkamp, I., Menges, B., Jonas, U., and Knoll, W. (2007) Responsive Thin Hydrogel Layers from Photo-Cross-Linkable Poly(N-isopropylacrylamide) Terpolymers†, Langmuir 23, 2231-2238.
67. Bell, C. L., and Peppas, N. A. (1996) Water, solute and protein diffusion in physiologically responsive hydrogels of poly(methacrylic acid-g-ethylene glycol), Biomaterials 17, 1203-1218.
68. Hirokawa, Y., Tanaka, T., and Sato, E. (1985) Phase transition of positively ionized gels, Macromolecules 18, 2782-2784.
69. Katayama, S., and Ohata, A. (1985) Phase transition of a cationic gel, Macromolecules 18, 2781-2782.

70. Kwon, I. C., Bae, Y. H., and Kim, S. W. (1991) Electrically credible polymer gel for controlled release of drugs, Nature 354, 291-293.
71. Kokufuta, E. (1993) Novel applications for stimulus-sensitive polymer gels in the preparation of functional immobilized biocatalysts, In Responsive Gels: Volume Transitions II (Dušek, K., Ed.), pp 157-177, Springer Berlin / Heidelberg.
72. Gliko-Kabir, I., Penhasi, A., and Rubinstein, A. (1999) Characterization of crosslinked guar by thermal analysis, Carbohydrate Research 316, 6-13.
73. Cunha, P. L. R., Castro, R. R., Rocha, F. A. C., de Paula, R. C. M., and Feitosa, J. P. A. (2005) Low viscosity hydrogel of guar gum: Preparation and physicochemical characterization, International Journal of Biological Macromolecules 37, 99-104.
74. Sandolo, C., Coviello, T., Matricardi, P., and Alhaique, F. (2007) Characterization of polysaccharide hydrogels for modified drug delivery, European Biophysics Journal 36, 693-700.
75. Ulbrich, K., Strohalm, J., and Kopeček, J. (1982) Polymers containing enzymatically degradable bonds. VI.Hydrophilic gels cleavable by chymotrypsin, Biomaterials 3, 150-154.
76. Obaidat, A. A., and Park, K. (1996) Characterization of Glucose Dependent Gel-Sol Phase Transition of the Polymeric Glucose-Concanavalin A Hydrogel System, Pharmaceutical Research 13, 989-995.
77. Tada, D., Tanabe, T., Tachibana, A., and Yamauchi, K. (2005) Drug release from hydrogel containing albumin as crosslinker, Journal of Bioscience and Bioengineering 100, 551-555.
78. Miyata, T., Asami, N., and Uragami, T. (1999) Preparation of an Antigen-Sensitive Hydrogel Using Antigen−Antibody Bindings, Macromolecules 32, 2082-2084.
79. Miyata, T., Asami, N., and Uragami, T. (1999) A reversibly antigen-responsive hydrogel, Nature 399, 766-769.
80. Alemdaroglu, F. E., and Herrmann, A. (2007) DNA meets synthetic polymers-highly versatile hybrid materials, Organic & Biomolecular Chemistry 5, 1311-1320.
81. He, X., Wei, B., and Mi, Y. (2010) Aptamer based reversible DNA induced hydrogel system for molecular recognition and separation, Chemical Communications 46, 6308-6310.
82. de Jong, S. J., De Smedt, S. C., Wahls, M. W. C., Demeester, J., Kettenes-van den Bosch, J. J., and Hennink, W. E. (2000) Novel Self-assembled Hydrogels by Stereocomplex Formation in Aqueous Solution of Enantiomeric Lactic Acid Oligomers Grafted To Dextran, Macromolecules 33, 3680-3686.
83. Wang, C., Stewart, R. J., and KopeCek, J. (1999) Hybrid hydrogels assembled from synthetic polymers and coiled-coil protein domains, Nature 397, 417-420.
84. Kopeček, J., Tang, A., Wang, C., and Stewart, R. J. (2001) De novo design of biomedical polymers: hybrids from synthetic macromolecules and genetically engineered protein domains, Macromolecular Symposia 174, 31-42.
85. Tanaka, T. (1992) Phase Transitions of Gels, In Polyelectrolyte Gels, pp 1-21, American Chemical Society.

86. Petit, F., Audebert, R., and Iliopoulos, I. (1995) Interactions of hydrophobically modified poly (sodium acrylate) with globular proteins, Colloid and Polymer Science 273, 777-781.
87. Akiyoshi, K., Deguchi, S., Tajima, H., Nishikawa, T., and Sunamoto, J. (1997) Microscopic structure and thermoresponsiveness of a hydrogel nanoparticle by self-assembly of a hydrophobized polysaccharide, Macromolecules 30, 857-861.
88. Desbrieres, J., Martinez, C., and Rinaudo, M. (1996) Hydrophobic derivatives of chitosan: characterization and rheological behaviour, International journal of biological macromolecules 19, 21-28.
89. Xie, X., and Hogen-Esch, T. E. (1996) Copolymers of N, N-dimethylacrylamide and 2-(N-ethylperfluorooctanesulfonamido) ethyl acrylate in aqueous media and in bulk. Synthesis and properties, Macromolecules 29, 1734-1745.
90. Ng, W., Tam, K., and Jenkins, R. (2001) Rheological properties of methacrylic acid/ethyl acrylate co-polymer: comparison between an unmodified and hydrophobically modified system, Polymer 42, 249-259.
91. Petka, W. A., Harden, J. L., McGrath, K. P., Wirtz, D., and Tirrell, D. A. (1998) Reversible hydrogels from self-assembling artificial proteins, Science 281, 389-392.
92. Petit, F., Iliopoulos, I., Audebert, R., and Szönyi, S. (1997) Associating polyelectrolytes with perfluoroalkyl side chains: Aggregation in aqueous solution, association with surfactants, and comparison with hydrogenated analogues, Langmuir 13, 4229-4233.
93. Akiyoshi, K., Deguchi, S., Moriguchi, N., Yamaguchi, S., and Sunamoto, J. (1993) Self-aggregates of hydrophobized polysaccharides in water. Formation and characteristics of nanoparticles, Macromolecules 26, 3062-3068.
94. Borrega, R., Tribet, C., and Audebert, R. (1999) Reversible gelation in hydrophobic polyelectrolyte/protein mixtures: An example of cross-links between soft and hard colloids, Macromolecules 32, 7798-7806.
95. Iliopoulos, I., Wang, T., and Audebert, R. (1991) Viscometric evidence of interactions between hydrophobically modified poly (sodium acrylate) and sodium dodecyl sulfate, Langmuir 7, 617-619.
96. Butler, L. G. (1975) Enzyme immobilization by adsorption on hydrophobic derivatives of cellulose and other hydrophilic materials, Archives of biochemistry and biophysics 171, 645-650.
97. Nishikawa, T., Akiyoshi, K., and Sunamoto, J. (1994) Supramolecular assembly between nanoparticles of hydrophobized polysaccharide and soluble protein complexation between the self-aggregate of cholesterol-bearing pullulan and. alpha.-chymotrypsin, Macromolecules 27, 7654-7659.
98. Suzuki, M., Mikami, T., Matsumoto, T., and Suzuki, S. (1977) Preparation and antitumor activity of O-palmitoyldextran phosphates, O-palmitoyldextrans, and dextran phosphate, Carbohydrate Research 53, 223-229.
99. Lapasin, R., De Lorenzi, L., Pricl, S., and Torriano, G. (1995) Flow properties of hydroxypropyl guar gum and its long-chain hydrophobic derivatives, Carbohydrate polymers 28, 195-202.

100. Chowdhury, P., Samui, S., Kundu, T., and Nandi, M. (2001) Graft polymerization of methyl methacrylate onto guar gum with ceric ammonium sulfate/dextrose redox pair, Journal of applied polymer science 82, 3520-3525.
101. Holmes, V. (2007) The application of controlled radical polymerization processes on the graft copolymerization of hydrophobic substituents onto guar gum and guar gum derivatives, Faculty of the Louisiana State University and Agricultural and Mechanical College In partial fulfillment of the Requirements for the degree of Doctor of Philosophy In The Department of Chemistry By Veronica Holmes BS, Southern University.
102. Bahamdan, A., and Daly, W. H. (2007) Hydrophobic guar gum derivatives prepared by controlled grafting processes, Polymers for Advanced Technologies 18, 652-659.
103. Bahamdan, A., and Daly, W. H. (2006) Poly (oxyalkylene) grafts to guar gum with applications in hydraulic fracturing fluids, Polymers for Advanced Technologies 17, 679-681.

Chapter 2 On formulating ophthalmic emulsions

Most of the experiments and analysis in chapter 2 were conducted by me. Guar hydrolysis and GPC measurements were conducted with the help of my summer student, Cameron Gray.
Dr. Pelton revised the versions I wrote, helped to analyze data and re-wrote the final version.

Colloids and Surfaces B:
Biointerfaces 122 (2014) 7–11

Contents lists available at ScienceDirect

Colloids and Surfaces B:
Biointerfaces

journal homepage:
www.elsevier.com/locate/colsurfb

On formulating ophthalmic emulsions

Roozbeh Mafi [a], Cameron Gray [a], Robert Pelton [a,*], Howard Ketelson [b], James Davis [c]

[a] Department of Chemical Engineering, McMaster University, Hamilton, ON L8S 4L7, Canada
[b] Alcon Research, Ltd., 6201 South Freeway, Fort Worth, TX 76134-2099, USA
[c] Alcon Research, Ltd., 11460 Johns Creek Parkway, Johns Creek, GA 30097, USA

article info

Article history:
Received 12 May 2014
Received in revised form 16 June 2014
Accepted 18 June 2014
Available online 24 June 2014

Keywords: Emulsion
stability Depletion
flocculation Guar
Eye drop formulation
Overlap concentration

abstract

The formulation of dilute, transparent ophthalmic emulsions (eye drops) with long shelf lives is a challenge because of the tendency of the emulsion droplets to aggregate, particularly in the presence of the water-soluble polymers typically used in eye drops. While many functions of eye drops, such as lubricity and residence time in the eye, are promoted by high concentrations of high molecular weight water-soluble polymers, emulsified lipids and drugs aggregate in the eye drop bottle if the polymer concentration is above the critical flocculation concentration (CFC). The purpose is to develop a simple approach to predict the CFC for polymers based on information readily available in the literature. High molecular weight guar was hydrolyzed to give a series of guar samples spanning a wide range of average molecular weights. The CFC values and critical viscosity concentrations were measured as functions guar properties, using electrophoresis, dynamic light scattering and rheology measurements. The higher the guar molecular weight, the lower was the CFC, the maximum concentration that can be tolerated in the eye drop formulation. The guar CFC values were approximately equal to the overlap concentrations where guar molecules start to overlap in solution. We propose that the CFC can be estimated for any water-soluble polymer using the polymer molecular weight and the readily available Mark–Houwink parameters, thus providing a design rule for ophthalmic emulsions.

1. Introduction

Eye drops are important vehicles for delivering materials to the front of the eye. From a physical chemical perspective, there are two classes of eye drops–homogeneous solutions of water-soluble ingredients, and emulsions. Homogeneous solutions are attractive because they are clear, stable and have long shelf lives. However, water–insoluble materials do not form homogeneous solutions. Instead they must be formulated as emulsions where the water–insoluble materials are present as dispersed emulsion droplets [1]. Emulsions offer many challenges, particularly with respect to shelf life and product clarity. Herein we present some ophthalmic emulsion design guidelines based on results from model emulsions.

Emulsions can undergo creaming, aggregation, and coalescence—these are briefly described. Ophthalmic emulsions are oil-in-water emulsions, and buoyancy forces cause the lower density emulsion drops to rise (cream) toward the surface [2]. Creaming rates are lowered by continuous mixing, by decreasing the emulsion drop diameter, or by increasing the viscosity of the suspending aqueous phase by addition of water–soluble polymers. Small (diameter <50 nm) droplets offer the additional advantage of high transparency.

Like any colloidal or nanoparticle suspension, emulsion droplets have a natural tendency to aggregate. Surfactants and polymers present during the emulsification process concentrate at the oil/water interface and can prevent aggregation (colloidal instability) because of electrostatic and/or steric repulsive forces [3]. If emulsions do aggregate, they either remain as clumps of droplets, or the droplets coalesce into larger droplets, eventually producing an oil layer on top of the aqueous phase. Creaming, aggregation and coalescence are undesirable outcomes for ophthalmic products.

In this work we illustrate the challenges in formulating ophthalmic emulsions by using a model emulsion of hexadecane stabilized by phosphatidylcholine, a biological surfactant. The aqueous phase includes guar, a nonionic water–soluble polymer used in products to alleviate dry eye symptoms [4]. Depending upon molecular weight and concentration, guar can either improve or degrade emulsion properties. Rules are presented for optimizing the water–soluble polymer components of ophthalmic emulsions.

* Corresponding author. Tel.: +1 905 529 7070x27045.
E-mail address: peltonrh@mcmaster.ca (R. Pelton).

http://dx.doi.org/10.1016/j.colsurfb.2014.06.039
0927-7765/

2. Experimental

2.1. Materials

Native guar with a molecular weight of ~3 MDa was provided by Alcon Laboratories (Fort Worth, TX, USA). Hexadecane, NaN_3, (4-(2-hydroxyethyl)-1-piperazineethanesulfonic acid) (HEPES) and NaCl were purchased from Sigma-Aldrich (Oakville, ON, Canada), and l-α-phosphatidylcholine was purchased from Avanti Polar Lipid (Alabaster, AL, USA). Aqueous solutions were made with 18.2 M cm, Barnstead Nanopure Diamond system (Iowa, USA) water.

2.2. Guar hydrolysis

Guar samples with molecular weights varying between 130 kDa and 427 kDa were prepared by the acid hydrolysis of high molecular weight guar using Prud'homme's method [5]. A 0.1% (w/w) high molecular weight guar was prepared by dissolving guar powder in water with vigorous stirring using a mechanical stirrer for 24 h to maximize hydration. A volume of 200 mL guar solution was placed in a sealed 500 mL three-neck round bottom flask maintained at 50 °C in a water bath. The pH of the guar solution was maintained at 1 by 1 N HCl addition. Periodically, over a period of 24 h, 20 mL samples of partially hydrolyzed guar solutions were isolated and the pH adjusted to 6 by 1 N NaOH addition. The samples were then purified by dialysis for two weeks and then freeze dried (Millrock Tech., BT48A, NY, USA).

Guar molecular weight distributions were determined by gel permeation chromatography using a Waters 515 HPLC pump, three Waters Ultrastyragel Linear columns, and a Waters 2414 refractive index detector. The mobile phase was 300 mM $NaNO_3$ in 50 mM phosphate buffer at pH 7. MW calibration was based on poly(ethylene glycol) standards (Waters, MA, USA).

2.3. Viscosity measurements

Guar solutions were prepared at concentrations varying from 0.02% (w/w) to 0.6% (w/w) by dissolving dried samples of guar in water with 20 ppm of NaN_3 preservative. All samples were stirred for 24 h to ensure complete dissolution and followed by at least 2 h rest before viscosity measurements. The viscosity of samples was measured at 25 °C as a function of shear rate using an ATS controlled stress rheometer (Rheologica Stress Tech HR,) equipped with bob and cup geometry (CC25). Temperatures were controlled within ±0.2 °C using a water-bath.

2.4. Emulsion preparation

An amount of 10 mg l-α -phosphatidylcholine in chloroform solution (25 mg/mL) was evaporated in a round-bottom flask using a rotary evaporator at room temperature, followed by 10 min exposure to a nitrogen gas stream. To the flask were added 140 mg of hexadecane and 10 mL solution containing 5 ppm NaN_3, 10 mM HEPES buffer and 5 mM NaCl. The mixture was sonicated for 15 min using a Misonix Sonicator (S-4000 Ultrasonic Processors, USA, 20 kHz). The ultrasonic probe (90% amplitude and output power setting of 60) was immersed directly into the emulsion.

2.5. Electrophoresis

Electrophoretic mobility measurements were made with a Brookhaven Zeta PALS instrument at 25 °C in phase analysis light scattering mode (PALS software version 2.5). The reported mobility values were the average of 10 cycles, each comprised of 15 scans. The samples were all made in 5 mM NaCl.

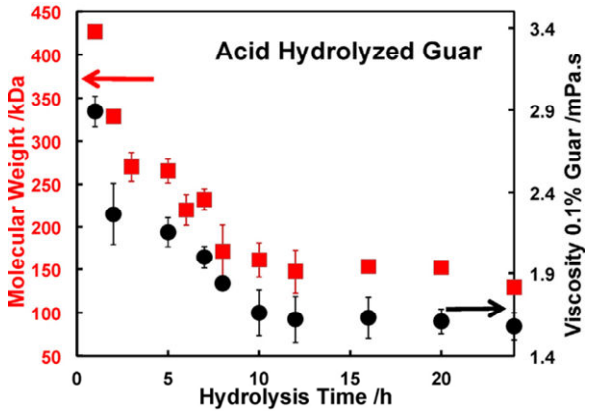

Fig. 1. The molecular weight (GPC) and viscosities of hydrolyzed guar samples as functions of the hydrolysis times. Viscosity measurements were made at 25 °C using a shear rate of 200 s^{-1}. Error bars are the standard deviation of triplicate measurements—in some cases the error bars are hidden within symbols.

2.6. Dynamic light scattering

Measurements were carried out at 25 °C using a BI-APD 8590 digital correlator (Brookhaven, NY, USA) apparatus at a fixed 90° scattering angle and a 35 mW 632.8 nm laser as the light source. Using the CONTIN program, the cumulative intensity distribution method was used to calculate the emulsion droplet diameter. Reported diameters are the average of 5 measurements.

Dynamic light scattering was used to determine the critical flocculation concentrations (CFC) of guar added to emulsions. CFC values corresponded to the first significant slope change in plots of average diameter versus guar concentration.

2.7. Creaming measurements

A volume of 0.2 mL emulsion were mixed with 2 mL of guar solution in a 5 mL vial and mixed for 120 s using a mini vortexer (VWR, VM-3000, USA). The emulsions were immediately transferred to glass test tubes (50 × 6 mm) and maintained at 23 °C. The thickness of the serum layer at the bottom of the tube was visually determined over a period of 500 h.

3. Results

A series of guar solutions of varying molecular weight was prepared by the controlled hydrolysis of very high molecular weight guar. The molecular weights of the purified products were measured by gel permeation chromatography. Fig. 1 shows the molecular weights and the viscosities of 0.1% solutions as functions of the hydrolysis times. This series of samples was used to assess the influence of water–soluble polymer molecular weight on ophthalmic emulsion stability.

Fig. 2 shows the viscosity versus concentration plots for three guar samples from the series of hydrolyzed samples—results for the remaining samples are shown in Fig. 2 of the supporting information file. As expected, the higher molecular guar gave the highest viscosity when compared at the same concentration. The inflection points in the log–log plots of viscosity versus guar concentration gave the minimum overlap concentration C^*. This is the lowest guar concentration where neighboring polymer coils in solution start to interact—the "dilute" to "semi-dilute" transition concentration [6].

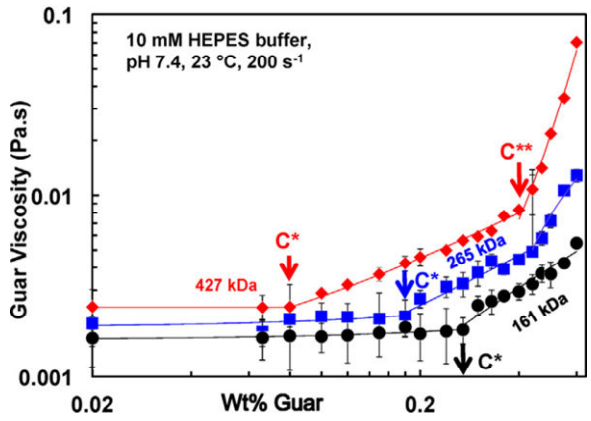

Fig. 2. Viscosities of three guar solutions as functions of the guar concentrations. The error bars depict the standard deviation based on three measurements.

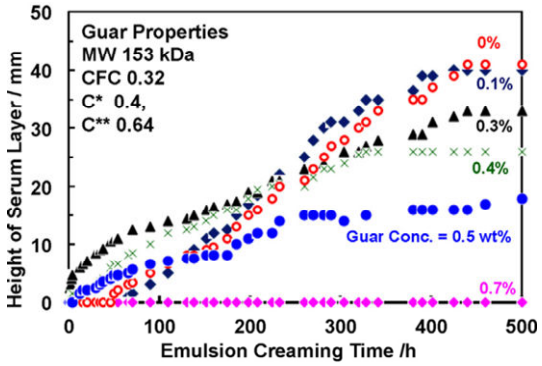

Fig. 3. The height of the boundary between the lower clear serum zone and the more turbid emulsion zone as a function of the creaming time. Each data set corresponds to a different guar concentration. The initial emulsions were 0.2% (v/v) hexadecane emulsions at 23 °C. Increasing guar concentration lowered creaming rates.

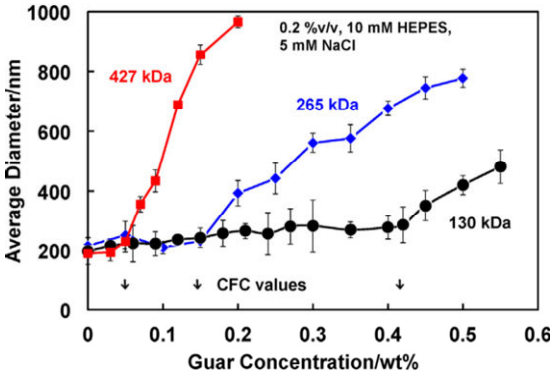

Fig. 4. Examples of emulsion size as functions of polymer concentration. The CFC values correspond to the onset of aggregation as evidenced by the increase in particle diameter. Error bars are the standard deviations based on five repeated measurements.

We show below that C^* is a critical design parameter for ophthalmic emulsions.

Also shown in Fig. 2 is the C^{**} value for the 427 kDa guar. C^{**} is the guar concentration corresponding to the onset of the concentrated polymer solution regime where the chains are fully entwined. Solution concentrations above C^{**} are probably too viscous for applications as eye drops.

Model emulsions consisting of 1.4 wt% hexadecane and 0.1 wt% phosphatidylcholine dispersed in 10 mM HEPES buffer and 5 mM NaCl were prepared by ultrasonic dispersion. Hexadecane was chosen as a pure, well-defined surrogate for the mineral oil used in commercial emulsions. The average emulsion droplet diameter was about 200 nm with a polydispersity of 0.1, as determined by dynamic light scattering. Note that these emulsion drops are sufficiently large to give turbid dispersions and significant creaming rates (see below).

Electrophoresis measurements were used to confirm that guar did not adsorb on the emulsion droplets. Table 1 shows the electrophoretic mobility of the emulsion particles as a function of guar concentration. In all cases the electrophoretic mobilities were negative, indicating that the emulsion surfaces had a net negative surface charge density. Although phosphatidylcholine is zwitterionic and should not give a net surface charge at neutral pH, most lecithin samples contain small quantities of anionic phospholipids that give a net negative charge [7]. Adsorption of a nonionic polymer, such as guar, onto an anionic colloid, shifts the shear plane out from the charged particle surface, dramatically decreasing the magnitude of the electrophoretic mobility. The results in Table 1 were insensitive to guar addition, suggesting no adsorption.

Classical macroscopic creaming measurements were performed by placing emulsions in test tubes and measuring the height of the interface between the clear serum layer at the bottom, and the more turbid layer above. Fig. 3 shows serum height measurements versus time for emulsions with various concentrations of 153 kDa guar ($C^* = 0.32$ wt% and $C^{**} = 0.64$%). The highest guar concentration (0.7%) was above C^{**} and this high viscosity prevented creaming. Guar concentrations between C^* and C^{**} gave intermediate extents of creaming, whereas below C^* the large emulsion drops displayed rapid creaming.

In addition to increasing viscosity, high concentrations of non-adsorbing water–soluble polymers such as guar can induce emulsion droplet aggregation by a mechanism called depletion flocculation [8,9]. This is an excluded volume phenomenon where the system minimizes the amount of water inaccessible to the water–soluble polymer. In previous work we showed that hydroxypropyl guar induces depletion flocculation of liposomes [10]. Fig. 4 shows examples of emulsion diameters as functions of guar concentration. The critical flocculation concentrations (CFC values) corresponded to the guar concentration, which gave a jump in average diameter as measured by dynamic light scattering.

The CFC values for our series of guars are shown in Fig. 5 as a plot of CFC versus the guar molecular weight. The higher the polymer molecular weight, the lower the polymer concentration required to induce emulsion aggregation.

Also shown in Fig. 5 are the corresponding C^* values for the polymers, determined by viscosity measurements such as those in Fig. 2. There is a close correspondence between the C^*, the overlap concentrations, and the CFC values, particularly for the higher molecular weight polymers. We propose that this is a general observation that applies to any water–soluble polymer. The discussion section presents a predictive approach for designing ophthalmic emulsions that exploits C^* as an upper estimate of the allowable concentration of water–soluble polymer.

Table 1
Emulsion droplet electrophoretic mobility values as functions of native guar ($M_w \sim 3$ MDa) concentrations. Measurements were performed in 10 mM HEPES buffer and 5 mM NaCl at pH 7.4.

Guar Concentration (wt%)	0	0.025	0.050	0.075	0.1	0.125	0.15	0.175	0.2
Electrophoretic mobility 10^{-8} $m^2/V/s$	−2.86	−2.98	−2.82	−2.76	−2.81	−2.54	−2.63	−2.36	−2.49

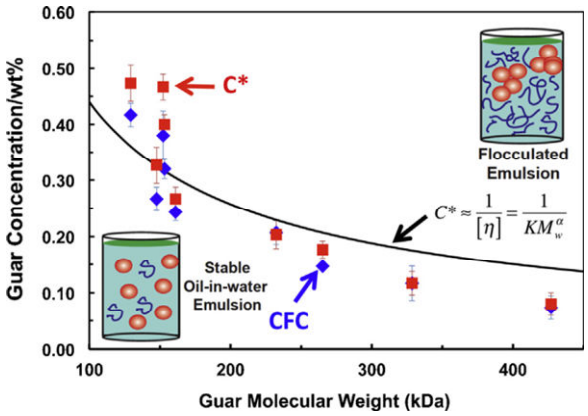

Fig. 5. Experimental critical flocculation concentrations (CFC) and dilute to semi-dilute transition concentrations (C^*) as functions of guar molecular weight. Measurements were made in 10 mM HEPES buffer and 5 mM NaCl. The error bars denote one standard deviation based on triplicate samples.

4. Discussion

The design of ophthalmic emulsions is an exercise in optimizing conflicting objectives. On the eye, the goal is to increase comfort by mechanisms such as increasing tear film lubricity, adsorption of protective layers on damaged cornea surfaces, supplementing the lipid film and possibly delivering drugs. The contributions of water–soluble polymers are to increase viscosity, possibly increasing residence time on the eye, and possibly to form protective layers on damaged surfaces. One might predict that for these functions, viscous, high molecular weight polymers are the most effective.

Emulsion droplets are added to deliver lipids to the surface of the tear film, or possibly to act as a carrier for hydrophobic drugs. For these roles the emulsions droplets must spontaneously deposit onto the desired locations, such as the lipid film, or on the hydrophobic surfaces of damaged corneal cells. Very stable (in the colloidal sense) emulsions will simply drain out of the eye, because stable emulsions tend not to deposit onto surfaces. To summarize, on the eye, viscous polymers and marginally stable emulsions should give the best results.

In the eye drop bottle, the requirements are different. The emulsion droplets are the biggest challenge. If they are too large, or if the aqueous phase viscosity is too low, they will cream while sitting on the shelf. If the water–soluble polymer concentration is too high, the polymer will induce depletion flocculation of the emulsion, which will enhance creaming and coalescence rates. Finally, if the emulsion is too colloidally unstable, aggregation and deposition on the walls of the container will limit shelf life.

The results in Fig. 5 show that to avoid depletion flocculation, the water–soluble polymer concentration/molecular weight combination should be below C^*. The link between C^* and the onset of depletion flocculation has been known for some time [11]. However, the correlation is not perfect; the results in Fig. 5 show that the CFC is systematically lower than the C^* values for low molecular weight guar, but not for the high molecular weight samples. Tuinier showed the opposite trend for skim milk stability in the presence of guar [12]. Although it is relatively easy to measure C^*, for most polymers it can be estimated from information in the literature. Specifically, C^* is approximately the inverse of the intrinsic viscosity of the polymer given by the following equation, where: [η] is the intrinsic viscosity of the polymer; M_w is the polymer molecular weight (usually provided by the supplier); and, K and α are the Mark–Houwink coefficients that are available for most water–soluble polymers.

$$C^* \approx \frac{1}{[\eta]} = \frac{1}{KM_w^\alpha} \quad (1)$$

To illustrate the approach, we used Eq. (1) with published Mark–Houwink coefficients for guar ($K = 3.04 \times 10^{-4}$ dL/g, $\alpha = 0.747$) [13]. The solid line in Fig. 5 was plotted using these values and is in reasonable agreement with the experimental CFC values. The C^* values estimated from Eq. (1) overestimated the experimental C^* values for high molecular guar, whereas agreement was better for lower molecular weights. Some of the older literature suggests that $C^* = 4/[\eta]$ [14] which gives poorer predictions of our flocculation data. In summary, we view C^* as an estimate of the maximum polymer concentration tolerated by an emulsion—a tool for guiding experimental design. More accurate determination of flocculation limits requires experimental determination. We suspect our approach has general utility. However, this remains to be verified with other water–soluble polymers.

Finally, this work has focused on factors influencing the physical stability of eye drop emulsions. Efficacy, safety and sterility are critical issues not addressed in this study.

5. Conclusions

(1) Water–soluble polymers can stabilize ophthalmic emulsions by lowering creaming rates. However, the same polymers can induce emulsion droplet aggregation if the water–soluble polymer concentrations are too high.
(2) The key formulation variables are the molecular weight and the concentration of the water–soluble polymer. These two properties are captured in a single parameter, C^*, the polymer concentration corresponding to the semi-dilute to dilute transition. C^* is determined by viscosity measurements as a function of polymer concentration, or can be approximately estimated from published Mark–Houwink parameters.
(3) Water–soluble polymer concentrations just below C^* give the lowest creaming rates, whereas above C^* the emulsions aggregate by a mechanism called depletion flocculation.

Acknowledgements

We thank the National Sciences and Engineering Research Council of Canada (NSERC) and Alcon Laboratories (Grant no. CRDPJ 418217-11) for funding this project. Some measurements were performed in the McMaster Biointerfaces Institute funded by Canadian Foundation for Innovation. R.P. holds the Canada Research Chair in Interfacial Technologies.

Appendix A. Supplementary data

Supplementary data associated with this article can be found, in the online version, at http://dx.doi.org/10.1016/j.colsurfb.2014.06.039.

References

[1] S. Ding, Recent developments in ophthalmic drug delivery, Pharm. Sci. Technol. Today 1 (1998) 328–335.
[2] M.M. Robins, Emulsions—creaming phenomena, Curr. Opin. Colloid Interface Sci. 5 (2000) 265–272.
[3] E. Dickinson, Structure, stability and rheology of flocculated emulsions, Curr. Opin. Colloid Interface Sci. 3 (1998) 633–638.
[4] M.T. Christensen, S. Cohen, J. Rinehart, F. Akers, B. Pemberton, M. Bloomenstein, M. Lesher, D. Kaplan, D. Meadows, P. Meuse, C. Hearn, J.M. Stein, Clinical evaluation of an Hp-guar gellable lubricant eye drop for the relief of dryness of the eye, Curr. Eye Res. 28 (2004) 55–62.

[5] Y. Cheng, K.M. Brown, R.K. Prud'homme, Characterization and intermolecular interactions of hydroxypropyl guar solutions, Biomacromolecules 3 (2002) 456–461.
[6] Q. Ying, B. Chu, Overlap concentration of macromolecules in solution, Macromolecules 20 (1987) 362–366.
[7] C. Washington, A. Chawla, N. Christy, S.S. Davis, The electrokinetic properties of phospholipid-stabilized fat emulsions, Int. J. Pharm. 54 (1989) 191–197.
[8] D.J. McClements, Comments on viscosity enhancement and depletion flocculation by polysaccharides, Food Hydrocolloids 14 (2000) 173–177.
[9] J.L. Burns, Y.-d. Yan, G.J. Jameson, S. Biggs, The effect of molecular weight of nonadsorbing polymer on the structure of depletion-induced flocs, J. Colloid Interface Sci. 247 (2002) 24–32.
[10] A. Khanal, Y. Cui, L. Zhang, R. Pelton, Y. Ren, H. Ketelson, J. Davis, Cationic liposome colloidal stability in the presence of guar derivatives suggests depletion interactions may be operative in artificial tears, Biomacromolecules 11 (2010) 2460–2464.
[11] D. Meyuhas, S. Nir, D. Lichtenberg, Aggregation of phospholipid vesicles by water–soluble polymers, Biophys. J. 71 (1996) 2602–2612.
[12] R.E. Tuinier, E.t. Grotenhuis, C.G. de Kruif, The effect of depolymerised guar gum on the stability of skim milk, Food Hydrocolloids 14 (2000) 1–7.
[13] Y. Cheng, K.M. Brown, R.K. Prud'homme, Preparation and characterization of molecular weight fractions of guar galactomannans using acid and enzymatic hydrolysis, Int. J. Biol. Macromol. 31 (2002) 29–35.
[14] E.R. Morris, A.N. Cutler, S.B. Ross-Murphy, D.A. Rees, J. Price, Concentration and shear rate dependence of viscosity in random coil polysaccharide solutions, Carbohydr. Polym. 1 (1981) 5–21.

Appendix 1: Supporting Information for Chapter 2

SI Table 1: Variation of viscosity as a function of acid hydrolysis time for guar samples. Viscosity measurements were made at 25 °C using a shear rate of 200s $^{-1}$.

Hydrolysis Time (Hours)	Viscosity (Pa.s)			Average	Std. Dev
1	0.00300	0.00282	0.00289	0.00290	9.26E-05
2	0.00245	0.00208	0.002275	0.00227	1.87E-04
5	0.00214	0.00206	0.00224	0.00215	9.02E-05
7	0.00193	0.00206	0.002013	0.00200	6.54E-05
8	0.00183	0.00180	0.00189	0.00184	4.58E-05
10	0.00182	0.00157	0.00159	0.00166	1.39E-04
12	0.00148	0.00173	0.00165	0.00162	1.26E-04
16	0.00157	0.00162	0.001718	0.00164	7.54E-05
20	0.00158	0.00154	0.001703	0.00161	8.32E-05
24	0.00154	0.00163	0.001571	0.00158	4.56E-05

SI Table 2: The molecular weight (GPC) of hydrolyzed guar samples as functions of the hydrolysis times.

Hydrolysis Time (Hours)	MW (kDa)			Average	Std. Dev
1	426963	_	_	426963	0
2	328526	_	_	328526	0
3	289086	257290	263194	269857	16913
5	260016	281211	254324	265184	14169
6	206476	241112	212512	220033	18502
7	220046	243863	233066	232325	11926
8	134952	189092	189765	171270	31454
10	184012	145225	154063	161100	20328
12	142103	174650	126024	147592	24773
16	159363	147212	153040	153205	6077
20	153040	147185	156525	152250	4720
24	123049	133026	131941	129339	5474

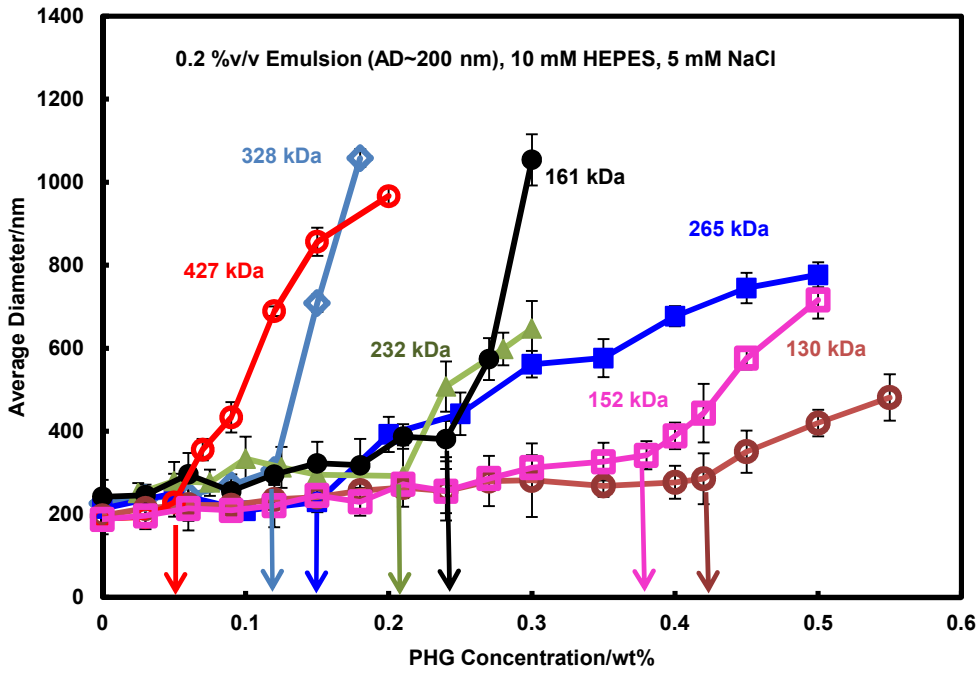

SI Figure 1: The influence of PHG concentration on the average emulsion diameter. CFC has been defined as the slope change in the curves.

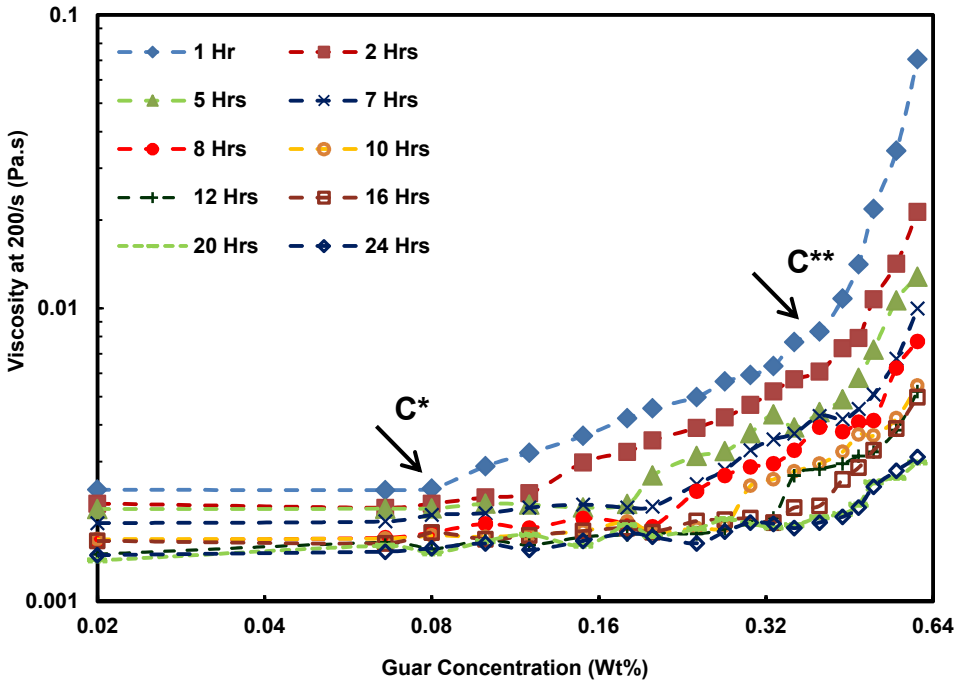

SI Figure 2: Defining critical viscosity concentrations (C* and C) for guar samples hydrolysed for different time intervals under acidic environment from curves of viscosity versus concentration. Results are shown as a double logarithmic plot.**

SI Table 3: Defining C* and CFC for guar samples hydrolysed for different hours to express a range of different molecular weights

Hydrolysis Time (Hours)	MW (kDa)	C* (wt%)			Average	Std. Dev.	CFC (wt%)			Average	Std. Dev.
1	427	0.08	0.06	0.1	0.08	0.02	0.05	0.09	0.08	0.07	0.02
2	329	0.1	0.14	0.11	0.12	0.02	0.09	0.11	0.15	0.12	0.03
5	265	0.16	0.18	0.19	0.18	0.02	0.14	0.15	0.15	0.15	0.01
7	232	0.18	0.23	0.2	0.20	0.03	0.19	0.23	0.2	0.21	0.02
8	171	0.2	0.2	0.21	0.20	0.01	0.19	0.2	0.2	0.20	0.01
10	161	0.25	0.29	0.26	0.27	0.02	0.23	0.26	0.24	0.24	0.02
12	148	0.29	0.34	0.35	0.33	0.03	0.25	0.26	0.29	0.27	0.02
16	153	0.42	0.39	0.39	0.40	0.02	0.33	0.33	0.3	0.32	0.02
20	152	0.48	0.44	0.48	0.47	0.02	0.43	0.35	0.36	0.38	0.04
24	130	0.51	0.46	0.45	0.47	0.03	0.44	0.4	0.41	0.42	0.02

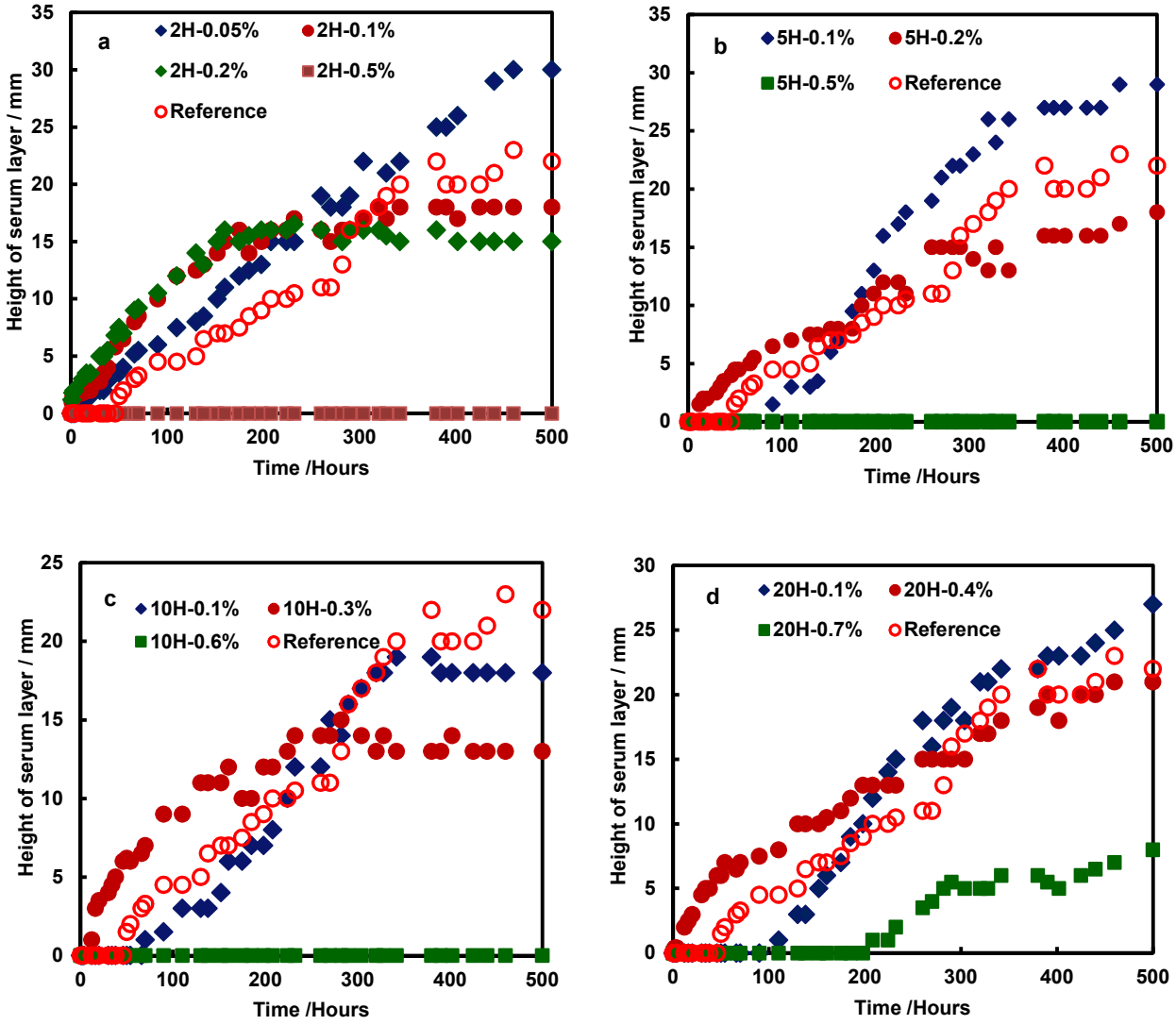

SI Figure 3: Height of visible boundary between creaming and serum layer during creaming of 0.2% (v/v) hexadecane emulsions at 25°C, showing the effect of variation in guar concentration hydrolysed for different hours(a. 2 hours, b. 5 hours, c. 10 hours and d. 20 hours) on creaming.

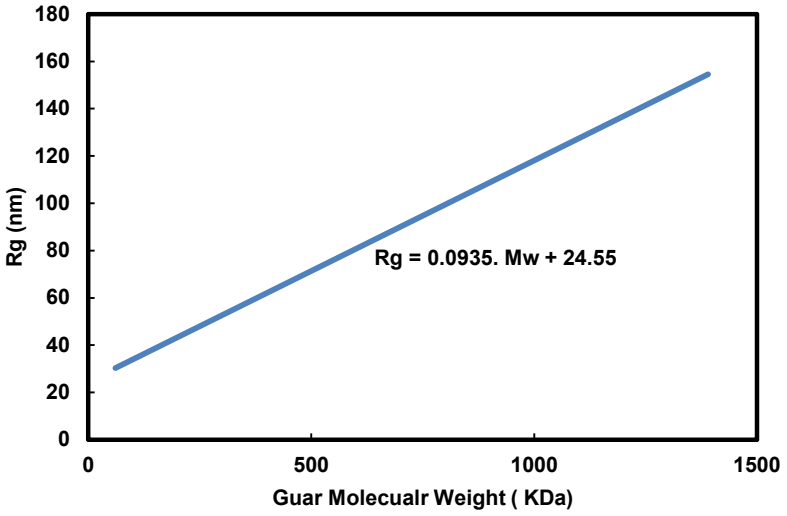

SI Figure 4: Radius of gyration of hydrolysed guar as a function of the molecular weight (From: Tuinier, R., ten Grotenhuis, E., and de Kruif, C. G. (2000) The effect of depolymerised guar gum on the stability of skim milk, *Food Hydrocolloids 14*, 1-7).

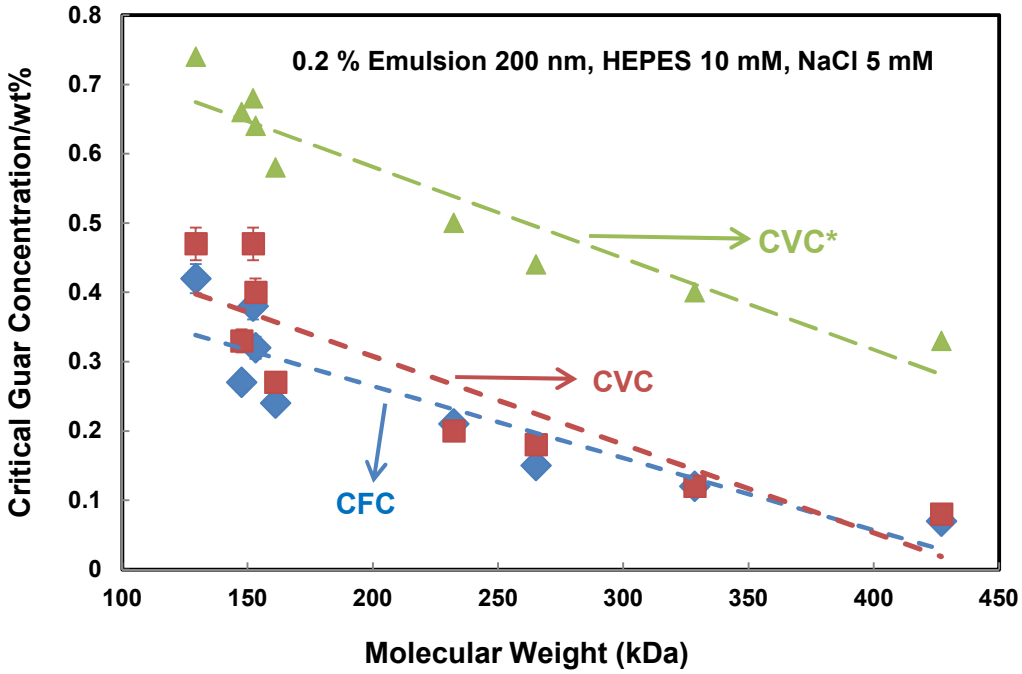

SI Figure 5: Dependency of CVC, CFC and CVC* on molecular weight of native guar.

Chapter 3. Emulsions at solid interfaces - A QCM-D study

In this Chapter, all QCM-D experiments were done by myself. My summer student, Wing Yan Lam helped with making emulsions for the inverted QCM-D experiments. Dr. Pelton revised the versions I wrote and edited them to the final version.

Emulsions at solid interfaces - A QCM-D study

Roozbeh Mafi and Robert Pelton*
Department of Chemical Engineering, McMaster University, 1280 Main Street West, Hamilton, Ontario, Canada L8S 4L8

3.1 Abstract

The interactions of oil-in-water emulsions with solid surfaces were determined with Quartz Crystal Microbalance (QCM-D) measurements. Conventional measurements, in flow, gave adsorption information whereas quiescent measurements with inverted QCM-D sensors probed the initial stages of consolidated (cream) layer formation next to the surface. A series of polydisperse emulsions with various oil content and stabilities have been prepared using hexadecane as the oil phase and L-α- phosphatidylcholine as the surfactant. Observation of frequency and dissipation variation suggests that non-creaming emulsions are inducing a single step change, which occurs during the flow and is due to the adsorption of emulsion droplets onto the surface. On the other hand, unstable emulsions are going through a two-step variation in frequency and dissipation. The second change occurs upon stopping the flow. Through viscoelastic modeling, the changes in viscoelastic properties of the close packed layer on top of the creaming layer are detectable.

Keywords
Emulsion; Creaming; Quartz crystal microbalance; Viscoelastic; Phospholipid; Adsorption

3.2 Introduction

Emulsions are droplets of one fluid dispersed in an immiscible fluid, stabilized by a surfactant. Studying the properties and stability of oil-in-water emulsions and defining the creaming process parameters is crucial for process control, improving the formulation of products containing emulsions and defining the shelf-life of the product. Metastable emulsion droplets tend to rise to the top of a container and cream out over time owing to the difference in the densities of droplets and the medium. Method of emulsion preparation, properties of the surfactant and oil defines the stability of oil in water emulsions. The size of emulsion droplets undergoes a number of time-dependent instabilities through flocculation, aggregation, Ostwald ripening and coalescence(*1*), which are all involving the spatial rearrangement of droplets. The rate of creaming for droplets with different diameters varies and is higher for larger particles.

Upwards movement of emulsion droplets, results in formation of three layers: serum layer on the bottom, creaming zone in the middle and a close packed layer on top(*2*). The emulsion eventually separates into a bottom serum phase, which is generally visible and a top oil phase. The rise of lower aqueous serum layer initiates with a so-called delay phase without any visible movement of the bottom layer. At the end of the delay period, clear serum layer starts the upwards movement, which is usually at a constant rate until a dense cream layer is reached on top(*3*).

There are various techniques to observe and evaluate the creaming process. The easiest and most conventional method is visual observation of the change in the thickness of serum layer of sample in which a clear phase separation occurs during the creaming process. In spite of its popularity, visual observation is a time consuming method and not very accurate for polydisperse emulsions. The diffuse boundary between serum phase and creaming layer is not easily detectable(*4*). Other techniques have been proposed to improve the accuracy or to reduce the experiment time. A non-intrusive method to monitor the creaming of emulsions is by measuring the velocity of ultrasound passing through different phases of the emulsion(*5*). Turbiscan, a method developed by Mengual *et al*.(*6*), is an optical technique has been employed by many researchers to evaluate the emulsions stability during the creaming process(*7*). Conductometric method is another technique of monitoring the creaming process with time, where the conductivity of top region was continuously measured initially. Due to the confusion of creaming with compaction process, the use of a pair of suspending electrodes in areas with different heights of emulsion has been substituted. The pair of electrodes monitors the boundary of creaming layer while it passes over the controlled regions through conductivity measurement(*8*). A video imaging device coupled with image analysis software is another technique to monitor the creaming process in a test tube as has been reported previously(*9*).

A simple and fast method is helpful for a better understanding of physical processes and different stages involved in creaming. Observation in short test vessel reduces the time of experiment. However, this is not possible to monitor the changes through the visual monitoring test. Quartz crystal microbalance-dissipation (QCM-D) experiment provides the opportunity to track the creaming process within the total height of about 65 μm. The height is about three orders of magnitude less than the one for conventional creaming test vessels. Lowering the tracking height significantly reduces the experiment time in comparison with visual observation techniques.

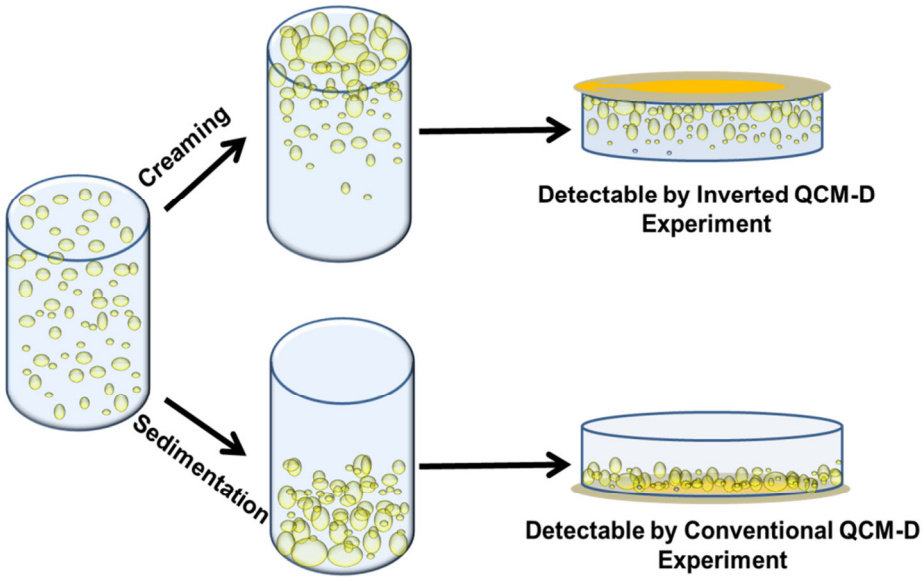

Figure 1: Schematic representation of creaming and sedimentation processes and appropriate method of QCM-D to detect the instability. Surface of the sensor is facing toward the droplets in both cases.

QCM-D is sensitive to the changes in resonant frequency and measures the adsorbed amount on the surface of the chip and the energy loss, which shows the viscoelastic properties of the adsorbed film. QCM-D also shows the variation in viscosity and density of the medium over the chip by a shift in frequency.
Viscosity varies with the change in the oil volume fraction of emulsions. The dependency of viscosity to the emulsion concentration has been shown before by Bullard *et al.*(*10*) and various equations has been developed to explain this dependency(*11*). QCM-D has been already employed to study the adsorption and desorption of concentrated phospholipid liposome solutions and phospholipid stabilized oil-in-water emulsions by Stalgren *et al.* (*12*). They found an initial rapid adsorption for the 20% oil-in-water emulsion sample. The big change was then followed by an increase in resonance frequency and a decrease in dissipation. They interpreted this as partial desorption of emulsion and droplet spreading on the gold sensor surface.
Inverted QCM-D module experiment, as shown in Figure 1 allows evaluation of the variation in the top layer, which is the close packed zone. Especially for dilute emulsions, variation in the top layer during the emulsion creaming is more significant compared to the bottom phase. The oil volume fraction on the top layer, which is also called consolidating zone increases with time due to upwards movement of droplets. The formed layer behaves as an elastic fluid or an elastic solid. The viscoelastic property depends on the size of droplets, volume fraction and their ability to resist coalescence(*13*). Deformability of droplets in polydisperse emulsions allows dense packing at concentrations much higher than the critical volume fraction (ϕ^*=0.64) of an equivalent monodisperse hard sphere suspension(*14*). Emulsions are viscose fluids at low

concentrations. They behave more like elastic solids with increasing the concentration over the critical volume fraction (*15*).
In this work, we evaluate the stability of emulsion systems by inverting the modules of QCM-D system. The viscoelastic behavior of the close packed layer, which forms on top of the creaming zone, will be defined. Variation in consolidating zone can be studied more accurately comparing to conventional visual observation experiments.

3.3 Experimental

Preparation of Emulsions- In a typical experiment, 10 mg of a 25mg/mL solution of L-α- phosphatidylcholine in chloroform was poured into a round-bottom flask. Removal of the solvent was done using a rotary evaporator at room temperature and exposure to the stream of nitrogen gas. This resulted in a dried film. 140 mg of hexadecane was then added to the flask followed by a 10 mL solution, which contained 5ppm NaN_3, 10 mM HEPES buffer and 5 mM NaCl. The mixture was ultrasonicated (90% amplitude and output powersetting of 60) for half an hour using a Misonix Sonicator (S-4000 Ultrasonic Processors, USA, 20 kHz) with the ultrasonic probe, which was immersed directly into the emulsion. To produce unstable emulsions with different average diameters, mixture was ultrasonicated for 3 and 15 minutes respectively.
Dynamic Light Scattering- BI-APD 8590 digital correlator (Brookhaven, NY, USA) apparatus at the fixed scattering angle of 90° and 35 mW 632.8 nm laser as the light source was employed for Dynamic light scattering (DLS) measurements at 25 °C. For the calculation of emulsion droplet diameter, CONTIN program, a cumulative intensity distribution method has been used. Average of 5 measurements is reported.
QCM-D Studies- Polystyrene QCM-D sensors were immersed in a 1% solution of Deconex 11 in TYPE 1water for 30 min at 30°C followed by thorough rinse of milliQ water and 99% ethanol and dried with nitrogen gas. UV/ozone treatment has been also done for gold sensors.
Measurements were performed with an E1 QCM-D (Q-Sense AB, Gothenburg, Sweden) and monitored using Qsoft401 software version 2.5.2. All measurements were repeated two times. Processed data from the fifth overtone using Qtools software version 3.0.7 are shown and Δf values have been normalized by the fifth overtone.
Quartz crystal sensor mounted to a removable flow module which is placed in the E1 temperature control chamber. The whole chamber platform was inverted. Measurements then initiated in air by obtaining the resonance frequencies of the sensor crystal. A solution, which contains 10 mM HEPES buffer and 5 mM NaCl was injected at a constant flow rate of 150 µL/min using an IPC-N935 tubing pump with planetary drive from Ismatec to produce a base line. It followed then by injection of emulsion to reach a plateau, keeping the flow rate constant at 150 µL/min. The flow stopped then and acquisition continued for several hours to observe further changes which indicate the creaming process. Afterwards, the sensor was rinsed with the buffer at 150 µL/min.
SEM photographs of nitrogen dried gold-coated QCM-D sensors were obtained on a JEOL JSM-7000F scanning electron microscope with 5kV and 20kV accelerating voltage. Optical microscopy was performed using the window QCM-D module mounted

to a stereo microscope type NIKON AZ 100 M equipped with an image analysis software. Intense illumination was provided by fibre-optic light source.
To observe the spreading behavior of oil droplets on different QCM-D surfaces in water, the oil droplet placed on the surface of PS and gold QCM-D chips suspended horizontally below the surface of water. The spreading behavior of droplets on various surfaces was observed using a Krüss contact angle measuring instrument and Drop Shape Analysis (DSA) 1.80.0.2 software.

3.4 Results

To evaluate the ability of inverted QCM-D to detect the creaming process and stability of emulsions, samples of unstable emulsions with the properties listed in Table 1 has been prepared. In addition to the samples listed in Table 1, SYSTANE BALANCE as an example of non-creaming emulsion was tested. The average emulsion droplet diameter was measured by dynamic light scattering. In this work, we only evaluated the behavior of dilute emulsions, i.e. below 2 V/V%.

Table 1: Characterization of the emulsion samples. Emulsions contain hexadecane as the oil phase and L-α- phosphatidylcholine as the surfactant and were ultrasonicated for half an hour. Each formulation was reproduced and the properties listed below are the average of three measurements.

Oil Fraction (%V/V)	Sonication Time (min.)	Average Diameter (nm)	PDI	Viscosity (mPa.s)
0.3	30	190	0.13	1.8±0.4
0.5	30	185	0.09	2±0.3
1	30	180	0.10	2.4±0.5
2	15	205	0.15	2.5±0.4
2	3	383	0.22	1.7±0.8

Droplet Spreading. Emulsion droplets adsorb and spread on both hydrophilic (silicon dioxide) and hydrophobic polystyrene surfaces. Visual observation of hexadecane, the oil phase of the emulsion system, spreading on the sample hydrophobic surface, PS sensor, in water revealed that the test droplet immediately wets the entire PS surface. Compared to oil droplets, emulsion droplets may have limited spreading due to the presence of surfactants. Rafai *et al.* studied the influence of various surfactants that can either improve the wetting or lower the extent of spreading (*16*).
Upwards movement of metastable emulsion droplets can be detected by a window equipped QCM-D module mounted to an optical microscope. Adsorption and spreading were detected on the surface of the glass window of the module. Depending on their position, they form various shapes. Non-adsorbed droplets can be determined by their circular shape and dark edge color, while adsorbed and spread ones have an irregular shape with brighter edges(*17*). Spread coalesced droplets have larger diameter and the surrounding ring has almost faded (Figure 2).

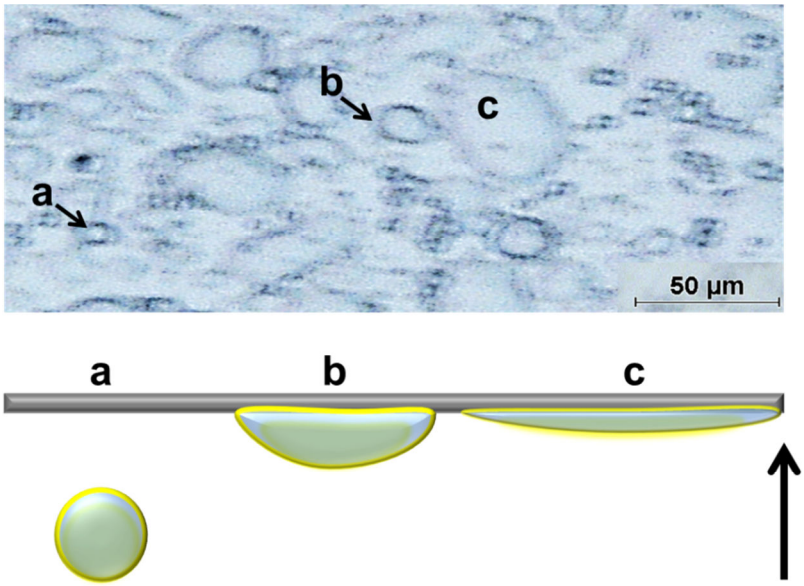

Figure 2: Optical light microscopic image of a sample emulsion showing various shapes of droplets during their upwards movement and spreading over clean glass (up) and side view shapes of the droplet: a) free droplet; b) adsorbed and partially spread droplet; c) fully spread droplet.

Scanning electron microscopy (SEM) was used to characterize the pattern of adsorbed droplets on QCM-D sensors. On SiO_2 substrate, residual droplets after rinsing have not covered the whole surface area (Figure 3-a) while the entire surface of Poly Styrene substrate is uniformly coated with fully spread and coalesced droplets (Figure 3-b).

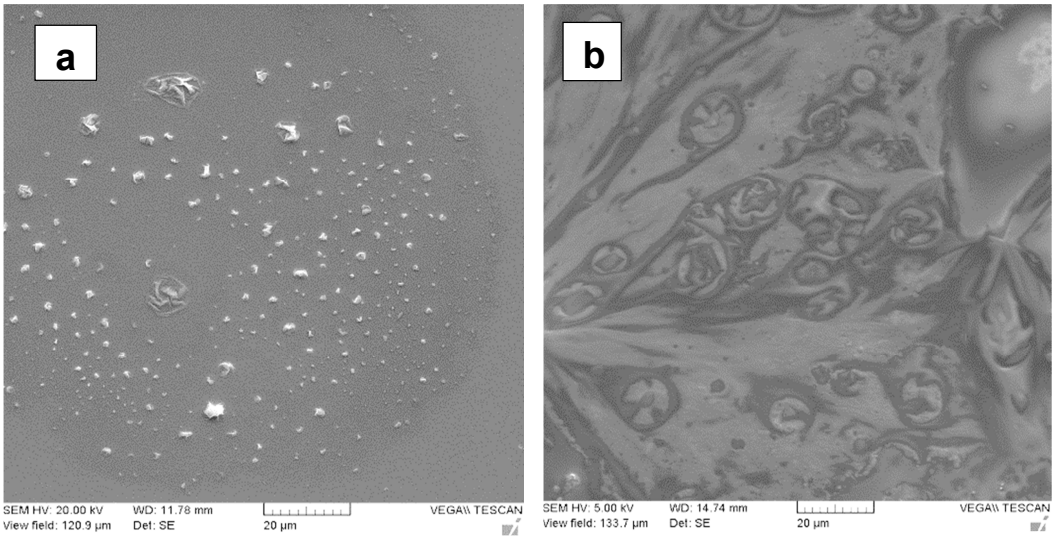

Figure 3: Scanning electron microscopy of the spreading pattern of emulsion droplets on a) SiO_2 and b) Polystyrene surface of QCM sensors

Emulsions at Solid Surfaces. Normal and inverted QCM-D experiments were employed to evaluate the adsorption of 2%(V/V) emulsion on gold and polystyrene sensors and typical raw data of measured changes in frequency, Δf_5, is displayed as a function of time in Figure 4.

In normal orientation, immediately after introducing the emulsion, the resonance frequency drops significantly during the first few minutes. . Emulsion droplets adsorb on gold and polystyrene surfaces. However, with running the flow for more than 30 hours, no further deposition onto the surface occurred. This is shown in SI Figure 8 for a 2% V/V emulsion with the average diameter of 205 nm over the PS sensor. On both normal QCM-D frequency curves for gold and PS sensors, no further decrease in frequency has been observed after stopping the flow of emulsion over the sensor. This indicates the inability of normal QCM-D measurements to track the changes occur in unstable emulsions during the creaming of dilute emulsions.

Figure 4 shows a bigger drop of frequency on PS sensor compared to gold sensor. The emulsion droplets spread more on the PS sensor. There is a limit that QCM-D can detect the adsorbed mass. The variations in water and at 5 MHz is only detectible within about 250 nm away the resonator surface(*18*). The penetration depth of shear wave is lower for higher frequencies. For the fifth overtone is as low as about 100 nm. QCM can only sense a part of the adsorbed droplet on the gold sensor, which is within the length of 100 nm. Compared to the droplet on the hydrophilic surface, more volume of adsorbed droplet on PS is within the penetration depth and can be sensed by QCM. Similar interpretation has been used by Lin et al. to define the contact angle and surface tension by QCM-D(*19*).

In the inverted experiment on PS sensor, similar initial drop of about 60 Hz in frequency was observed during the flow of emulsion. This reveals that the adsorption during the flow is independent of the direction of QCM-D module. After a delay period, a gradual, almost linear decrease in frequency occurs for the inverted QCM-D curve of PS sensor. This second drop can be interpreted as the creaming process in the unstable emulsion. While creaming occurs, a delay period may exist prior to the creaming process(*4*). However, the delay, which is observed prior to the second change in frequency might have some other reasons in our proposed technique. During the creaming, the volume fraction of emulsion droplets next to the sensor increases. This leads to both a decrease in the density and an increase in viscosity. However, below the volume fraction of 20%, the increase in viscosity is not significant(*20*). This also can be seen in the curve of viscosity dependency to volume fraction based on Krieger and Dougherty equation (KD equation), which is shown in the appendix. Therefore, viscosity effect cancels the effect of density on frequency. The plot of the square root of density times viscosity (from KD equation) as functions of volume fraction (see supplementary information) shows an increasing trend in viscosity as the volume fraction of emulsion droplets raises. Frequency is a function of square root of density times viscosity. The plot can explain the drop in frequency during the creaming.

After the delay phase, the volume fraction raised enough to cause a change in the viscosity of the adsorbed layer, which is detectable by QCM-D. The second frequency decrease proceeds for several hours with a slower rate than the initial adsorption. A second plateau is achieved by the end of this process. The second plateau can be both due

to the upwards movement of all droplets or due to the inability of QCM-D to detect further changes.

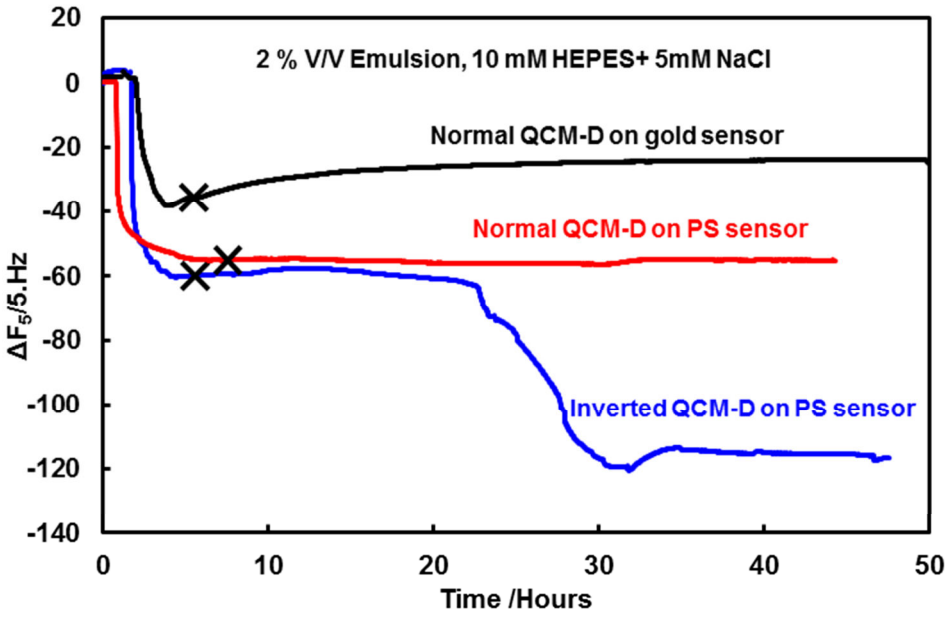

Figure 4: QCM-D measurements showing the changes in frequency during adsorption of emulsion droplets (2 % V/V) for 1) normal QCM-D measurement on gold sensor, 2) normal QCM-D measurement on PS sensor and 3) inverted QCM-D measurement on PS sensor. X on each data line shows the stop flow time.

Figure 5 shows the interaction of 2% milk and PS substrate. Inverted and normal module QCM-D was employed to evaluate the changes, which were occurred during the flow of buffer and milk, as well as the variations after stopping the flow. The buffer was the serum of milk, which was creamed off by centrifuging milk at 33,500 for 30 minutes. The continuous reduction of frequency during the flow of buffer to produce a stable base line was interpreted as the adsorption of casein. Therefore, casein formed a layer that inhibited the adsorption of emulsion droplets to PS surface during the flow of milk. However, presence of emulsion in the bulk lowered the density that caused an increase in the frequency in both normal and inverted QCM-D module experiments.
In normal method, Frequency and dissipation were almost plateaued after the initial increase during the flow. Upon stopping the flow, further increase in both frequency and dissipation was observed in the inverted method. The upwards movement of droplets lowered the density. This decrease has been detected by inverted QCM-D, while the normal method was almost insensitive to the changes occurred during the flow stoppage.

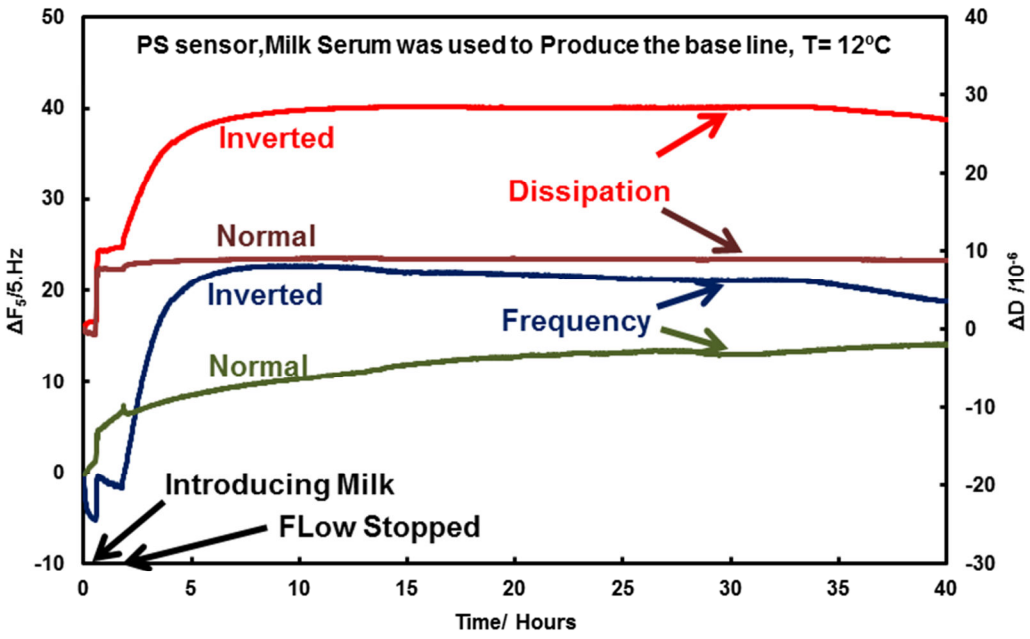

Figure 5: Evaluating the interaction of 2% milk and PS sensor through normal and inverted QCM-D technique. Buffer was the milk serum, which was produced by centrifuging the 2% milk at 35,000 and for half an hour.

During the creaming of a metastable 0.3 % (V/V) emulsion using the inverted QCM-D in Figure 6, dissipation is increasing in a similar trend but not identical to the *f*-shifts. 1×10^{-6} shift in dissipation corresponds to 10 nW power dissipation. In this dilute system addition of emulsion droplets to the initially adsorbed layer caused a continuous change in frequency. The thickness of final film forms with all the droplets is about 195 nm, which is within the penetration depth of shear wave and is detectable by QCM-D.

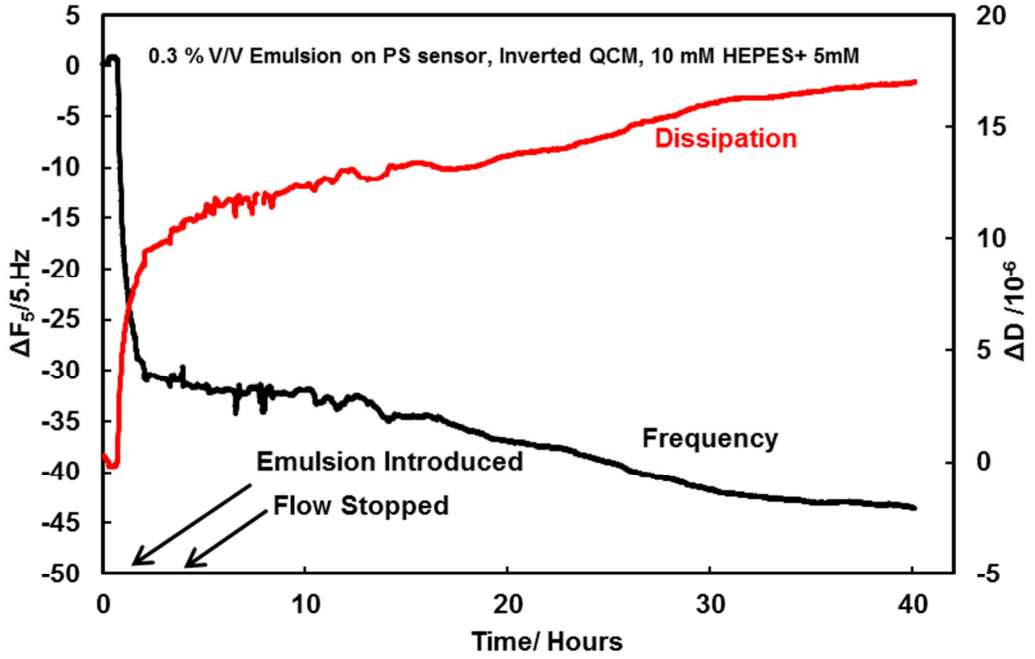

Figure 6: Observation of the effect of upwards movement of droplets after stopping the flow in a typical inverted QCM-D module measurement.

Stability. The inverted QCM-D is also able to define the stability of emulsion systems. Figure 7 compares three different systems. No creaming has been detected for the non-creaming emulsion, SYSTANE BALANCE lubricant eye drop. To produce unstable emulsions with the average diameter (AVD) of 205 nm and 383 nm, same composition of oil, surfactant and buffer were ultrasonicated for 3 and 15 minutes respectively. The larger droplets move to the interface more quickly, giving a volume fraction that can cause significant change in viscosity. The concentrated layer undergoes coalescence in a shorter time.

While the unstable emulsion with AVD of 205 nm creamed after a delay period of 23 hours, frequency change due to creaming occurred almost immediately upon stopping the flow for the one with AVD of 383 nm.

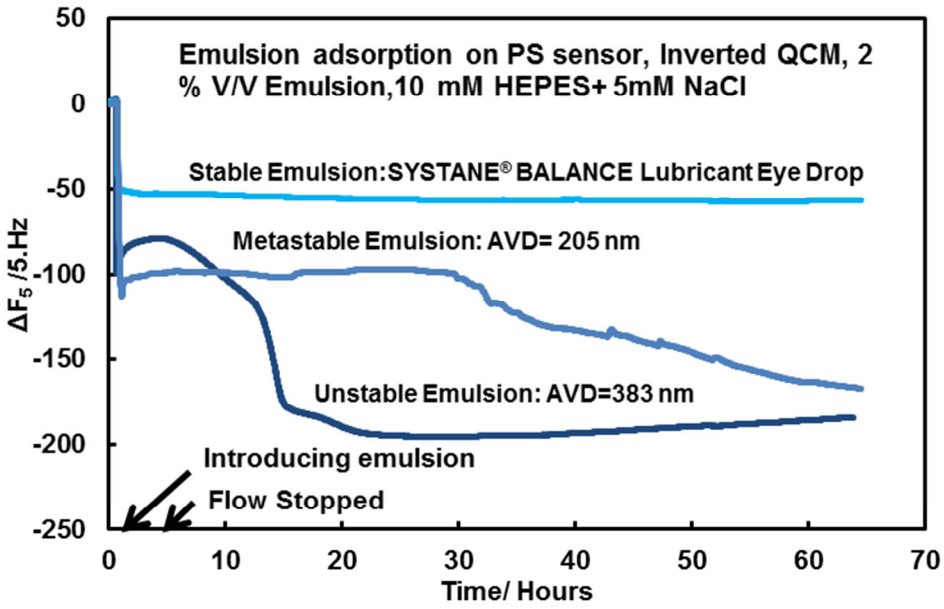

Figure 7: Ability of the inverted QCM-D to differentiate between non-creaming, metastable and unstable emulsions

Plotting the change in dissipation as a function of change in frequency (Δf–ΔD plot) gives an insight into the properties of the layer which extends further away from the surface(*21, 22*). Figure 8 shows Δf–ΔD plots of same QCM-D data displayed for non-creaming and unstable (AVD=383 nm) emulsions. The initial adsorption prior to stopping the flow, leads to an increase in dissipation with a frequency decline for both systems. According to the dissipation and frequency values, the layer formed at the end of this phase (at ΔD~ 25×10^{-6}) has the same structure with similar properties.
During the creaming of unstable emulsion, additional droplets including the coalesced droplets in the bulk, approach the previously formed layer. Extension of the adsorbed layer and formation of larger droplets next to the sensor leads to the formation of a softer layer.

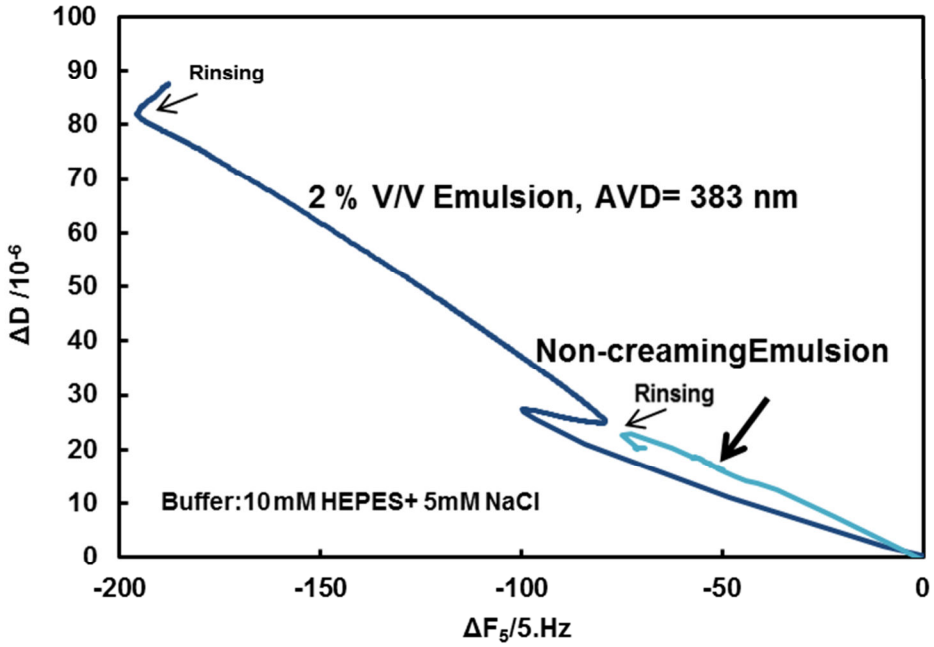

Figure 8: Comparing the properties of the formed layer on PS sensor for non-creaming and unstable emulsions using Δf–ΔD plot. The non-creaming Emulsion refers to SYSTANE® BALANCE Lubricant Eye Drop.

Growth of Droplet Size. Light microscopic images were taken from the top of a QCM-D window module for an emulsion sample with the oil content of 1 % V/V within a period of 60 hours presented in Figure 9 shows a gradual increase of droplet size during the creaming process as they coalesce. Images were taken after letting the emulsion stay in the module for 15 hours.

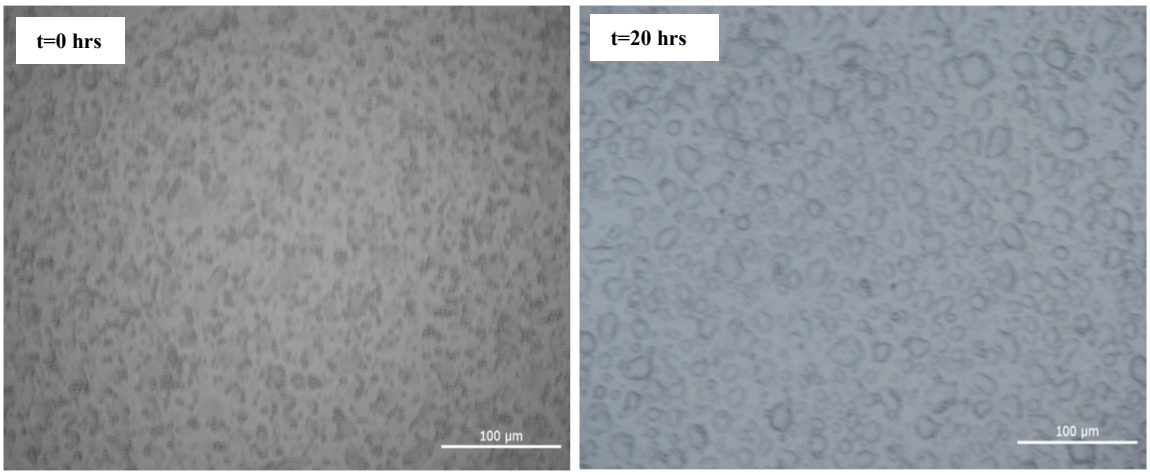

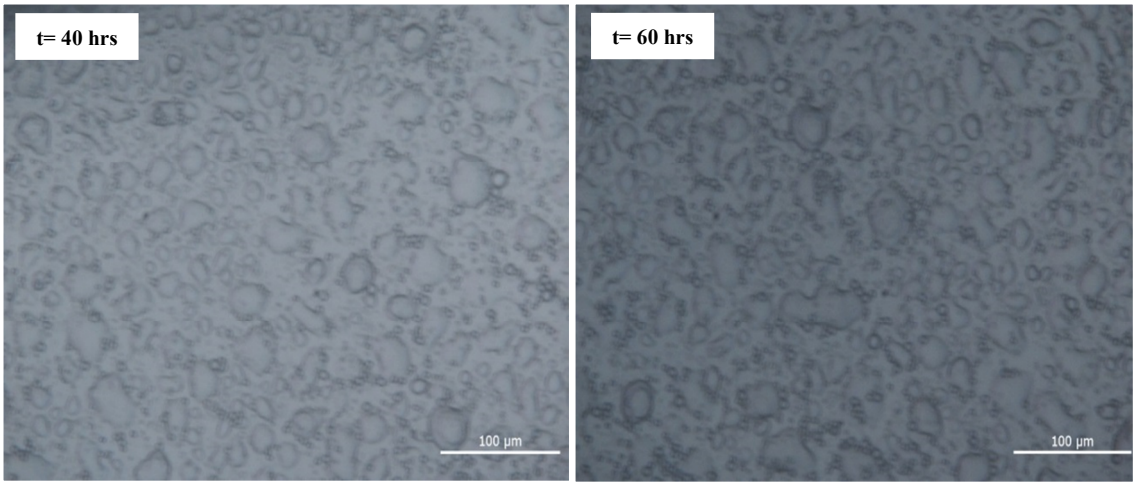

Figure 9: Light microscopic images of emulsion droplets (oil content 1%V/V) at t=0, 20, 40 and 60 hours (300 times original magnification) at room temperature.

Viscoelastic Modeling. Emulsions behave as elastic solids when the emulsion droplet concentration exceeds the critical volume fraction (*23-25*). The close packed layer on top of the creaming zone can be also considered as a highly concentrated emulsion(*20, 26*). To evaluate the elastic behavior of formed layer next to the sensor, we used the viscoelastic modeling on Q-Tools software for a closed packed layer and a Newtonian bulk over the film. The schematic depiction of different layers and the assumed value for modeling for each layer is shown in Figure 10.

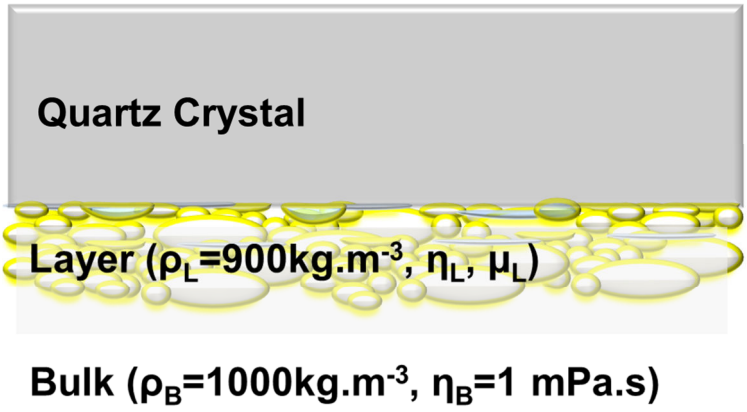

Figure 10: Schematic depiction of QCM sensor covered with a close packed layer of emulsion droplet and the bulk fluid over the layer.

Viscoelastic modeling on Q-Tools is possible when the bulk over the film is Newtonian and the adsorbed layer is homogeneous. The formed layer on PS sensor is assumed to be homogeneous. The adsorbed layer is coupled perfectly and is under no slip condition.

However, some of the droplets adjacent to the bulk are held within the adsorbed layer because of the difference in density of emulsion droplets compared to water. Resuming the flow might remove some of them. The removal of droplets due to the flow can be detected by QCM-D if only it is within the penetration depth of shear waves. Assuming that the bulk under the formed layer is a Newtonian liquid and the layer formed next to the sensor behaves as a solid layer, we can use Voigt-based extended viscoelastic model in Q-tools (*27, 28*). Q-tools 3.0.12 software was used for viscoelastic modeling. Third, fifth and seventh overtones were selected for modeling because frequency dependant behavior has been observed. Assumptions for some properties of the layers next to the QCM-D sensor are required. Fixed parameters used for the model were the bulk density (1000 $kg.m^{-3}$) and bulk viscosity (0.001 Pa.s). The density of the layer was also assumed to be constant (900$kg.m^{-3}$, which is the average density of water and oil). Assuming the formation of a layer of close packed droplets next to the sensor surface, viscosity, shear modulus and thickness of the layer were selected as the parameters to be fitted. To find the best possible fit for the layer, the following ranges were defined: viscosity of the layer varied between 0.001-100 Pa. s, shear modulus (0.1-10000 Pa), and thickness (10^{-9}-10^{-6} m).

It is worth mentioning that Sauerbrey equation significantly underestimates the thickness, when dissipation variation is not close to zero and viscoelastic effects play a role(*29*). Therefore, Sauerbrey is not valid for our system. It also must be considered that shear wave is not able to detect the variations occur beyond the penetration depth. It is as low as about 100 nm for the fifth overtone. However, with increasing the viscosity of the adjacent layer due to increasing the emulsion droplet volume fraction, ϕ, penetration depth goes to about 400 nm. Calculations are shown in the appendix.

Figure 11 and Figure 12 are comparing the variation of shear modulus of two unstable emulsions of 2% V/V with different average diameters during the creaming process. We observed two different behaviors by modeling shear modulus during the creaming process: For the system with smaller droplets, with the addition of emulsion droplets from the bulk and increasing the volume fraction of droplets in the layer next to the sensor, elastic modulus initially increased. After reaching the maximum of about 2600 Pa, shear modulus started to decline steadily. The decline can be due to the increase in the size of emulsion droplets, which can be the result of coalescence. The effect of packing density on shear modulus competes with the droplet size dependency of shear modulus. Formation of close packed layer raises the shear modulus; however, increasing the size of droplets due to coalescence lowers the shear modulus.

The dependency of elastic modulus to the size of droplet has been previously reported by Weiss and McClements (*30*). Their results show a drop of about 2500 Pa in shear modulus, when the droplet size increased from 75 nm to 90 nm in a 25 wt % *n*-octadecane oil-in-water emulsion.

In the unstable system with larger droplets, shear modulus declined rapidly during the creaming. Presumably, larger droplets have faster upwards movement and form a packed layer more quickly. The coalescence occurs immediately, leading to a decline in elastic modulus. The results might not perfectly match previously studied systems with similar size and volume fraction of emulsion droplets because the shear modulus refers to

frequencies in MHz scale (*31*). However, the trends clearly explain the behavior of droplets in the closed pack layer.

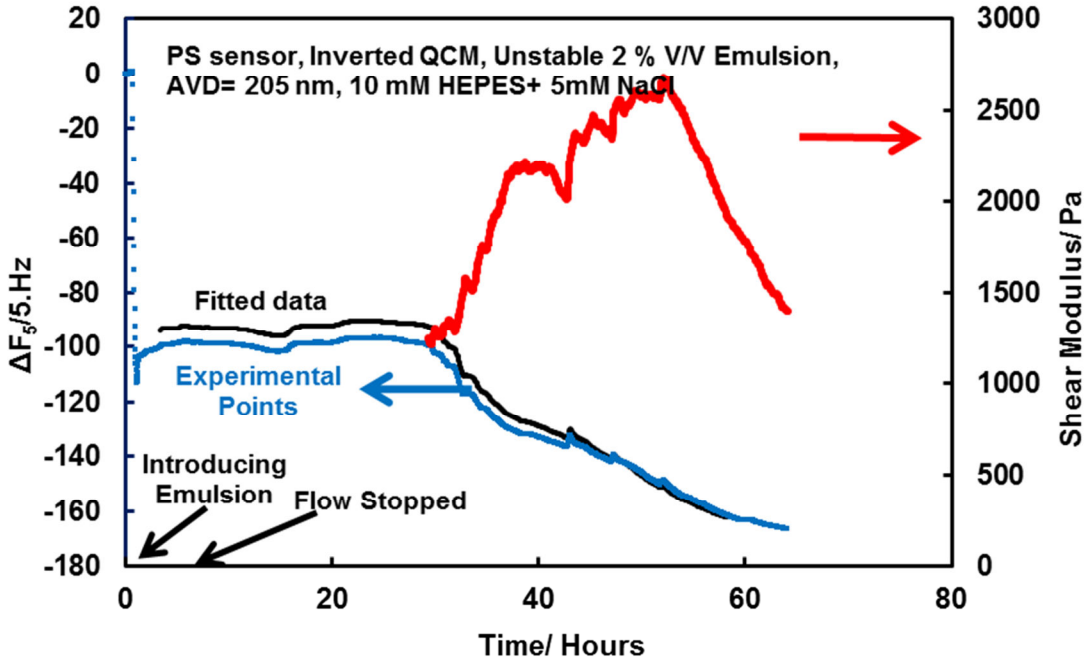

Figure 11: Time dependence shear modulus of 2% (V/V) unstable emulsion with AVD of 205 nm during creaming. 3rd, 5th and 7th overtones were used for Voigt-based extended viscoelastic modeling.

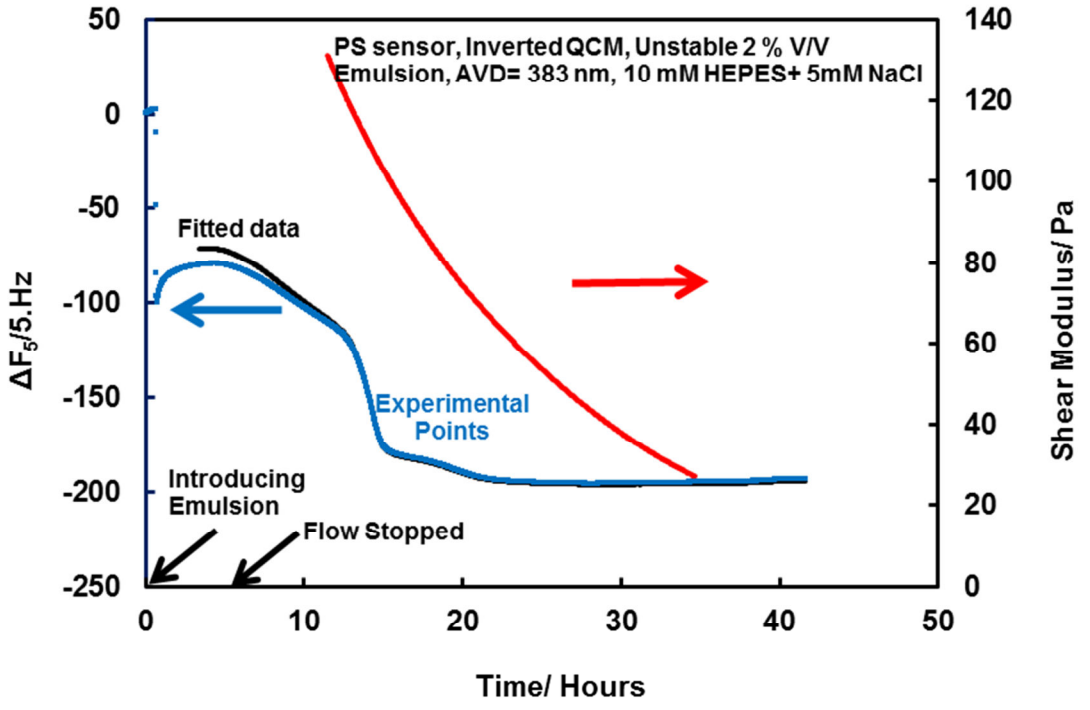

Figure 12: Time dependence shear modulus of 2% (V/V) unstable emulsion with AVD of 383 nm during creaming. 3rd, 5th and 7th overtones were used for Voigt-based extended viscoelastic modeling.

3.5 Discussion

In the visual observation method of creaming process, the movement of the boundary between bottom layer and creaming zone is monitored. Normal QCM-D experiment is unable to detect the variations in the serum layer, especially in dilute emulsions. The variation in viscosity and density is not significant to cause any change in frequency and dissipation. Moreover, upwards movement of droplets does not cause any further change and is not strong enough to isolate the adsorbed droplets from the surface of sensor. However, turning the test module upside down enabled us to evaluate the formation of top layer, which is an indication to the creaming process. Increasing the volume fraction of droplets causes a noticeable change in viscosity. Although the formation of a packed layer of emulsion droplets lowers the density of the layer next to the sensor, the impact of viscosity is more significant that results in frequency reduction.

Both non-creaming and unstable emulsions adsorb on sample hydrophobic QCM-D sensor. The adsorption causes a drop in frequency. Inverted QCM-D technique is able to differentiate stable emulsions from unstable emulsions. During the creaming and upon stopping the flow of unstable emulsions, further variation in frequency was observed. This can be due to the upwards movement of droplets. Addition of the droplets to the layer of already adsorbed droplets as is shown in Figure 13, results in the formation of a close packed layer. This causes an increase in the viscosity of the layer next to the sensor and eventually lowers the frequency value. Various equations were derived to explain the dependency of emulsion viscosity as a function of dispersed phase volume fraction(*11*). The Krieger and Dougherty equation and the related curve are shown in the appendix. On the other hand, the stable emulsions showed no variation during the flow stoppage and after the initial adsorption.

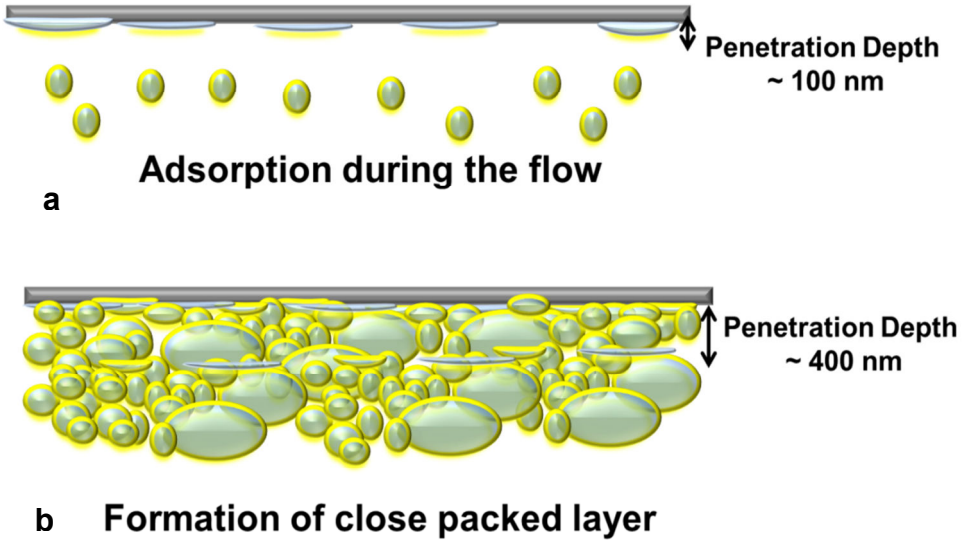

Figure 13: Schematic drawing of the structure of (a) the adsorbed layer during the flow of emulsion and (b) formation of close packed layer.

The increase in volume fraction of droplets right next to the sensor surface and formation of close packed layer also leads to an increase in dissipation. This indicates the elevated sensed elastic modulus. Variation of both storage and loss modulus of the viscoelastic layer affects the shifts in the resonance frequency and dissipation (*32*). Lacasse *et al*.(*33*) has previously reported the effect of oil volume fraction on elastic modulus. While the emulsion consists of repulsive droplets, compression of droplets leads to a noticeable change in dissipation. In their study, Mason *et al*.(*25*) showed that in a concentrated emulsion stabilized with surfactants of low molecular weight, elastic shear modulus significantly increases as oil volume fraction goes up from 0.5 to 0.9.
At low volume fractions, emulsion droplets keep their spherical shape due to the surface tension. In this case, theories for hard spheres and conventional models are applicable to emulsions. In a packed layer on top of the emulsion container, properties vary due to the increased density of droplets. Other than the volume fraction and packing density, droplet shape and size deformation due to emulsion instabilities such as Ostwald ripening or coalescence affects rheological behavior of emulsion(*30*). We observed the same behavior in samples of both metastable and unstable emulsions. Spreading of droplets on the surface also affects the elastic behavior of the adsorbed layer. Similar to previous studies with using Ellipsometric measurements(*34*), our SEM pictures shows that emulsion droplets spread easier on hydrophobic surfaces. However, the extent of spreading is limited at higher packing density.

3.6 Conclusion

1. Whereas conventional QCM-D measurements monitors the deposition of emulsion droplets onto surfaces, measurements made with an inverted QCM-D cell without flow gives insight into the gravity-induced build-up of a concentrated emulsion layer (consolidation layer) near the sensor surface.

2. Some emulsions only show deposition with no evidence of a consolidation layer – these tend to be dilute, small and colloidally stable. By contrast, larger and less stable emulsions display rich behaviours in both frequency shifts and dissipation over the period of hours as consolidation layers build up next to the QCM-D sensor surface.

3. Voigt-based viscoelastic modelling fits to inverted QCM-D data gives insight into the evolution of the properties of the consolidation layers with time.

4. Of the many excellent techniques available for measuring emulsion properties, inverted QCM-D measurements are unique in terms of characterizing the first 100 nm of the consolidation layer next to a solid surface.

3.7 References

1. Cao, Y., Dickinson, E., and Wedlock, D. J. (1990) Creaming and flocculation in emulsions containing polysaccharide, *Food Hydrocolloids 4*, 185-195.
2. Manoj, P., Fillery-Travis, A. J., Watson, A. D., Hibberd, D. J., and Robins, M. M. (1998) I. Creaming Behavior, *Journal of colloid and interface science 207*, 283-293.
3. Moates, G. K., Watson, A. D., and Robins, M. M. (2001) Creaming and oscillation rheology of weakly flocculated concentrated emulsions, *Colloids and Surfaces A: Physicochemical and Engineering Aspects 190*, 167-178.
4. Robins, M. M. (2000) Emulsions—creaming phenomena, *Current Opinion in Colloid & Interface Science 5*, 265-272.
5. Howe, A. M., Mackie, A. R., and Robins, M. M. (1986) Technique to measure emulsion creaming by velocity of ultrasound, *JOURNAL OF DISPERSION SCIENCE ANDTECHNOLOGY 7*, 231-243.
6. Mengual, O., Meunier, G., Cayre, I., Puech, K., and Snabre, P. (1999) Characterisation of instability of concentrated dispersions by a new optical analyser: the TURBISCAN MA 1000, *Colloids and Surfaces A: Physicochemical and Engineering Aspects 152*, 111-123.
7. Matsumiya, K., Inoue, T., Niida, J., Katagiri, T., Nishizu, T., and Matsumura, Y. (2014) Evaluation of long-term stability of milk beverages by a novel method for rapid determination of aggregation forces between colloidal particles, *Food Hydrocolloids 34*, 177-183.
8. Bury, M., Gerhards, J., Erni, W., and Stamm, A. (1995) Application of a new method based on conductivity measurements to determine the creaming stability of o/w emulsions, *International journal of pharmaceutics 124*, 183-194.
9. Novales, B., Papineau, P., Sire, A., and Axelos, M. (2003) Characterization of emulsions and suspensions by video image analysis, *Colloids and Surfaces A: Physicochemical and Engineering Aspects 221*, 81-89.
10. Bullard, J. W., Pauli, A. T., Garboczi, E. J., and Martys, N. S. (2009) A comparison of viscosity–concentration relationships for emulsions, *Journal of colloid and interface science 330*, 186-193.
11. Pal, R. (2001) Novel viscosity equations for emulsions of two immiscible liquids, *Journal of Rheology (1978-present) 45*, 509-520.
12. Stålgren, J. J., Claesson, P. M., and Wärnheim, T. (2001) Adsorption of liposomes and emulsions studied with a quartz crystal microbalance, *Advances in colloid and interface science 89*, 383-394.
13. Leal-Calderon, F., Thivilliers, F., and Schmitt, V. (2007) Structured emulsions, *Current Opinion in Colloid & Interface Science 12*, 206-212.
14. Princen, H., and Kiss, A. (1986) Rheology of foams and highly concentrated emulsions: III. Static shear modulus, *Journal of colloid and interface science 112*, 427-437.
15. Mason, T., Bibette, J., and Weitz, D. (1996) Yielding and flow of monodisperse emulsions, *Journal of colloid and interface science 179*, 439-448.

16. Rafaï, S., Sarker, D., Bergeron, V., Meunier, J., and Bonn, D. (2002) Superspreading: aqueous surfactant drops spreading on hydrophobic surfaces, *Langmuir 18*, 10486-10488.
17. Dresselhuis, D. M., van Aken, G. A., de Hoog, E. H., and Stuart, M. A. C. (2008) Direct observation of adhesion and spreading of emulsion droplets at solid surfaces, *Soft Matter 4*, 1079-1085.
18. Johannsmann, D. (2014) *The Quartz Crystal Microbalance in Soft Matter Research*, Springer.
19. Lin, Z., and Ward, M. D. (1996) Determination of contact angles and surface tensions with the quartz crystal microbalance, *Analytical Chemistry 68*, 1285-1291.
20. Chanamai, R., and McClements, D. J. (2000) Dependence of creaming and rheology of monodisperse oil-in-water emulsions on droplet size and concentration, *Colloids and Surfaces A: Physicochemical and Engineering Aspects 172*, 79-86.
21. Sundh, M., Svedhem, S., and Sutherland, D. S. (2010) Influence of phase separating lipids on supported lipid bilayer formation at SiO 2 surfaces, *Physical Chemistry Chemical Physics 12*, 453-460.
22. Tammelin, T., Merta, J., Johansson, L.-S., and Stenius, P. (2004) Viscoelastic properties of cationic starch adsorbed on quartz studied by QCM-D, *Langmuir 20*, 10900-10909.
23. Lequeux, F. (1998) Emulsion rheology, *Current Opinion in Colloid & Interface Science 3*, 408-411.
24. Mason, T. (1999) New fundamental concepts in emulsion rheology, *Current Opinion in Colloid & Interface Science 4*, 231-238.
25. Mason, T. G., Bibette, J., and Weitz, D. A. (1995) Elasticity of Compressed Emulsions, *Physical Review Letters 75*, 2051-2054.
26. Jeelani, S., Benoist, G., Joshi, K., Gunde, R., Kellenberger, D., and Windhab, E. (2005) Creaming and aggregation of particles in suspensions, *Colloids and Surfaces A: Physicochemical and Engineering Aspects 263*, 379-389.
27. Malmström, J., Agheli, H., Kingshott, P., and Sutherland, D. S. (2007) Viscoelastic Modeling of Highly Hydrated Laminin Layers at Homogeneous and Nanostructured Surfaces: Quantification of Protein Layer Properties Using QCM-D and SPR, *Langmuir 23*, 9760-9768.
28. Reviakine, I., Johannsmann, D., and Richter, R. P. (2011) Hearing what you cannot see and visualizing what you hear: interpreting quartz crystal microbalance data from solvated interfaces, *Analytical Chemistry 83*, 8838-8848.
29. Johannsmann, D. (2008) Viscoelastic, mechanical, and dielectric measurements on complex samples with the quartz crystal microbalance, *Physical Chemistry Chemical Physics 10*, 4516-4534.
30. Weiss, J., and McClements, D. (2000) Influence of Ostwald ripening on rheology of oil-in-water emulsions containing electrostatically stabilized droplets, *Langmuir 16*, 2145-2150.
31. Stengel, G., Höök, F., and Knoll, W. (2005) Viscoelastic Modeling of Template-Directed DNA Synthesis, *Analytical Chemistry 77*, 3709-3714.

32. Voinova, M. V., Rodahl, M., Jonson, M., and Kasemo, B. (1999) Viscoelastic acoustic response of layered polymer films at fluid-solid interfaces: continuum mechanics approach, *Physica Scripta 59*, 391.
33. Lacasse, M.-D., Grest, G. S., Levine, D., Mason, T. G., and Weitz, D. A. (1996) Model for the Elasticity of Compressed Emulsions, *Physical Review Letters 76*, 3448-3451.
34. Malmsten, M., Lindstrom, A.-L., and Wärnheim, T. (1995) Ellipsometry Studies of Interfacial Film Formation in Emulsion Systems, *Journal of colloid and interface science 173*, 297-303.

Appendix 2: Supporting Information for Chapter 3

A QCM-D study on the effect of tear film proteins on the adsorption of commercial eye drops on sample hydrophilic and hydrophobic surfaces

Quartz crystal microbalance-dissipation (QCM-D) has been employed to detect the influence of tear film proteins (HSA and lysozyme) on the adsorption of two conventional eye drops: SYSTANE ULTRA and SYSTANE BALANCE on sample hydrophobic surface. SYSTANE BALANCE contains emulsion droplets.

Sample preparation- Both eye drops were diluted with the buffer (10 mM HEPES+5 mM NaCl). Protein solutions were prepared by dissolving 0.2 wt% protein in buffer.

QCM-D Studies- Polystyrene QCM-D sensors were used as representatives of hydrophobic surfaces. For cleaning the sensors, following steps were taken: Polystyrene QCM-D sensors were immersed in a 1% solution of Deconex in milliQ water for 30 min at 30°C followed by thorough rinse of milliQ water and 99% ethanol and dried with nitrogen gas.

Measurements were performed with E4 QCM-D (Q-Sense AB, Gothenburg, Sweden) and monitored using Qsoft401 software version 2.5.2. All measurements were repeated two times. Processed data from the fifth overtone using Qtools software version 3.0.7 are shown and Δf values have been normalized by the fifth overtone.

Quartz crystal sensors mounted to removable flow modules, which are placed in the E4 temperature control chamber. Measurements then initiated in air by obtaining the resonance frequencies of the sensor crystals. A solution of 10 mM HEPES buffer and 5 mM NaCl was injected at a constant flow rate of 150 μL/min by using an IPC-N935 tubing pump with planetary drive from Ismatec to produce the baseline. It then followed by injection of eye drops, buffer, protein solution, buffer or protein solution, buffer, eye drop, buffer until reaching a plateau keeping the flow rate constant at 150 μL/min.

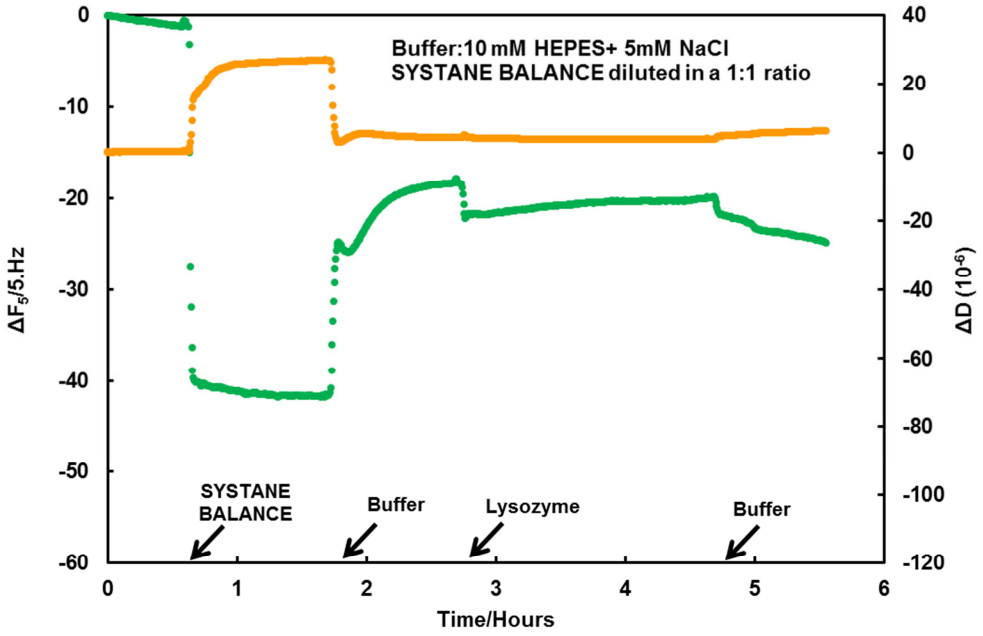

SI Figure 1: Adsorption of SYSTANE Balance on PS sensor followed by lysozyme solution at pH= 7.4.

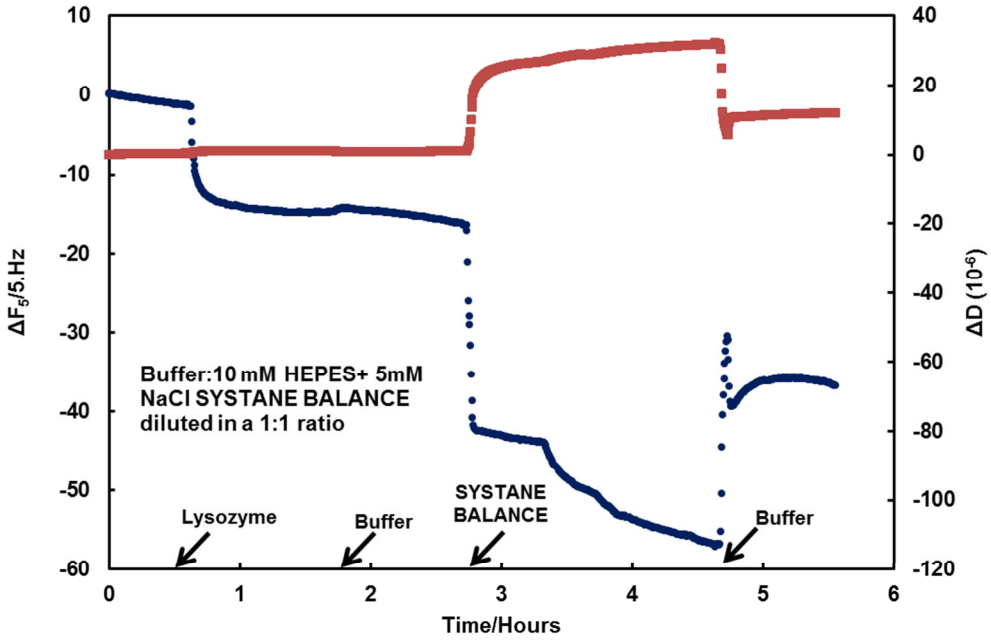

SI Figure 2: Adsorption of lysozyme on PS sensor followed by SYSTANE Balance at pH= 7.4.

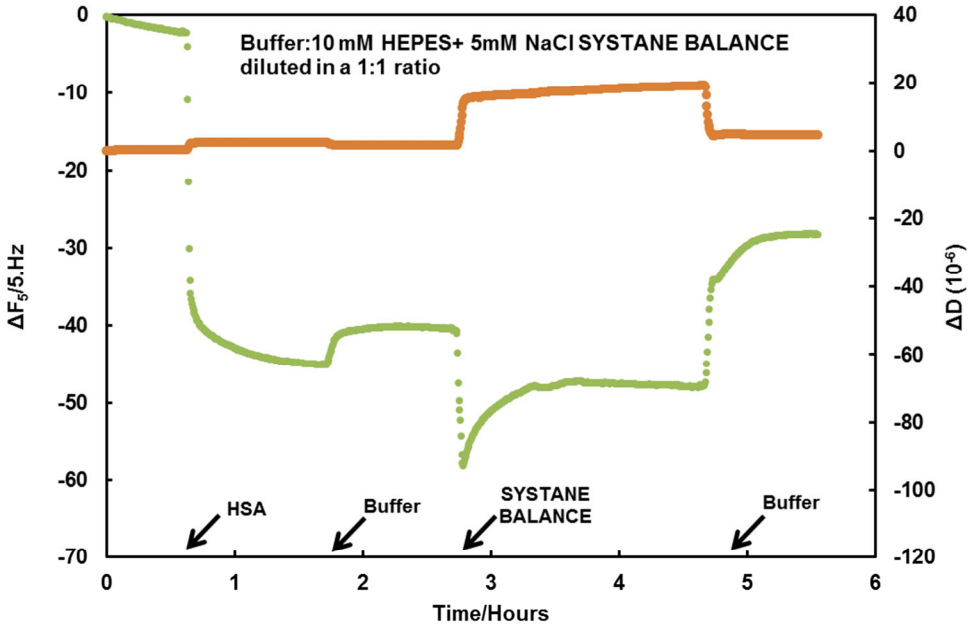

SI Figure 3: Adsorption of HSA on PS sensor followed by SYSTANE Balance at pH= 7.4.

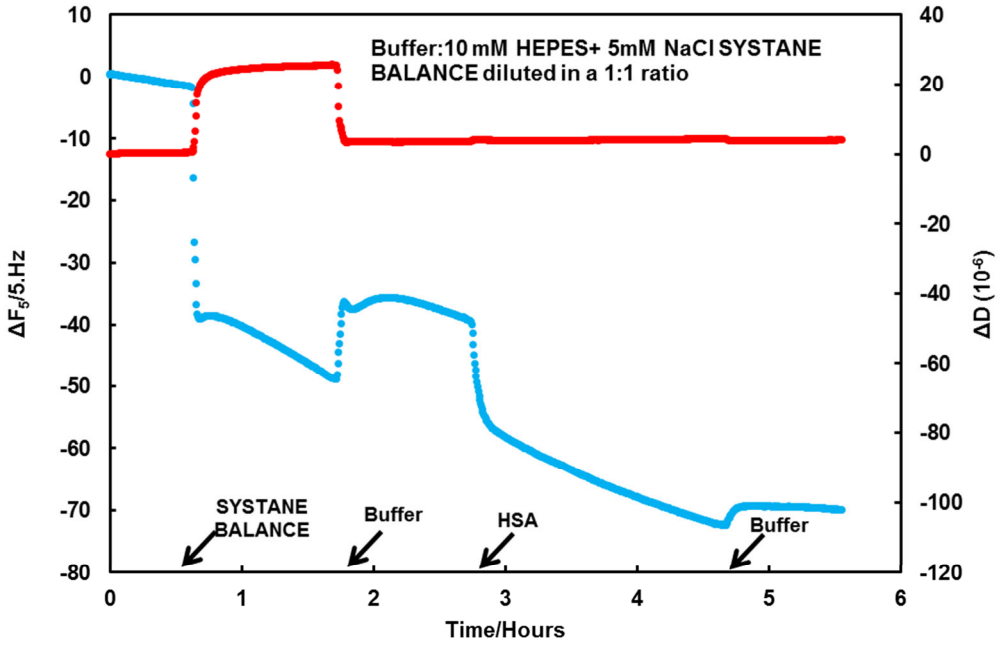

SI Figure 4: Adsorption of SYSTANE Balance on PS sensor followed by HSA solution at pH= 7.4.

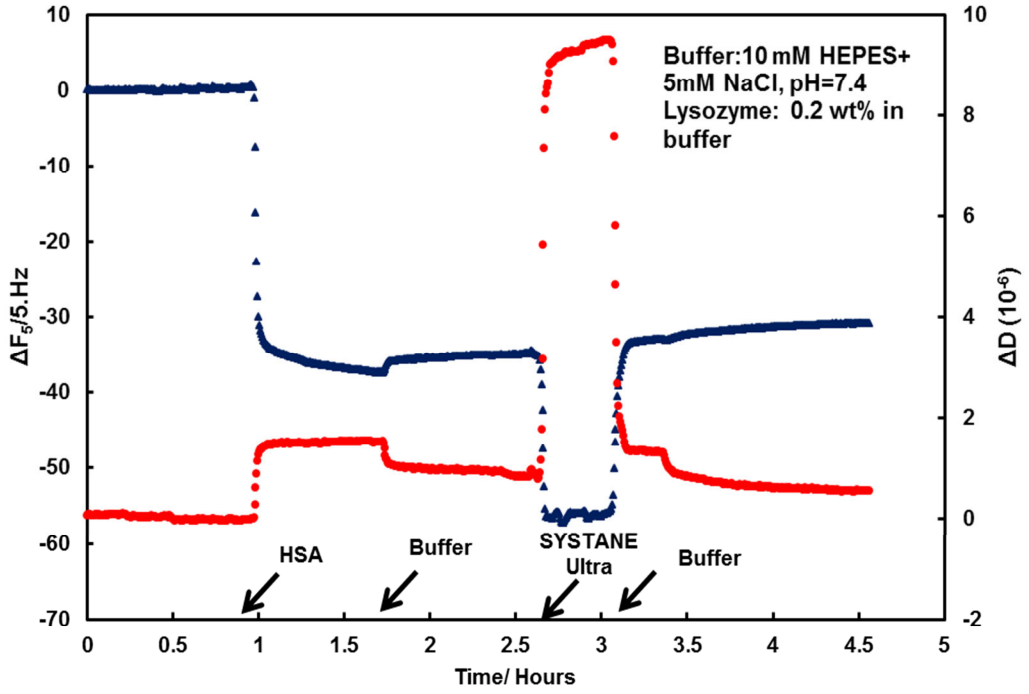

SI Figure 5: Adsorption of HSA on PS sensor followed by SYSTANE Ultra at pH= 7.4.

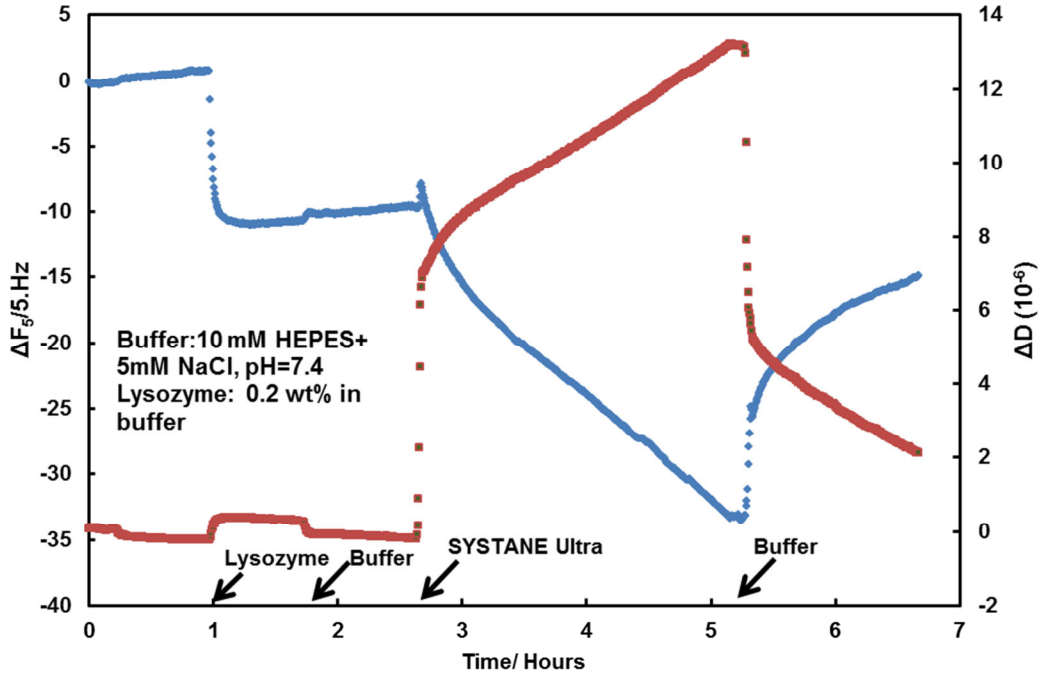

SI Figure 6: Adsorption of lysozyme on PS sensor followed by SYSTANE Ultra at pH= 7.4.

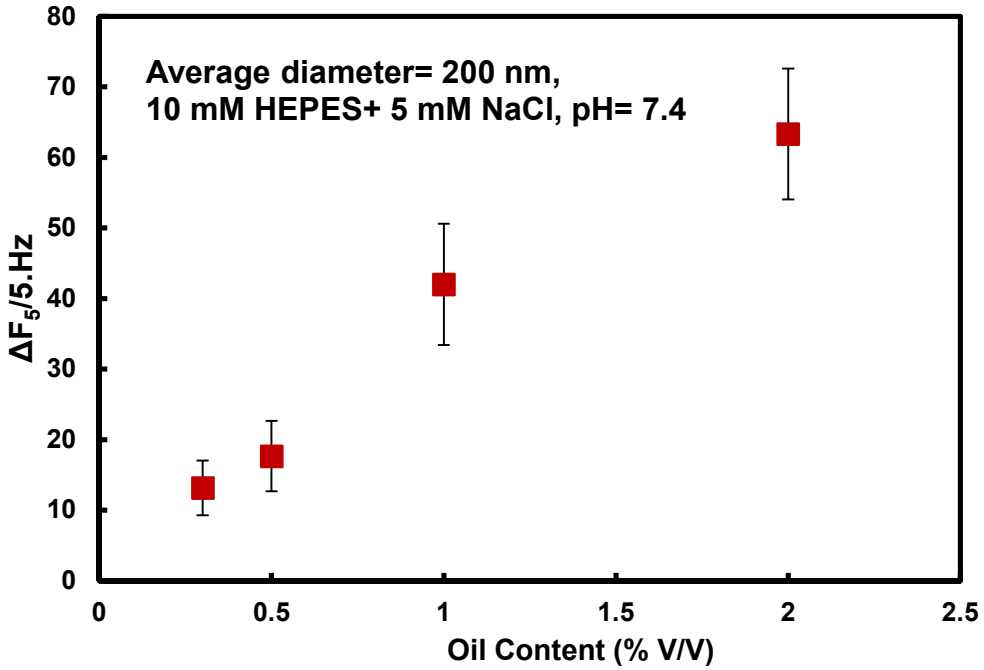

SI Figure 7: Frequency variation after stopping the flow as a function of oil content. The error bars are the standard deviation values based on 3 replicates. Increasing the oil content causes a bigger change in the frequency when the flow was stopped. The error bars are the standard deviation values based on 3 replicates.

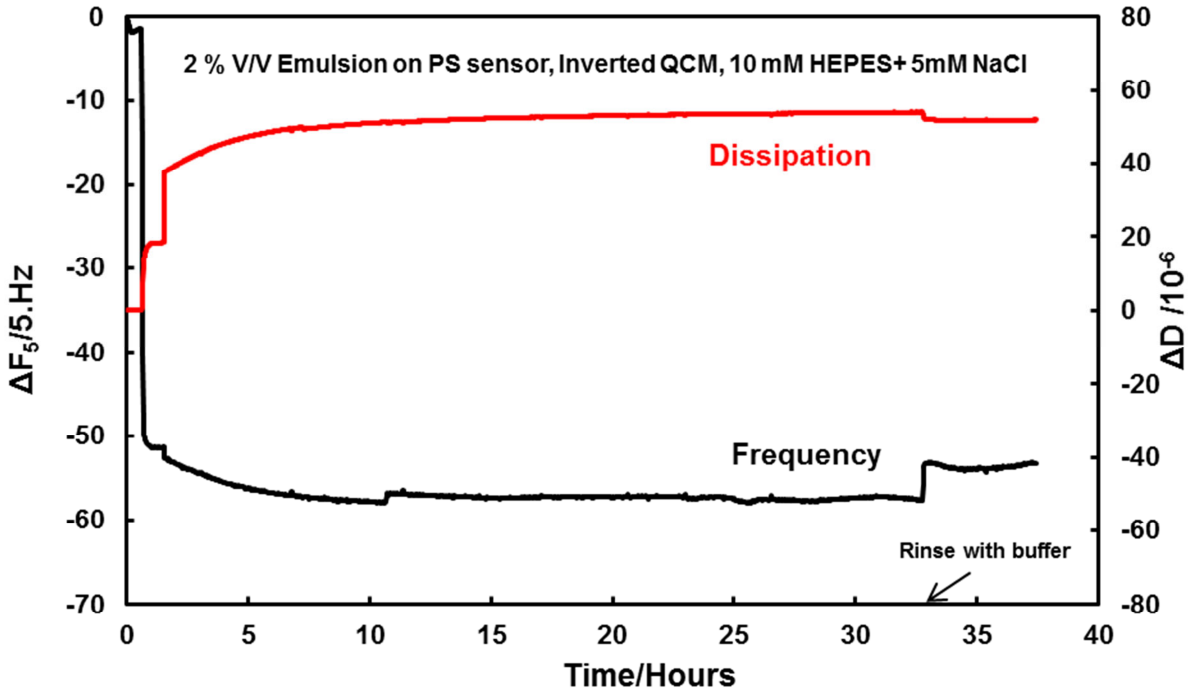

SI Figure 8: Variation of frequency and dissipation for a 2 %(V/V) emulsion with the average diameter of 205 nm. Flow continued for more than 30 hours.

Dependency of Density on oil concentration

$\rho_w := 1 \frac{gm}{cm^3}$

Density of continuous phase (water)

$\rho_{oil} := 0.773 \frac{gm}{cm^3}$

Hexadecane density

$\rho_v(\phi) := \phi \cdot \rho_{oil} + (1 - \phi) \cdot \rho_w$

$\phi := 0, 0.1 .. 1$

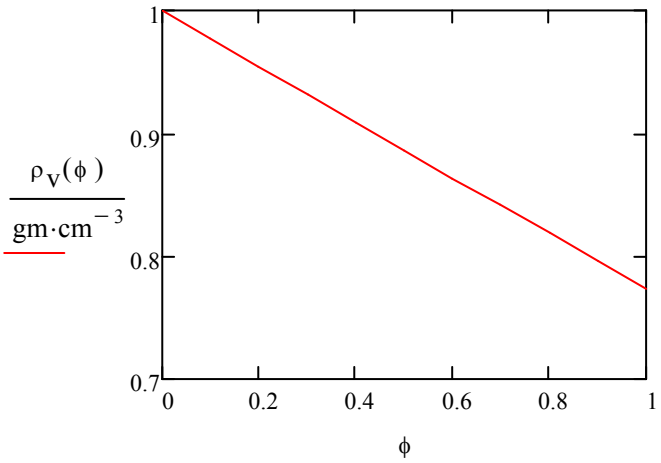

Calculating Penetration Depth of Shear Wave

$\eta := 0.001 Pa \cdot s$

Viscosity of continuous phase (water)

$\rho := 1 \frac{gm}{cm^3}$

Density of continuous phase (water)

$f_0 := 5 MHz$

ω is angular frequency and can be calculated as follow

$\omega := 2 \cdot \pi \cdot f_0 = 3.142 \times 10^7 \frac{1}{s}$

δ , viscous penetration depth can be calculated as follow

$\delta := \sqrt{\frac{2 \cdot \eta}{\rho \cdot \omega}} = 2.523 \times 10^{-7} m$

Variation of Penetration Depth with oil droplet fraction

Krieger and Dougherty equation

$\phi_m := 0.64$

The maximum packing concentration of particles

$\eta_{rKD}(\phi) := \exp\left(1 - \frac{\phi}{\phi_m}\right)^{-2.5\phi_m}$

$\eta_{KD}(\phi) := \eta \cdot \eta_{rKD}(\phi)$

$\phi := 0, 0.1 .. 1$

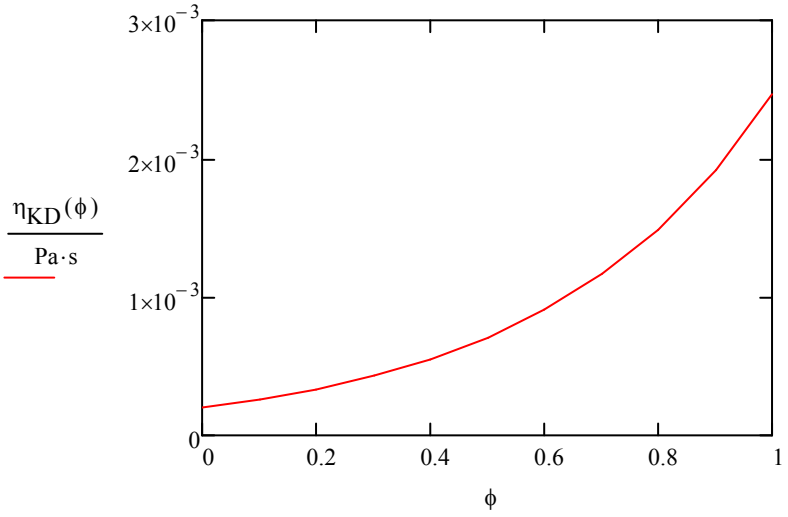

$\delta(\phi) := \sqrt{\frac{2 \cdot \eta_{KD}(\phi)}{\rho \cdot \omega}}$

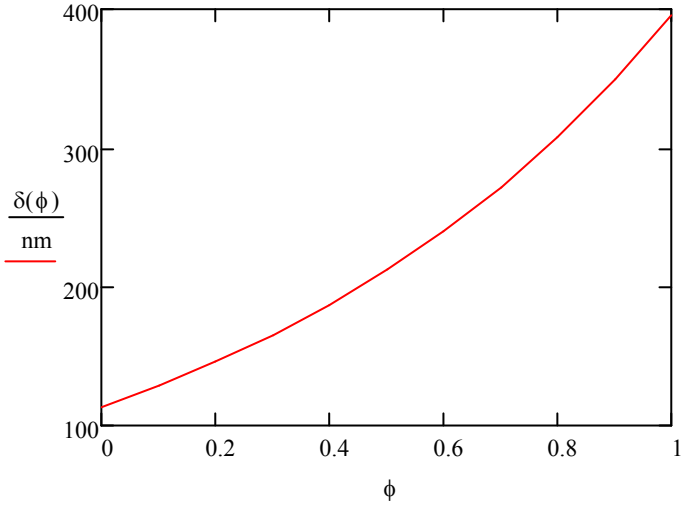
400
300
200
100
δ(ϕ)
nm
0
0.2
0.4
0.6
0.8
1
ϕ

Plot of the square root of viscosity times density

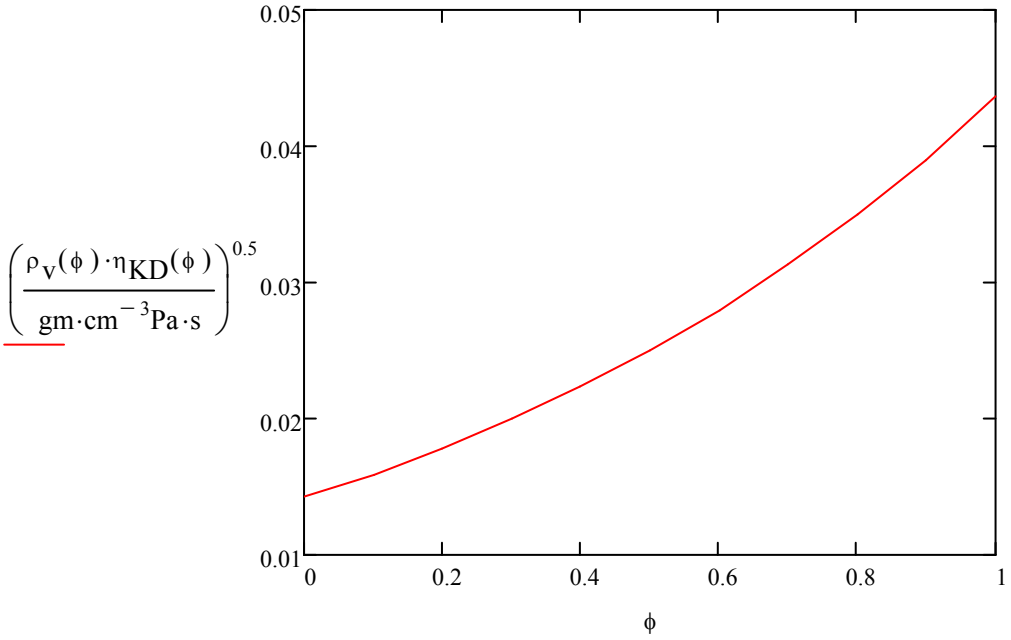

Chapter 4. Weak Gelation of Hydrophobic Guar by Albumin in Simulated Human Tear Solutions

Most of the experiments and analysis in chapter 4 were conducted by me. Modification of Guar has been done based on the method has been previously developed in our lab by Dr. Yuguo Cui. Protein binding experiments were conducted with the help of my summer student, Wing Yan (Joyce) Lam.
Dr. Pelton revised the versions I wrote, helped to analyze data and organized the final version.

Biomacromolecules

pubs.acs.org/Biomac

Weak Gelation of Hydrophobic Guar by Albumin in Simulated Human Tear Solutions

Roozbeh Mafi,[†] Robert Pelton,*[,†] Yuguo Cui,[†] and Howard Ketelson[‡]

[†]Department of Chemical Engineering, McMaster University, 1280 Main Street West, Hamilton, Ontario L8S 4L8, Canada

[‡]Alcon Research, Ltd., 6201 South Freeway, Fort Worth, Texas 76134-2099, United States

Supporting Information

ABSTRACT: This initial study shows that hydrophobic modification of guar polymers used in eye drops forms weak gels with human serum albumin (HSA), suggesting that modified guar may offer advantages for treatment of dry eye diseases that lead to elevated HSA concentrations in tears. Specifically, hydroxypropyl guar samples were oxidized and derivatized with linear alkyl amines to give a series of modified guar polymers (MGuar) bearing hydroxypropyl, N- alkylamide, and carboxyl moieties. MGuar interactions with lysozyme and HSA were measured by binding and rheological methods as functions of the alkyl chain length and the extent of hydrophobic modification. HSA binds MGuar, giving weak gels, whereas lysozyme shows little tendency to bind MGuar or to interfere with HSA binding. Six mole percent substitution of decyl hydrophobes gave the strongest gels in the presence of HSA.

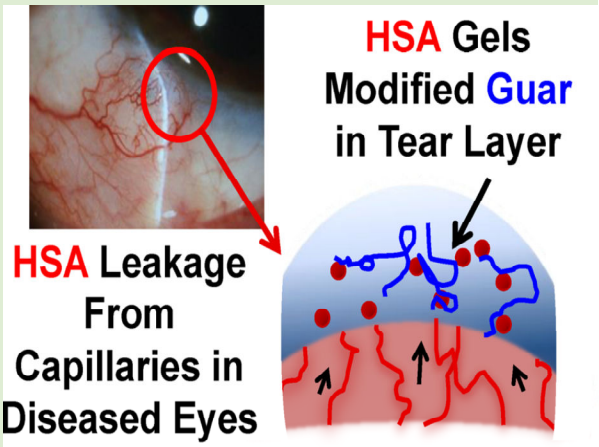

INTRODUCTION

Hydroxypropyl guar (HPG) is employed in eye drops used to treat the symptoms of dry eye disease.[1] The potential roles of HPG in eye drops include (1) increasing tear fluid viscosity,[2] which increases the residence time of eye drops on the eye,[3] (2) decreasing friction[4] when the eyelid moves over the eye, and (3) possibly adsorbing on hydrophobic cell surfaces, making them more hydrophilic. Each of these potential functions will be promoted by employing higher molecular weight fractions of hydroxypropyl guar. Guar gum is available as very high molecular weight polymers; however, they present significant practical difficulties in dry eye formulations including the following: Very high molecular weight guar or HPG is difficult to dissolve, guar gels could be too viscous to dispense as eye drops, and low concentrations of high molecular weight guar induce depletion flocculation of any emulsion particles in the eye drops.[5]

With a view toward enhancing the performance of guar-based polymers in ophthalmic applications, we report herein some properties of hydrophobically modified hydroxypropyl guar (MGuar). In particular, we show that some MGuar compositions bind to human serum albumin (HSA) in model tear fluids, producing weak structures that increase viscosity. These findings suggest the possibility of replacing high molecular weight HPG in eye drops with much lower molecular weight hydrophobically modified guar polymers that flow easily in the bottle but form weak gels on the eye.

Guar and HPG are hydrophilic nonionic polymers, and depletion is the dominant interaction with most protein solutions (repulsion).[6] Exceptions include specific proteins such as lectins[7] and antibodies[8] that can bind to aqueous guar. Hydrophobic modification is a well-established approach to increase the interactions of water-soluble polymers with proteins that have hydrophobic surface domains. Audebert's work in the mid 90s was particularly relevant. They reported an order of magnitude increase of solution viscosity when bovine serum albumin (BSA) was added to dilute solutions of poly(acrylic acid) with 1 mol % substitution of linear octadecyl groups.[9] They proposed that the protein behaved as a cross-linker, increasing the effective molecular weight of the hydrophobically modified polymer.

In the simplest case, the structure of hydrophobically modified polymers is defined by two average properties: the density of hydrophobic substituents and the length of linear hydrophobes. Gao and Dubin proposed the following as factors linking protein binding to the structure of hydrophobically modified polymers: (1) the minimum hydrophobe for protein binding is 3−4 methylene groups, (2) protein binding competes with intramolecular micellization of the pendent hydrophobes, and (3) charged groups of along the polymer backbone interfere with micellization and thus may promote protein binding.[10]

Hydrophobically modified guar has been described in a number of publications, usually with a view toward rheology control[11] or oil recovery.[12] For example, Lapasin reported the

Received: August 28, 2014
Revised: November 6, 2014

rheological properties of hydroxypropyl guar (HPG), modified with linear 22-carbon chains.[13]

In the following sections, we describe the preparation and characterization of a series of hydrophobically modified hydroxypropyl guars, MGuar. Lysozyme and HSA interactions with the MGuars are probed by rheological and protein binding measurements.

EXPERIMENTAL SECTION

Materials. Hydroxypropyl guar with a molecular weight of 2.4 MDa and degree of substitution of 0.36 was provided by Alcon Laboratories (Fort Worth, TX). NaN_3, 4-(2-hydroxyethyl)-1-piperazineethanesulfonic acid (HEPES), NaCl, HSA, lysozyme from chicken egg white, and a bicinchoninic acid (BCA) assay kit containing BCA solution, copper(II) sulfate solution, and protein standards containing bovine serum albumin (BSA) were purchased from Sigma-Aldrich (Oakville, ON). Centrifugal filter devices with a mesh size of 100 000 and 30 000 nominal molecular weight limit (NMWL) were purchased from Millipore (Billerica, MA).
All solutions were made using Type 1 water (18.2 MΩ cm, Barnstead Nanopure Diamond system). Most measurements were performed in either low (5 mM NaCl, 10 mM HEPES, 5 ppm of NaN3) or high (150 mM NaCl, 10 mM HEPES, 5 ppm of NaN3) ionic strength buffers.

HPG Oxidation. In a typical experiment, HPG (116.2 mg) was dissolved in 100 mL of water. TEMPO (2.2 mg) and NaBr (12.4 mg) were added, and the solution was stirred and cooled in an ice bath (~3°C). Sodium hypochlorite (15%, ~30 mL) was adjusted to pH 9.4 by 1 M HCl and cooled (~3 °C). Of the sodium hypochlorite solution, 0.6 mL was added to the guar solution, and the pH was maintained at 9.4 by 0.01 M NaOH. After 30 min, the reaction was quenched by 0.6 mL of methanol and neutralized to pH 6 by 0.1 M HCl. Sodium borohydride (56.2 mg) was added, and the solution was stirred for several hours to remove residual NaOCl and to reduce aldehydes back to alcohols. To precipitate the oxidized HPG, 100 mL of 2-propanol was added with mixing, and the product was centrifuged (Allegra X-12R, Beckman Coulter) at 7500 rpm for 15 min. The product was placed on filter paper and washed with 80:20 2-propanol/water. The washed product was dissolved in sufficient water to dissolve the gelled product, and the solution was then freeze-dried for 2 days. Conductometric titration was used to determine the carboxyl content, and an example titration curve is shown in Supporting Information Figure S1.

Alkylation of Oxidized HPG To Give MGuar. Taking decylamide MGuar as an example, oxidized HPG (100 mg) dissolved in 100 mL of 0.1 M MES buffer at pH 4.7 was placed in a 250 mL round-bottomed flask, fitted with a magnetic stirring bar. To this was added 57.3 mg of decylamine, a 10-fold molar excess based on HPG carboxyl content, dissolved in 10 mL of dichloromethane with stirring at room temperature, and the solution was mixed for 30 min. For shorter alkyl chains, alkylamine was added directly to oxidized HPG solution. Next 56.5 mg of N-(3-(dimethylamino)propyl)-N′-ethylcarbodiimide hydrochloride (EDC) was added to the flask. This EDC dosage was a 10-fold molar excess based on the content of carboxyl groups on the oxidized HPG. After 2 h of mixing, the solution was dialyzed against water for 24 h in Spectra/Por Dialysis membranes (Spectrum Laboratories Inc.) with a molecular weight cutoff of 3500. The purified polymer was freeze-dried for storage. FTIR and NMR were used to confirm the product structure (examples are shown in Supporting Information Figures S2 and S3).

Potentiometric and Conductometric Titration. To define the degree of substitution for various hydrophobically modified guars, both potentiometric and conductometric titrations were performed with a PCTitrate titrator (Man-Tech Associates) equipped with a Burivar-I/2 buret and a conductivity electrode connected to a 4010 conductivity meter controlled by PC-Titrate software. A 100 mL titration cell that was thermostated with an mgw Lauda RM6 pump controlled by an mgw Lauda RMS system was employed. Samples were dissolved in 5 mmol/L of KCl. The pH of samples was initially adjusted to about 3.0 using hydrochloric acid. Then, either 0.1 or 1 mol/L NaOH was used as a titrant with an injection rate of 60 mV/pH by the base into acid titration method.

The example calculation in the Supporting Information file illustrates the complex calculations required to convert free carboxyl contents, measured by titration, into the degrees of substitution of hydrophobic substituents. Each hydrophobic DS value in Table 1 is based on two titration values and bears the accumulated uncertanties of two titrations.

Table 1. Carboxyl Contents before and after Alkylation[a]

	carboxyl degree of substitution		
MGuar designation	before alkylation	after alkylation	hydrophobe DS
1C6	0.142	0.132	0.01
3C6	0.142	0.105	0.037
6C6	0.201	0.143	0.058
10C6	0.201	0.104	0.097
1C8	0.142	0.130	0.012
6C8	0.201	0.146	0.055
1C10	0.142	0.127	0.015
3C10	0.142	0.112	0.030
6C10	0.201	0.142	0.059
9C10	0.201	0.114	0.087
1C12	0.142	0.132	0.01
5C12	0.201	0.150	0.051
1C18	0.142	0.130	0.012

[a]For the MGuar designations xCy, x is approximately the hydrophobic DS expressed as a percentage, and y is the number of carbons in the hydrophobic chain.

Protein Binding to MGuar. Protein (lysozyme or HSA) binding to MGuar was determined by mixing protein with MG, filtering the mixture through a 100 kDa filter, and using the BCA protein assay kit (Sigma, USA) to measure the unbound protein in the filtrate. In a typical experiment, 0.25 mL of 0.2% (w/w) in high ionic strength buffer and 0.25 mL of 0.4% HSA in buffer were added to 0.5 mL centrifuge tubes (Amicon Ultra-0.5 mL, Millipore) fitted with a 100 kDa filter (Millipore) and mixed for ~30 s with a mini-vortexer (VWR VM-3000, USA).

The unbound protein was isolated immediately or 24 h after mixing. The solutions were centrifuged for 20 min at 14 500 rpm (14 000g) with an Eppendorf Mini Spin Plus centrifuge (Hamburg, Germany). The filtrate was collected, and the filter cake was washed by two rounds of adding 0.01 mL of buffer followed by centrifugation. For experiments involving mixtures of HSA and lysozyme, the filtrates were filtered a second time through a 30 kDa filter (Millipore), which should allow only lysozyme to pass.

The protein concentrations in filtrates were measured as follows: 0.1 mL of protein solution was combined with 1.9 mL of the BCA solution prepared by mixing 50 parts of reagent A (sodium carbonate, sodium bicarbonate, bicinchoninic acid, and sodium tartrate in 0.1 N NaOH) with 1 part of reagent B (copper sulfate solution). After vortex mixing, the solutions were incubated at 37 °C for 30 min followed by 2 h at room temperature. The absorbance at 562 nm was measured, and the corresponding protein concentration in each sample was determined with a linear calibration curve.

Rheological Characterization. Rheological measurements were performed with an ATS controlled stress rheometer equipped with a CC25 concentric cylinder cell (Rheologica Stress Tech HR). After loading sample solution into the cup, sufficient time was allowed for the stresses to relax and to reach thermal equilibrium to 25 °C, controlled within ±0.1 °C using a water bath.

Dynamic viscometry experiments were performed with varying applied stress in the range of 0.01 to 100 Pa while the delay and integration times were both 1 s. The zero-shear viscosity values were

obtained by extrapolation. Figure S6 in the Supporting Information shows a typical example of viscosity as a function of shear rate.

The linear viscoelastic region was characterized with stress sweep tests. With the stress fixed at 0.055 Pa, the frequency was varied from 0.01 to 100 Hz in the dynamic oscillatory tests. Supporting Information Figure S5 shows an example result with and without the presence of HSA. The elastic modulus, G′, for samples with different protein concentrations was compared at a frequency of 10 Hz, conditions in the linear viscoelastic regime.

Turbidity Measurements. The UV absorbance at 285 nm was used to probe MGuar solubility. Solution/suspensions were dispersed using a mini vortexer, transferred into a standard 10 mm optical path length quartz cuvette, and placed in a Beckman Coulter DU800 spectrophotometer. Ten millimolar HEPES buffer with 5 mM or 150 mM NaCl was used as a blank.

RESULTS AND DISCUSSION

Herein, we report results from initial testing of the hypothesis that hydrophobically modified hydroxypropyl guar may offer advantages over unmodified guar in eye drop formulations for treating dry eye symptoms. Specifically, we have focused on the possibility of exploiting HSA binding to MGuar to give weak gels on the eye. We chose HSA as the target protein because it is present at elevated levels in some eye disease states.[14]

The last sentence in Borrega's 1999 publication suggests that specific protein binding to polymers could be exploited to give "biospecific thickeners";[15] our work describes our initial attempts to exploit this idea in eye drop formulations. Specifically, in situ guar gelation could increase residence time on the eye, lubrication, and tear film stability with a relatively low molecular weight MGuar. Although very high molecular weight unmodified guar gives viscous solutions and weak gels, the solutions are too viscous for easy dispensing from the eye drop bottle, and the guar induces depletion aggregation of emulsified products in the formulation, impacting shelf life. In other words, in situ gelation may offer the advantages of relatively low molecular weight MGuar in the eye drop bottle with the properties of high molecular weight MGuar on the eye.

Modified Guars. A series of hydrophobically modified guar (MGuar) polymers was prepared first by TEMPO-mediated oxidation of 2.4 MDa hydroxypropyl guar, converting some C6 hydroxyls to carboxyls.[16] In a second alkylation step, alkyl amines were conjugated to the carboxyl groups, forming amide linkages. The extent of hydrophobic modification was determined by measuring the carboxyl contents before and after alkylation. Table 1 summarizes the carboxyl and alkyl contents of the modified guars expressed as substitution (DS) values, defined as the number of substituents per hexose ring.

Our modified guar structures are complex, bearing hydroxypropyl, alkylamide, and carboxyl groups (Figure 1). Native guar is a linear polymannose chain with pendent galactose units approximately on every other mannose ring. Our starting material was a hydroxypropyl guar with a hydroxypropylation DS (groups per hexose ring) of 0.36. The literature suggests that the hydroxypropylation reaction has about twice the probability of occurring at one of the two types of C6 hydroxyls compared to that at any of the other seven types of secondary hydroxyls.[17] More recent work has shown that the hydroxypropyl moieties are present as individual groups with no poly(propylene glycol) oligomer formation.[16]

TEMPO-mediated HPG oxidation occurs exclusively at the unsubstituted primary hydroxyl groups, giving carboxyl groups. In the alkylation step, some carboxyls are converted to the corresponding alkyl amides (Figure 1). The maximum carboxyl

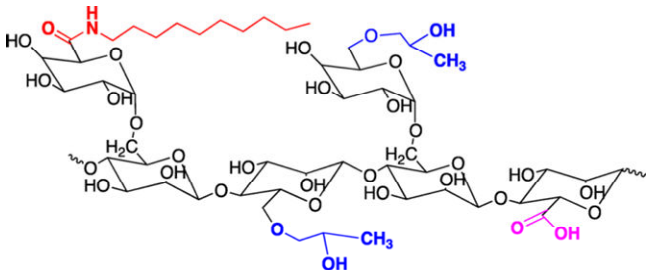

Figure 1. Segment of modified guar bearing hydroxypropyl, decylamide, and carboxyl groups. The carboxyl and alkyamide groups locate on either the mannose or galactose primary alcohols, whereas the hydroxypropyl groups could be substituted on any of the alcohol groups.

content in Table 1 was 0.20, and the maximum conversion of carboxyls to alkyl corresponded to sample 10C6. To summarize, the modified guar samples had approximately three hexose rings for every hydroxypropyl group, whereas the number of hexose rings per hydrophobe varied from about 10 hexose rings per hydrophobe (sample 10C6) to 100 hexose rings per hydrophobe (1C6 and 1C12). In addition, all of the modified guars had significant contents of residual carboxyl groups (DS values ranging from 0.07 to 0.13), giving the polymers some polyelectrolyte character.

The hydrophobic modification of hydroxypropyl guar decreases water solubility. Figure 2 shows the influence of

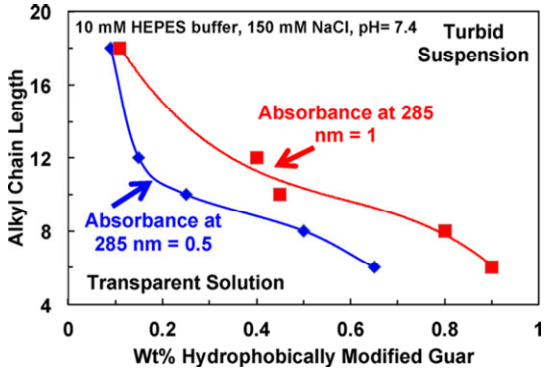

Figure 2. Influence of hydrophobic chain length on the solubility of modified guars with a hydrophobe DS 0.8−1.

hydrophobe chain length on the modified guar concentrations corresponding to the transition of from clear-to-turbid solutions and turbid-to-precipitation. These results were obtained in 10 mM HEPES + 150 mM NaCl at pH 7.4, conditions chosen to mimic human tear ionic strength.[18] As expected, the longer the alkyl chains, at constant hydrophobe DS, the lower the concentration corresponding to the onset of phase separation. MGuar 1C18 was too hydrophobic to have a useful solubility range. The following sections show that C12 and C10 modified guars gave interesting results.

Some experiments were also performed in lower ionic strength buffer solutions (5 vs 150 mM NaCl). The aggregation and precipitation boundaries were slightly shifted to higher concentrations (see Supporting Information Figure S4).

Comparing MGuar Polymers at Low Ionic Strength. Initial measurements were performed in 10 mM HEPES and 5 mM NaCl; these conditions correspond to an osmolality of about 20 mOsm/kg, which is much less than that of human

tears (293−326 mOsm/kg[18]). More detailed studies with the more promising guars were subsequently performed under conditions of higher osmolality (~300 mOsm/kg from 10 mM HEPES and 150 mM NaCl). Initial experimentation with concentrated (0.35 wt %) 8C10 MGuar showed that addition of 0.15% HSA gave strong gels with G′ > G″ over the measured frequency range (see plots in Supporting Information Figure S5). Because strong hydrogels are unlikely to be acceptable for on-eye application, we restricted our measurements to more dilute mixtures giving weak gels or a suspension soluble complexes just below the gel point concentration. Following the lead of Audebert's classic studies, we used viscosity measurements to probe these weakly gelling systems.[9]

Figure 3 shows the zero-shear viscosity of C6 and C10 modified guar samples as a function of HSA concentration. An

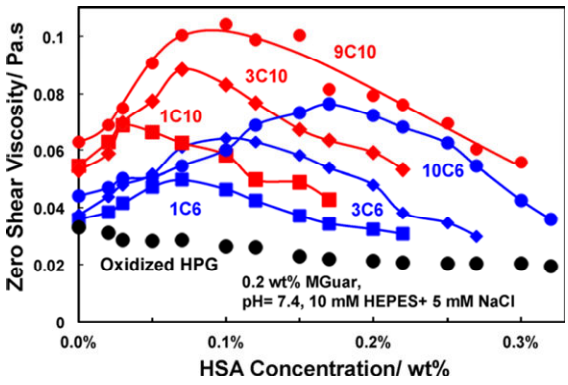

Figure 3. Influence of HSA on zero-shear viscosity of hydrophobically modified guars. The parent oxidized hydroxypropyl guar had a carboxyl DS of 0.201 (Table 1).

example of viscosity versus shear rate data, used to obtain zero-shear viscosity, is shown in Supporting Information Figure S6. The hydrophobic guars showed increased zero-shear viscosity in the presence of HSA, whereas the parent oxidized hydroxypropyl guar showed a slight decrease in viscosity with HSA addition. When comparing the decyl (xC10) results to those from the hexyl (xC6) series, the longer hydrophobes gave the highest viscosities, with maximum values occurring at lower HSA concentrations compared to the shorter hexyl series. For both series, the maximum viscosity increased with DS, as did the corresponding HSA concentration.

Lysozyme is the most prominent protein in tears. Figure 4 compares the abilities of HSA and lysozyme to promote gelation of guar 9C10 under low ionic strength conditions. In spite of potential electrostatic interactions between cationic lysozyme and anionic 9C10, HSA gave greater increases in storage modulus than did lysozyme. Similar results were reported by Borrega et al., who showed that hydrophobically modified poly(acrylic acid) gave stronger gels with BSA compared to that of gels formed with lysozyme.[15]

MG−Protein Interactions in Model Tear Solutions. To more closely mimic tear fluid conditions, measurements were made in buffered 150 mM sodium chloride solutions. Mixtures of 0.1% lysozyme and 0.1% HSA were prepared and the extent of protein−MGuar binding was measured for a series of modified guars. The results, summarized in Figure 5, show that the C10 and C12 modified guars had the highest HSA and the lowest lysozyme binding. These results suggest there is potential for HSA to bind MGuar in the tear film where lysozyme concentrations are relatively high.

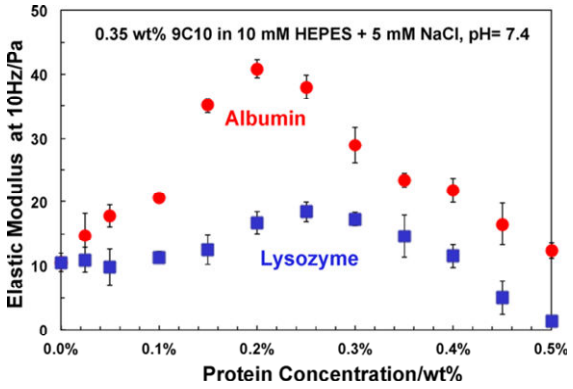

Figure 4. Elastic modulus (10 Hz with a constant stress of 0.055 Pa) of 0.35 wt % MGuar 9C10 versus the concentration of added albumin or lysozyme.

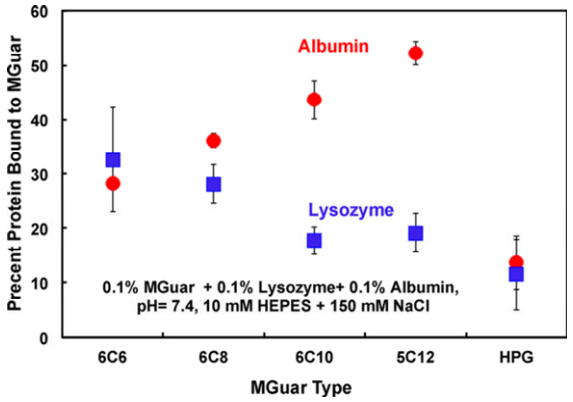

Figure 5. Competitive binding of HSA and lysozyme to MGuar. The parent oxidized hydroxypropyl guar had a carboxyl DS of 0.201 (Table 1). The error bars are the standard deviation values based on three replicates.

HSA binding to MGuar is rapid. Supporting Information Table S2 shows that binding results measured 24 h after mixing were the same as those determined immediately after mixing HSA with MGuar.

The ability of HSA bound to multiple MGuar chains to increase viscosity is of interest if the effects occur under ophthalmically relevant HSA concentrations. Figure 6 shows the viscosity of 6C10/HSA mixtures and the corresponding amounts of bound HSA. At the HSA concentration giving the highest viscosity, the binding measurements indicate that the MGuar was about half saturated with bound HSA. These conditions facilitate inter guar chain coupling by bound HSA, as predicted by the analysis of Borrega et al.[15] The maximum amount of bound HSA was about 0.35 g/g of MGuar; this value is about an order of magnitude less than maximum values reported by Porcar et al.[19] for HSA binding to poly(acrylic acid) with 3 mol % dodecyl hydrophobic substituents. The relatively poor HSA binding characteristics of 6C10 MGuar could be a reflection of the lower chain length of our hydrophobe, the high ionic strength and low pH (compared to that in Porcar et al.), repulsion from residual carboxyls, and/or the inability of the protein to compete with micellization of the hydrophobes along the polymer chain. Of these possibilities, we speculate that hydrophobe chain length and ionic strength/pH differences are the key factors.

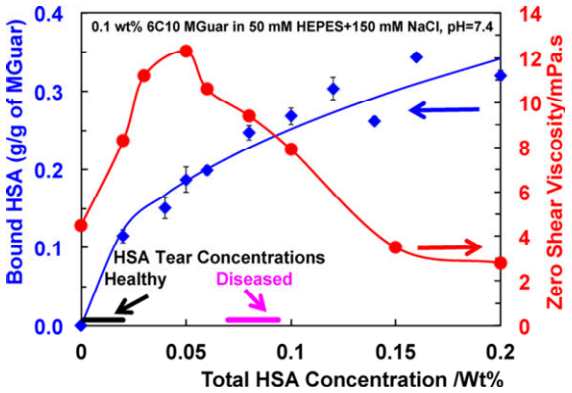

Figure 6. MGuar 6C10 viscosity (steady shear measurements extrapolated to zero-shear rate) and the corresponding content of MGuar-bound HSA as a function of the total HSA concentration. HSA concentrations in healthy eyes have been reported to be between 0.001 wt %[20] and 0.02 wt %,[14] whereas diseased eye concentrations have been reported from 0.07 wt %[21] to 0.094 wt %.[14]

The results in Figure 6 suggest that it is indeed possible to achieve HSA-induced gelation of MGuar; however, there are three important questions: (1) are the tear fluid HSA concentrations sufficiently high to produce weak gels, (2) are the gels sufficiently strong, and (3) do other tear film components influence gelation? These questions are now considered.

HSA is a minor component of tear fluid in healthy eyes; however, some disease conditions cause HSA leakage from blood capillaries, giving higher BSA concentrations in tears. The bars on the bottom of Figure 6 show a range of HSA contents in healthy (0.001 wt %[20] to 0.02 wt %[14]) and diseased eyes (0.07 wt %[21] to 0.094 wt %[14]). Our results show that MGuar−HSA gels can be formed at ophthalmically relevant concentrations, but are the gels strong enough?

Figure 6 shows a 3-fold increase in the zero-shear viscosity at the optimum MGuar−HPG ratio. Without clinical test results, we cannot comment on whether this is sufficient to improve the performance of dry eye drop formulations. Petit et al.[9] showed that with higher polymer and BSA concentrations viscosity can be increased by an order of magnitude. Therefore, we believe there is scope to optimize MGuar structures to obtain higher gel strengths.

Tear fluids are complex mixtures. With our simple model formulations, we have shown that lysozyme is unlikely to interfere with MGuar−HSA interactions. However, it is well-known that surfactants strongly interact with hydrophobically modified polymers.[22] Therefore, we might expect that other amphophilic materials in tears could compete with HSA.

Shear Thinning in a Blink of the Eye. The human tear layer is a dynamic environment. We blink every few seconds, and with each blink, the eyelid induces shear rates as high as 4250−28 500 s^{-1}.[23] The weak gelation of eye drop polymers on the eye should increase residence time and may also lubricate the blinking eyelid. However, the gels must not be too rigid. Figure 7 shows the results of cyclic viscosity measurements indicating that shear rates between 10 and 100 s^{-1} are sufficient to break MGuar−HSA structures. Therefore, we propose that MGuar−HSA structures are likely to be disrupted by a blinking eye.

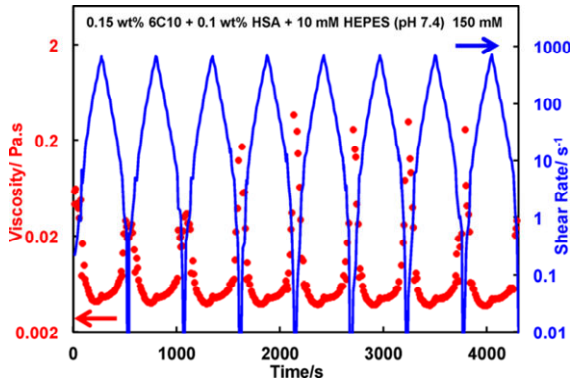

Figure 7. Cyclic viscosity measurements showing the reproducible shear thinning behavior of 6C10-MGuar−HSA complex. Red points show the shear viscosity, and solid lines represent the applied shear rate. Each point was measured with an integration time of 10 s.

CONCLUSIONS

In summary, we have shown that hydrophobically modified guar gives weak gels in the presence of HSA. Specifically, hydrophobically modified guar (MGuar) binds HSA in model tear fluid, resulting in a maximum viscosity increase of about a factor of 2 when the mass concentration ratios of MGuar−HSA were between 1 and 4, depending upon the alkyl group chain length and the degree of alkyl substitution. On the basis of the comparison of a small set of modified guars, the largest viscosity increase was obtained with 6C10, a 2.4 MDa hydroxypropyl guar that was bearing both carboxyl (DS = 0.07) and decylamide groups (DS = 0.06). Furthermore, MGuar−HSA complex structures are shear-thinning and are sufficiently weak to break down reversibly in a blink. On the basis of these initial results, we propose that higher tear HSA concentrations associated with some eye diseases can be exploited to increase tear viscosity when mixed with eye drops containing hydrophobically modified guar.

ASSOCIATED CONTENT

* Supporting Information

Figure S1: Example potentiometric and conductometric titration of oxidized HPG. Figure S2: FTIR spectra of HPG before and after oxidation. Figure S3: Proton NMR spectra of oxidized HPG and 5C12 MGuar. Figure S4: Influence of hydrophobic chain length on the solubility of modified guars with a hydrophobe DS 0.8−1 in low ionic strength. Figure S5: Influence of HSA on the dynamic rheological behavior of concentrated 8C10 MGuar at low ionic strength. Figure S6: Log plots of viscosity vs shear rate showing the reproducible shear thinning behavior of 6C10-MGuar with HSA. Table S1: Titration data for MGuars before and after alkylation. Table S2: Influence of time on protein binding to MGuar. Calculation of MGuar DS values from conductometric titration. This material is available free of charge via the Internet at http://pubs.acs.org.

AUTHOR INFORMATION

Corresponding Author

*E-mail: peltonrh@mcmaster.ca.

Notes

The authors declare no competing financial interest.

ACKNOWLEDGMENTS

The authors acknowledge the technical assistance of Wing Yan Lam, McMaster, and James Davis, Alcon. We thank the National Sciences and Engineering Research Council of Canada (NSERC) and Alcon Laboratories for funding this project. Some measurements were performed in the McMaster Biointerfaces Institute funded by the Canadian Foundation for Innovation. R.P. holds the Canada Research Chair in Interfacial Technologies

REFERENCES

(1) Christensen, M. T.; Cohen, S.; Rinehart, J.; Akers, F.; Pemberton, B.; Bloomenstein, M.; Lesher, M.; Kaplan, D.; Meadows, D.; Meuse, P.; Hearn, C.; Stein, J. M. Clinical evaluation of an HP-guar gellable lubricant eye drop for the relief of dryness of the eye. Curr. Eye Res. 2004, 28, 55−62.

(2) Lu, C.; Kostanski, L.; Ketelson, H.; Meadows, D.; Pelton, R. Hydroxypropyl guar-borate interactions with tear film mucin and lysozyme. Langmuir 2005, 21, 10032−10037.

(3) Davis, J. W.; Ketelson, H. A.; Campbell, E. E.; Meadows, D. L.; Rangarajan, R. Ophthalmic compositions with improved dessication protection and retention. US Patent 2013/0296264 Al, 2013.

(4) Meyer, A. E.; Baier, R. E.; Chen, H. G.; Chowhan, M. Tissue-on-tissue testing of dry eye formulations for reduction of bioadhesion. J. Adhes. 2006, 82, 607−627.

(5) Mafi, R.; Gray, C.; Pelton, R.; Ketelson, H.; Davis, J. On formulating ophthalmic emulsions. Colloids Surf., B 2014, 122, 7−11.

(6) Doublier, J. L.; Garnier, C.; Renard, D.; Sanchez, C. Protein−polysaccharide interactions. Curr. Opin. Colloid Interface Sci. 2000, 5, 202−214.

(7) Roy, I.; Sardar, M.; Gupta, M. N. Cross-linked alginate-guar gum beads as fluidized bed affinity media for purification of jacalin. Biochem. Eng. J. 2005, 23, 193−198.

(8) Pettolino, F. A.; Hoogenraad, N. J.; Ferguson, C.; Bacic, A.; Johnson, E.; Stone, B. A. A (1→4)-beta-mannan-specific monoclonal antibody and its use in the immunocytochemical location of galactomannans. Planta 2001, 214, 235−242.

(9) Petit, F.; Audebert, R.; Iliopoulos, I. Interactions of hydrophobically modified poly(sodium acrylate) with globular proteins. Colloid Polym. Sci. 1995, 273, 777−781.

(10) Gao, J. Y.; Dubin, P. L. Binding of proteins to copolymers of varying hydrophobicity. Biopolymers 1999, 49, 185−193.

(11) Zody, G. M.; Morgan, M. E. Hyrophobically modified non-ionic polygalactomannan ethers. US Patent 4,870,167, 1989.

(12) Young, N. W. G.; Williams, P. A.; Meadows, J.; Allen, E. A promising hydrophobically-modified guar for completion applications. Soc. Pet. Eng. J. 1998, 2, 463−470.

(13) Lapasin, R.; De Lorenzi, L.; Pricl, S.; Torriano, G. Flow properties of hydroxypropyl guar gum and its long-chain hydrophobic derivatives. Carbohydr. Polym. 1995, 28, 195−202.

(14) Versura, P.; Bavelloni, A.; Grillini, M.; Fresina, M.; Campos, E. C. Diagnostic performance of a tear protein panel in early dry eye. Mol. Vision 2013, 19, 1247−1257.

(15) Borrega, R.; Tribet, C.; Audebert, R. Reversible gelation in hydrophobic polyelectrolyte/protein mixtures: an example of cross-links between soft and hard colloids. Macromolecules 1999, 32, 7798−7806.

(16) Wu, X. Y.; Ye, Y. Q.; Chen, Y. N.; Ding, B.; Cui, J. J.; Jiang, B. Selective oxidation and determination of the substitution pattern of hydroxypropyl guar gum. Carbohydr. Polym. 2010, 80, 1178−1182.

(17) Reuben, J. Description of heteropolysaccharide ethers▪ hydroxypropyl guar and carboxymethyl guar. Macromolecules 1985, 18, 2035−2037.

(18) Craig, J.; Simmons, P.; Patel, S.; Tomlinson, A. Refractive index and osmolality of human tears. Optom. Vision Sci. 1995, 72, 718−724.

(19) Porcar, I.; Gareil, P.; Tribet, C. Formation of complexes between protein particles and long amphiphilic polymers: Binding isotherms versus size and surface of the particles. J. Phys. Chem. B 1998, 102, 7906−7909.

(20) Balasubramanian, S. A.; Pye, D. C.; Willcox, M. D. P. Levels of lactoferrin, secretory IgA and serum albumin in the tear film of people with keratoconus. Exp. Eye Res. 2012, 96, 132−137.

(21) Bron, A.; Mengher, L. The ocular surface in keratoconjunctivitis sicca. Eye 1989, 3, 428−437.

(22) Kastner, U.; Zana, R. Interactions between quaternary ammonium surfactant oligomers and water-soluble modified guars. J. Colloid Interface Sci. 1999, 218, 468−479.

(23) Tiffany, J. M. The viscosity of human tears. Int. Ophthalmol. 1991, 15, 371−376.

dx.doi.org/10.1021/bm501278g | Biomacromolecules XXXX, XXX, XXX−XXX

Appendix 3: Supporting Information for Chapter 4

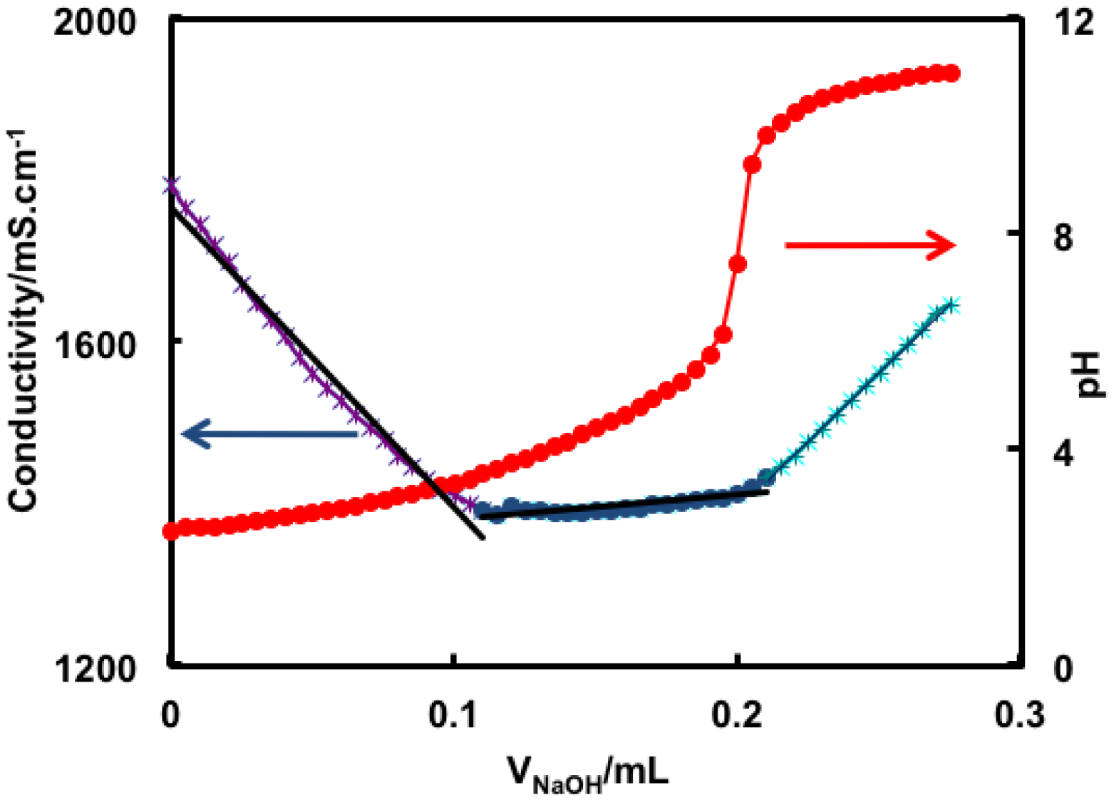

SI Figure 1: Example potentiometric and conductometric titration of oxidized HPG.

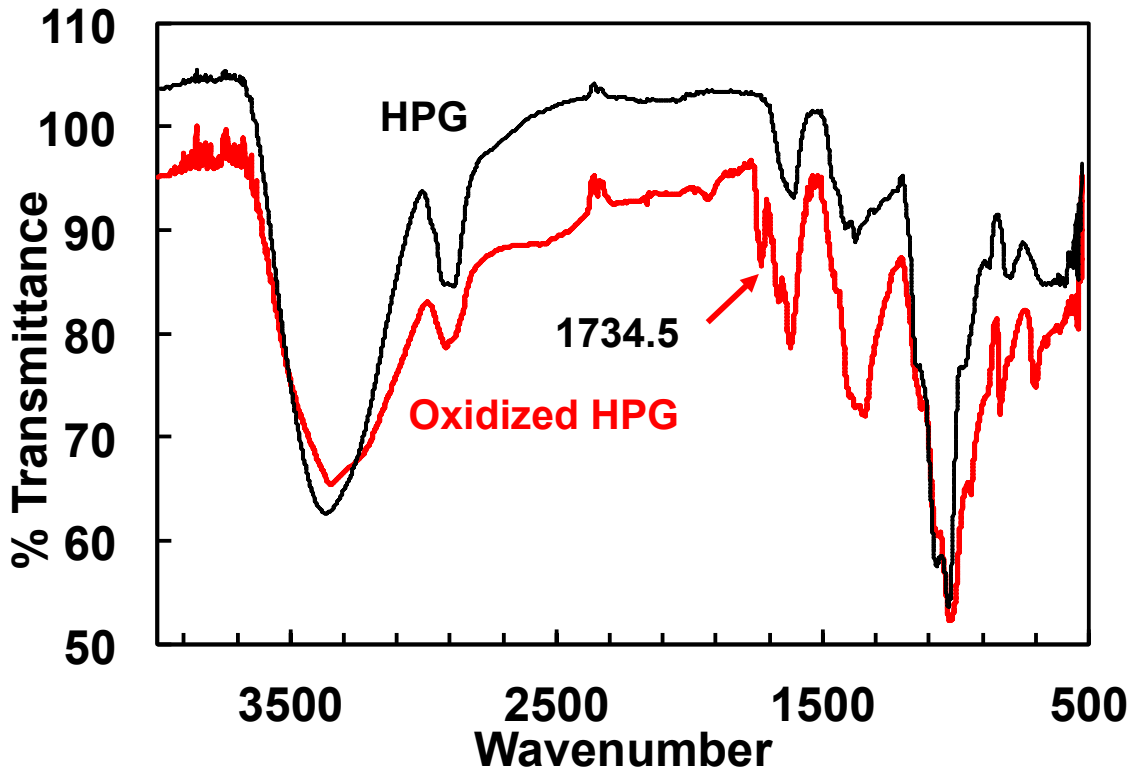

SI Figure 2: FTIR spectra of HPG before and after oxidation.

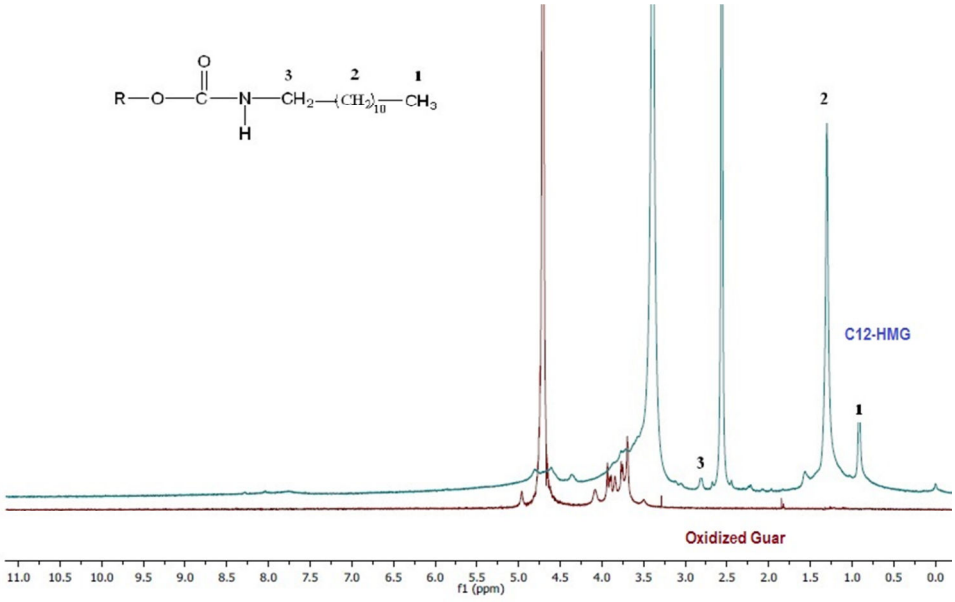

SI Figure 3: Proton NMR spectra of oxidized HPG and 5C12 MGuar

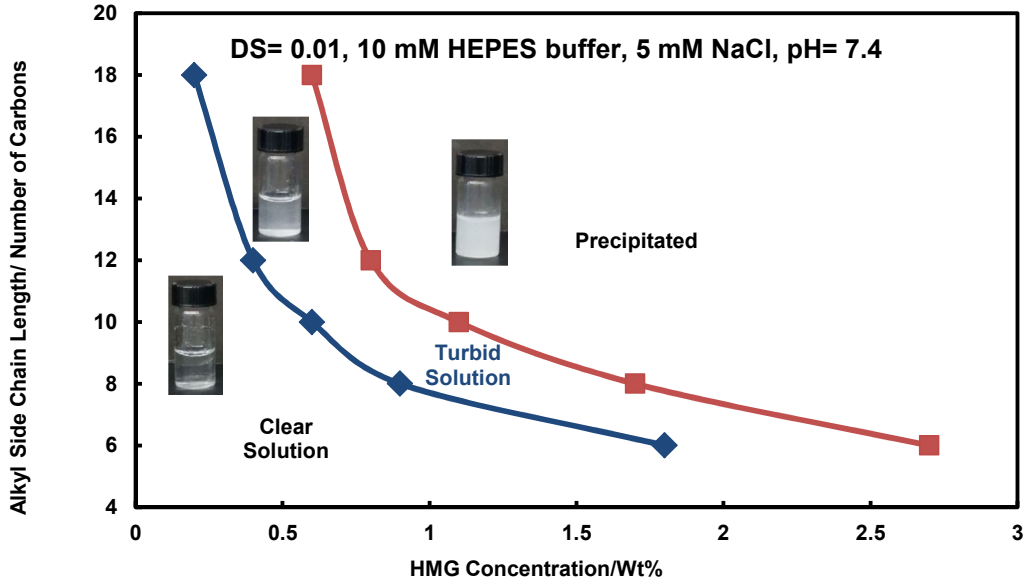

SI Figure 4: The influence of hydrophobic chain length on the solubility of modified guars with a hydrophobe DS 0.8-1 in low ionic strength.

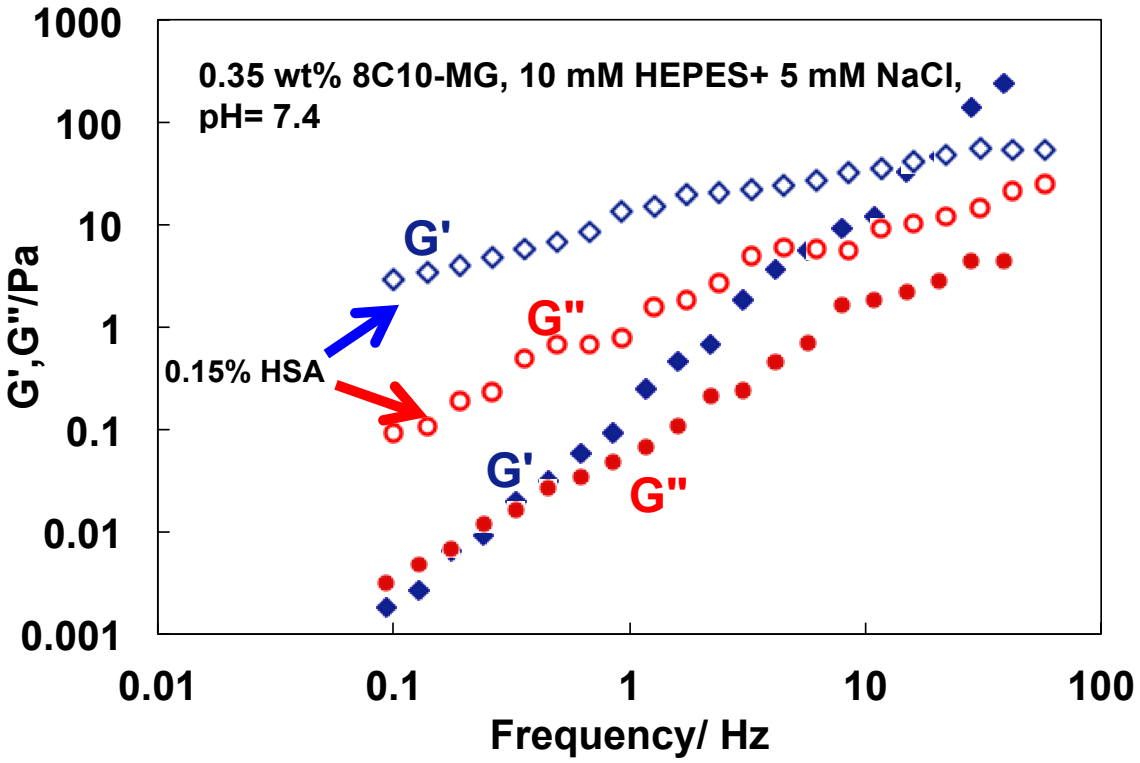

SI Figure 5: The influence of HSA on the dynamic rheological behaviour of concentrated 8C10 MGuar at low ionic strength. 10 mM HEPES+ 5 mM NaCl, pH= 7.4

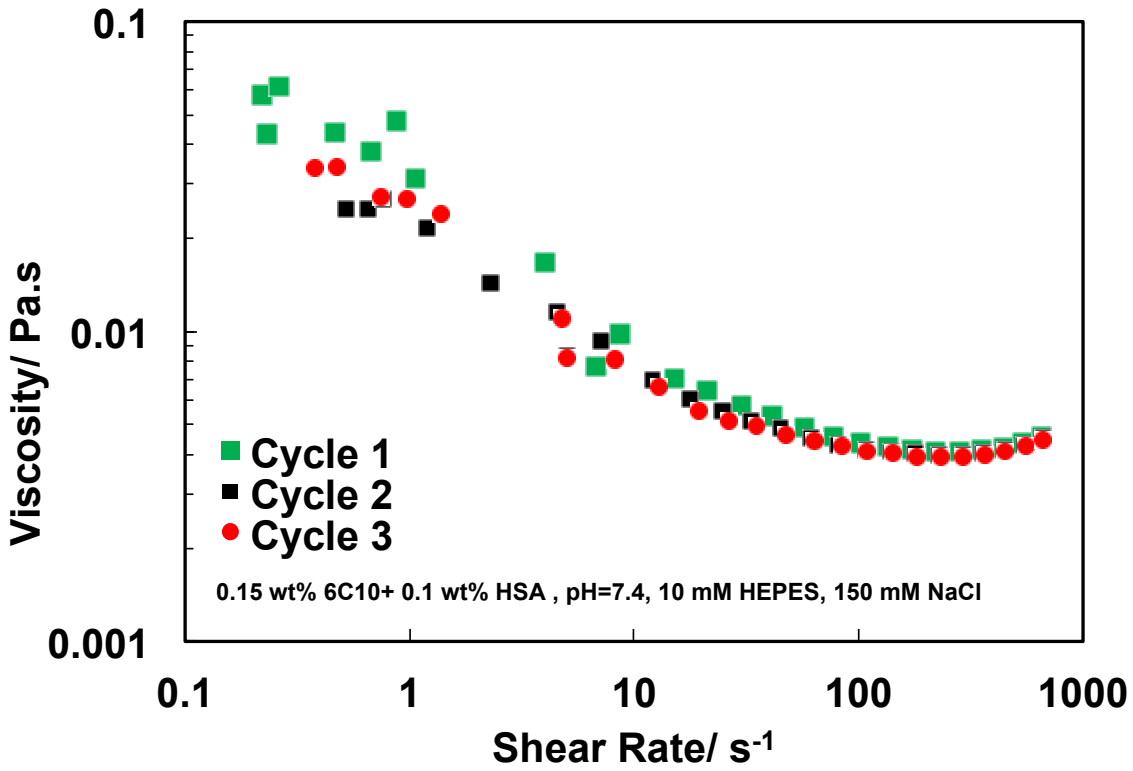

SI Figure 6: An example of viscosity as function of shear rate, showing the shear thinning behavior for the first three cycles of cyclic viscosity measurement in Figure 7.

SI Table 1: Titration data for MGuars before and after alkylation.

MGuar Designation	MGuar Carboxyl Contents (meq/g)		Hydrophobe DS
	Before Alkylation	After Alkylation	
1C6	0.765	0.714	0.009
3C6	0.765	0.569	0.037
6C6	1.08	0.777	0.058
10C6	1.08	0.582	0.097
1C8	0.765	0.700	0.012

6C8	1.08	0.793	0.055
1C10	0.765	0.684	0.015
3C10	0.765	0.605	0.030
6C10	1.08	0.771	0.059
9C10	1.08	0.640	0.087
1C12	0.765	0.713	0.01
5C12	1.08	0.817	0.051
1C18	0.765	0.702	0.012

SI Table 2: The influence of time on protein binding to MGuar.

Type of MG	Bound Albumin (%)	
	Immediate	24 hours
6C6	12.7±2.1	12.0±1.8
6C8	19.4±1.8	21.8±3.1
6C10	27.6±2.2	32.6±6.1
5C12	37.7±2.2	39.9±2.1
HPG	6.8±2.6	7.7±4.4

Introduction

HPG has three structural parameters, MW, DS and the fraction of glactose groups (F_g)

The goal of this calculation is determine the hydrophobic DS from titration data, before and after alkylation.

Nomenclature

C - mass fraction
M - mol/m^3
MW - Da

Quantifying the Structure of Hydroxypropyl Guar

Objective - to convert mass concentration of guar into a molarity of various types of diol units

Input parameters describing HPguar

1.7 Average number of manose groups per galactose

$F_g := \frac{1}{1 + 1.7}$ Mole fraction of galactose units

$DS := 0.36$ Degree of substitution of hydroxy propyl groups on guar

$MW_{HPG} := 1.7 \cdot 10^6 \cdot Da$

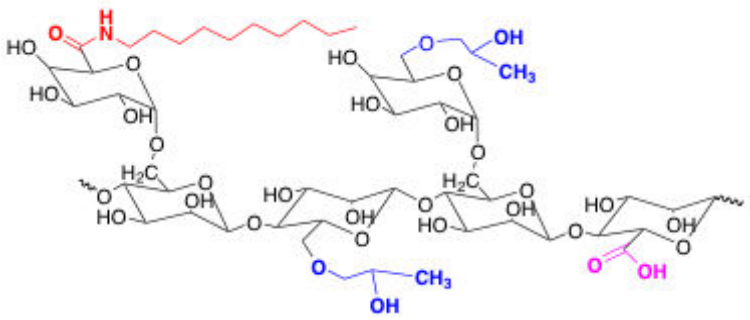

Molecular weight of sugar rings

$MWman := 6 \cdot AM_C + 5 \cdot AM_O + 9 \cdot AM_H = 161.1071 \cdot Da$ MW of Mannose - 1 H

$MWgla := 6 \cdot AM_C + 5 \cdot AM_O + 11 \cdot AM_H = 163.1229 \cdot Da$ MW of galactose - 1O

Consider the polymer to be made of two types of mannose
Type 1 is unsubstituted mannose
Type 2 is a substituted mannose to a galactose pair

$1 - F_g$ Mole fraction of type 1 mannose rings

$F_g = 0.3704$ Mole fraction of type 2 mannose rings and mole fraction of galactose rings and type 2 segments

Average molecular weight of sugar rings in HP guar as function of DS

$$MW_r(DS) := F_g \cdot (MWgla) + \left(1 - F_g\right) \cdot \left(MWman + AM_H\right) + DS \cdot \left(3 \cdot AM_C + AM_O + 6 \cdot AM_H\right)$$

$MW_r(DS) = 183.3951 \cdot Da$ $MW_r(0) = 0.1625\,mol^{-1} \cdot kg$

Derivation

$$MW_{rcooh} = MW_r + DS_{cooh}\cdot\left(AM_O - 2AM_H\right)$$

Molecular weight per sugar ring

$$DS_{cooh} = \frac{Mol_{cooh}}{Mol_{rcooh}} = \frac{EW_{cooh}\cdot gm}{\frac{gm}{MW_{rcooh}}} = EW_{cooh}\cdot MW_{rcooh} = EW_{cooh}\cdot MW_r + EW_{cooh}\cdot\left[DS_{cooh}\cdot\left(AM_O - 2AM_H\right)\right]$$

$$AM_O = AM_O \qquad AM_H = AM_H$$

$$DS_{cooh} = EW_{cooh}\cdot MW_r + EW_{cooh}\cdot DS_{cooh}\cdot\left(AM_O - 2AM_H\right) = X + DS_{cooh}\cdot Y$$

$$DS_{cooh} = \frac{X}{1 - Y} = \frac{EW_{cooh}\cdot MW_r}{1 - EW_{cooh}\cdot\left(AM_O - 2AM_H\right)}$$

Derivation

$$MW_{ralk} = MW_{rcooh} + DS_{alk}\cdot MW_{hp}$$

Average molecular weight per ring after alkylation

$$DS_{alk} = \frac{Mol_{coohinit} - Mol_{coohfinal}}{Mol_{ralk}} = \left(EW_{cooh} - EW_{alk}\right)\cdot MW_{ralk} = \left(EW_{cooh} - EW_{alk}\right)\cdot\left(MW_{rcooh} + DS_{alk}\cdot MW_{hp}\right) = x\cdot MW_{rcooh} + x\cdot\left(DS_{alk}\cdot MW_{hp}\right)$$

$$DS_{alk} = \frac{MW_{rcooh}\cdot\left(EW_{cooh} - EW_{alk}\right)}{1 - \left(EW_{cooh} - EW_{alk}\right)\cdot MW_{hp}}$$

Tempo Oxidized HPG

$meq := 0.001\,mole$

$EW_{cooh} := 1.08\frac{meq}{gm}$ From conductometric titration for 1C6

$DS_{cooh}(DS, EW_{cooh}) := \frac{EW_{cooh} \cdot MW_r(DS)}{1 - EW_{cooh} \cdot (AM_O - 2AM_H)}$

$DS_{cooh}(DS, EW_{cooh}) = 0.2011$

$MW_{rcooh}(DS, EW_{cooh}) := MW_r(DS) + DS_{cooh}(DS, EW_{cooh}) \cdot (AM_O - 2AM_H)$

$MW_{rcooh}(DS, EW_{cooh}) = 0.1862\,mol^{-1} \cdot kg$

Alkylated Oxidized HPG

Titration results for 5C6

$EW_{alk} := 0.777\frac{meq}{gm}$ alkylated sample

$EW_{cooh} := 1.08\frac{meq}{gm}$ parent oxidized HPG

$MW_{hp} := AM_N - AM_O + 6 \cdot AM_C + 13 \cdot AM_H$ Molecular weight of hydrophobe - 1 proton

$MW_{hp} = 0.0832\,mol^{-1} \cdot kg$

$DS_{alk}(DS, EW_{cooh}, EW_{alk}, MW_{hp}) := \frac{MW_{rcooh}(DS, EW_{cooh}) \cdot (EW_{cooh} - EW_{alk})}{1 - (EW_{cooh} - EW_{alk}) \cdot MW_{hp}}$

$DS_{alk}(DS, EW_{cooh}, EW_{alk}, MW_{hp}) = 0.0589$

$MW_{ralk}(DS, EW_{cooh}, EW_{alk}, MW_{hp}) := MW_{rcooh}(DS, EW_{cooh}) + DS_{alk}(DS, EW_{cooh}, EW_{alk}, MW_{hp}) \cdot MW_{hp}$

$MW_{ralk}(DS, EW_{cooh}, EW_{alk}, MW_{hp}) = 0.1943\,mol^{-1} \cdot kg$

Calculating number of hydrophobes per bound HSA

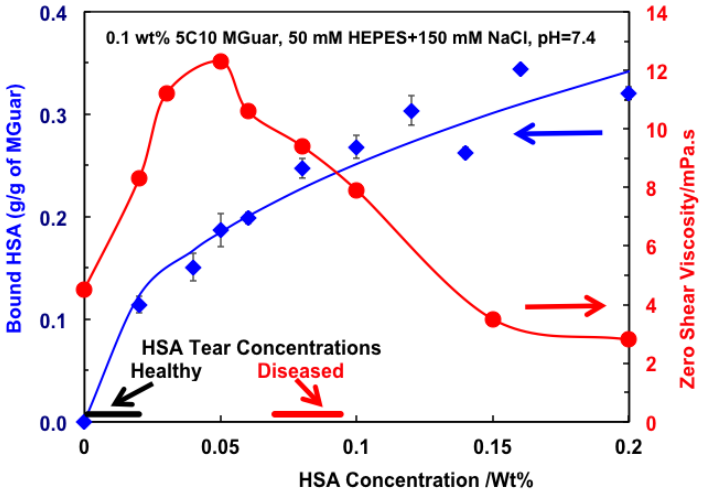

Basis 1 g of MGuar

$HSA := 0.2\,gm$ Mass of bound HSA corresponding to maximum viscosity

$N_{rings} := \frac{gm}{MW_{ralk}(DS, EW_{cooh}, EW_{alk}, MW_{hp})} = 5.1479 \times 10^{-3}\,mol$ number of sugar rings in 1 g of MGuar

$MW_{hsa} := 67000\,Da$

$DS_{hsa} := 1\frac{HSA}{MW_{hsa} \cdot N_{rings}} = 5.7986 \times 10^{-4}$

$\frac{DS_{alk}(DS, EW_{cooh}, EW_{alk}, MW_{hp})}{DS_{hsa}} = 166.83$ Number of hydrophobes per bound albumin

The behavior of emulsion droplets in the solutions containing MGuars while they are interacting with natural tear proteins

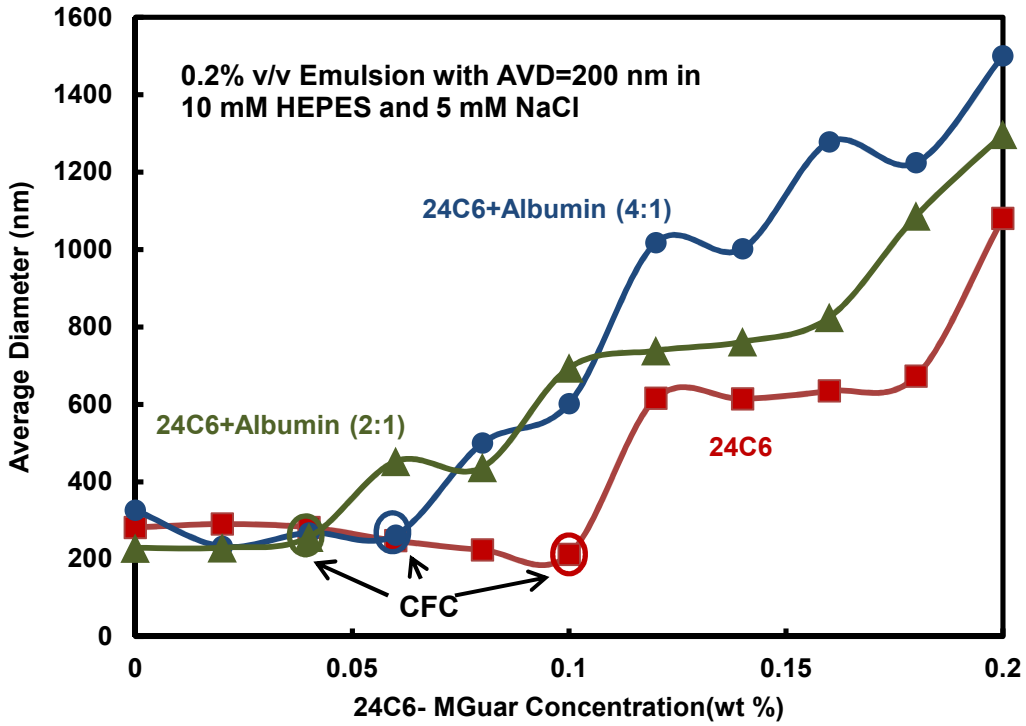

SI Figure 7: Decreasing the CFC due to the interaction of 24%C6-MGuar with HSA. Formation of MGuar/HSA complexes results in higher molecular weight polymers. They show the CFC at lower polymer concentrations. The CFC is considered as the slope change in Average diameter-MGuar concentration curves.

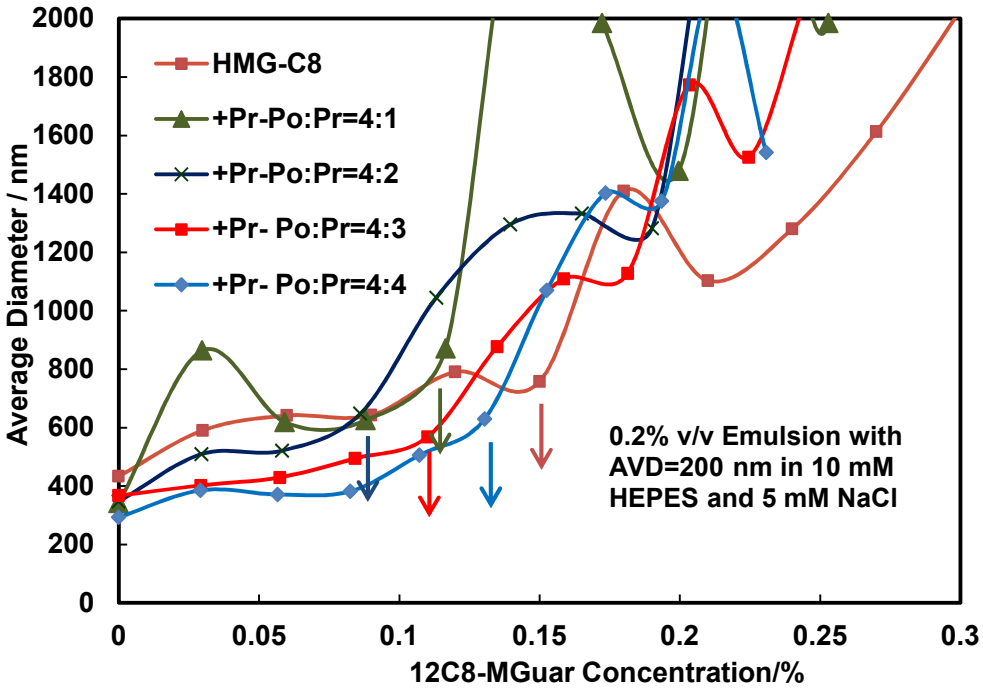

SI Figure 8: Reversible effect of 12C8- MGuar interaction with HSA on the CFC. Formation of MGuar/HSA complexes results in higher molecular weight polymers. They show the CFC at lower polymer concentrations. Saturation of MGuar backbone terminates the chain extension and results in complexes with similar initial molecular weight of the polymer. The 4:2 complex formed the complex that resembles the highest molecular weight. Higher protein ratios moved back the CFC to higher values, similar to the MGuar in the absence of protein. There is a chance that MGuar interacts with emulsion droplets. Data goes up and down at low concentrations as a result of bridging flocculation.

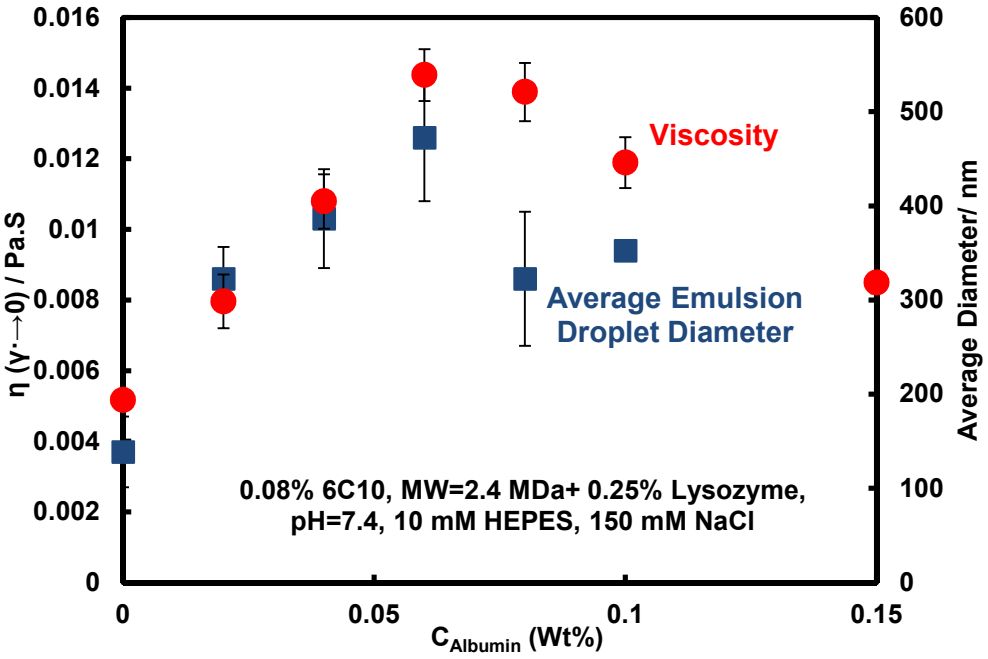

SI Figure 9: Variation of viscosity and average emulsion droplet diameter due to the interaction of 0.08% 6C10-MGuar with HSA as a function of HSA concentration in the ophthalmic environment. The error bars are the standard deviation values based on 3 replicates.

Chapter 5. *In-Situ* Chain Extension through Interaction of Modified Guars with Tear Proteins

In this Chapter, most of the experiments and data analysis were done by myself. Friction tests were done with the help of Wei Zhang. He helped to make the tip and substrate of friction pairs. Cameron Gray helped with QCM-D measurements and Wing Yan Lam helped with protein binding experiments. Dr. Pelton revised several versions and edited them to the final version.

In-Situ Chain Extension through Interaction of Modified Guars with Tear Proteins

Roozbeh Mafi and Robert Pelton*

Department of Chemical Engineering, McMaster University, 1280 Main Street West, Hamilton, Ontario, Canada L8S 4L8

5.1 Abstract

In-situ chain extension of hydrophobically modified guar (MGuar) in tear environment helps control the stability of ophthalmic emulsions and increase the residence time of eye drop over cornea. Low molecular weight MGuar can be optimized to out-perform high molecular weight guars without the complications of formulating eye drops with high molecular weight polymers. Lysozyme, a natural tear protein, is able to extend the effective chain length of MGuar through polymer/protein complex formation. Hydrophobic modifications on guar enable efficient interaction with proteins, through their mutual hydrophobic characteristics. Hydroxypropyl guar samples were oxidized and derivatized linear alkyl amines to give a series of MGuars. To elevate lysozyme affinity to MGuar, various alkyl chain lengths, degrees of substitution and a range of molecular weights were examined. Binding and rheological measurements were employed to evaluate MGuar interactions with lysozyme. Our results suggest that higher degrees of substitution and longer alkyl chain length give higher viscosity values. Lowering molecular weight allows for higher concentration while keeping the initial viscosity constant. Higher viscosity was achieved as the chain extension occurred. The influence of hydrophobic modification and molecular weight variation on lubrication behavior of MGuars has also been determined. Hydrophobic modification enhanced the lubrication between hydrophobic surfaces. However, saturation of hydrophobes with lysozyme abolished the lubricity.

5.2 Introduction

A major concern in producing ophthalmic emulsions is achieving long term stability over their shelf life period. A method to improve the stability is by using polymers. They lower the creaming rate by increasing the emulsion viscosity. On the other hand, polymers can also reduce the emulsion stability. High concentration of polymers in the formulation of emulsion-containing eye drops induces depletion flocculation(*1*). This defines a limit in polymer concentration, which is known as the critical flocculation concentration (CFC). A method for increasing polymer concentration without reaching the CFC is to use low

molecular weight polymers. The CFC occurs at higher values. Therefore, larger volumes of polymer can be incorporated in the formulation of ophthalmic emulsions.

However, even by using low molecular weight polymers, two problems still remain. First, the emulsion must cream quickly upon its application onto the eye. Fast creaming helps rebuild the structure of lipid layer on top of the tear film. Therefore, upon eye drop application, the polymer concentration must be over the CFC. Raising the polymer concentration after introducing the eye drop on the cornea seems impossible. Lowering the CFC by increasing the molecular weight of polymer appears to be a promising method. Secondly, a major part of topically applied liquid eye drops drains immediately after application. Extending the residence time of the eye drop on cornea surface would enhance the therapeutic performance as well. A conventional method to extend the residence time is through increasing the viscosity by using polymers in the formulation of eye drops. However, generating high initial viscosity of eye drops through the use of high polymer concentration or high molecular weight polymers is not desirable. High initial viscosity introduces difficulties during the application and spreading of the eye drop over the cornea. It also produces more resistance against blinking (*2*).

A method to control emulsion stability is through *in-situ* gel formation(*3*). The CFC occurs at low polymer concentration as the molecular weight increases. Depletion flocculation induced by the higher molecular weight polymers helps formation of larger droplets and faster upward movement. This helps rebuild the lipid layer in a much shorter time. *In-situ* chain extension that results in higher molecular weight polymers would also be helpful in extending the residence time of eye drop after its application. It should be noted that for ophthalmic applications, the gel must be weak enough to not inhibit blinking. For this purpose, hydrogels are good choices as they show shear thinning behavior. They flow under shear, exhibit less resistance against blinking and are able to rebuild their structure when shear is removed.

Guar and its derivatives are widely used for ophthalmic applications and have the ability to form hydrogels at very low concentrations and through various crosslinking reaction methods. Herein, we evaluate hydrophobic modification that enables modified guar (MGuar) to form complexes with natural tear proteins as a method of mild *in-situ* gelation. Audebert's research group reported extensive studies on the ability of proteins including lysozyme and albumin to act as reversible crosslinkers for hydrophobically modified polymers (HMPs) (*4-8*). It was observed that gelation for HMPs depended on protein concentration. In our previous work, we have demonstrated the ability of MGuars to interact with human serum albumin (HSA) to effectively increase the viscosity (Chapter 4). The results suggest the possibility of replacing high molecular weight HPG in eye drops with much lower molecular weight hydrophobically modified guar polymer

that is droppable but also forms weak gels on the eye. However, this application is limited to specific types of dry eye disease in which, the level of HSA is increased due to inflammation. HSA concentration in other types of dry eye syndrome or in normal tears is too low to lead to an effective viscosity enhancement.

Similar to HSA, lysozyme contains hydrophobic patches. Considering the protein profile in different tear samples (*9*), lysozyme has relatively high concentration in most types of tears varying from 0.6 to 2.6 mg/ml (*10*). Compared to HSA, its high concentration makes it a more appropriate target for general mild gelation method of MGuars allowing for a broader range of applications. Our previous modifications, however, did not significantly improve the viscosity upon the interaction of MGuar with lysozyme (Chapter 3).

Proteins act as connectors to hydrophobically modified water-soluble polymers when their concentration is in a specific ratio to polymer concentration(*5, 7*). Increasing the protein concentration to some extent induces inter chain links that raise the viscosity; while excessive protein concentration saturates the hydrophobes. As a result, proteins would not share the polymer chains anymore and they lose their effectivity in raising the viscosity(*8*). Due to the relatively high level of lysozyme in tear film, interaction might result in polymer backbone saturation without any viscosity enhancement. Possible solutions could be increasing the number of hydrophobes causing a higher degree of substitution, or using a solution with a higher polymer fraction. A high degree of substitution results in intramolecular associations. This is more significant for longer hydrophobes. Using high polymer concentration also causes the problems associated with high initial viscosity.

We propose two modifications on guar to enable MGuars to interact effectively with lysozyme at ophthalmic relevant concentrations: lowering the molecular weight of MGuars and increasing the degree of substitution of hydrophobes with short chain length. Lowering the molecular weight moves the critical flocculation concentration to higher values(*11*) and more polymer can be used in the formulation. To enable using MGuars with higher degree of substitution, hydrophobes with shorter alkyl chain length must be used.

An important function of the tear film is to reduce friction by acting as lubricant between the eyelid and conjunctiva and the cornea. Boundary lubrication(*12*) , hydrodynamic lubrication(*13*) , mixed film lubrication or squeeze film lubrication (*14*) have been already proposed as mechanisms for mucin and tear film lubrication. When tear film is lacking, blinking can produce dry spots as the eyelids encounter excessive friction. This may even lead to punctate wear of mucus layer and exposure of hydrophobic corneal surface(*15*). Adsorption of a polymer layer to a hydrophobic substrate lowers the

boundary friction coefficient (*16*). We evaluated the influence of applied modifications on the lubrication behavior of MGuar solutions for sample hydrophobic surfaces.

5.3 Experimental

Materials. Native guar with molecular weight of ~3 MDa and hydroxypropyl guar with MW of ~2.4 MDa and DS of 0.36 was provided by Alcon Laboratories (Fort Worth, TX, USA). NaN_3, 4-(2-hydroxyethyl)-1-piperazineethanesulfonic acid (HEPES), NaCl, lysozyme from chicken egg white and Bicinchoninic acid (BCA) assay kit were purchased from Sigma-Aldrich (Oakville, ON, Canada). Polydimethylsiloxane (PDMS)-Sylgard 184 elastomer kit from Dow Corning (MI, USA) was used to prepare hydrophobic elastomer surfaces for friction experiment. Centrifugal Filter Devices with mesh size of 30,000 Nominal Molecular Weight Limit were purchased from Milipore (Billerica, MA, USA). The pH of polymer solutions was adjusted using 0.1N HCl and 0.1 N NaOH. Type 1 water (18.2 MΩcm, Barnstead Nanopure Diamond system) was used to prepare all solutions.

Hydrolysis of Hydroxypropyl Guar (HPG). Using partial acid-heat hydrolysis method in dilute solutions, HPG was hydrolysed to achieve lower molecular weight samples. In a typical experiment, 300 mL of 0.1 wt% HPG solution was heated to 50 °C in a 500 mL sealed three-neck round bottom flask. By adding concentrated HCl (1 N), pH was adjusted 1.0. Equal volumes (30 mL) of solution were removed periodically over a period of a 24 hours and pH was adjusted to 6.0 using NaOH (1 N) to stop the acid hydrolysis reaction. The samples were then purified via dialysis using Spectra/Por Dialysis membranes (Spectrum Laboratories Inc.) with molecular weight cut off of 3500 for two weeks and freeze dried (MillrockTech., BT48A, NY, USA).
Polymer molecular weights (MW) and molecular weight distribution (MWD) were determined by gel permeation chromatography (GPC) system consisting of a Waters 515 HPLC pump, threeWaters Ultrastyragel Linear columns, and a Waters 2414 refractive index detector. The mobile phase was 300 mM NaNO3 in 50 mM phosphate buffer at pH 7. Degraded guar samples were diluted to 0.05 wt % and filtered through a 0.45 *í*m filter (Whatman Autovial) prior to analysis.

Preparation of Hydrophobically Modified Guar (MGuar). Hydrophobic guars were synthesized in a two-step process as has been explained in details in Chapter 4: HPG oxidation and alkylation of oxidized HPG to produce MGuars.

Potentiometric and Conductometric Titration. Potentiometric and conductometric titration were employed to define the degree of substitution (DS) of MGuars. A PCTitrate

titrator (Man-Tech Associates) equipped with a Burivar-I/2 buret and a conductivity electrode connected with a 4010 conductivity meter controlled by PC-Titrate software was used. 5 mmol/L polymer samples in of KCl were prepared and the initial pH was adjusted to about 3.0 using HCl. Using the base into acid titration method and with an injection rate of 60 mV/pH, 0.1 mol/L NaOH was added to titration vessel.

Lysozyme Binding. To determine the effect of ionic strength on the mechanism of lysozyme binding to MGuar, 0.25 mL lysozyme at 0.15 wt% and 0.25 mL MGuar (30C6 at 0.1 wt%) were mixed for about 30 s with a Mini-Vortexer (VWR VM-3000, USA) and transferred to 0.5 mL centrifuge tubes (Amicon Ultra-0.5 mL, Millipore). Protein and MGuar solutions were prepared in 10 mM HEPES buffer while NaCl concentration varied from 5 mM to 150 mM. The mixture was then filtered using 30 kDa filters (Millipore) which are fitted in centrifuge tubes. They were centrifuged for 20 minutes at 14500 (rcf: 14000xg) with an Eppendorf—Mini Spin Plus centrifuge (Hamburg, Germany). BCA protein assay kit (Sigma, USA) was employed to determine lysozyme fraction in the filtrate. 1.9 mL of 50:1 mixture of reagent A (sodium carbonate, sodium bicarbonate, bicinchoninic acid and sodium tartarate in 0.1N NaOH) and reagent B (copper sulphate solution) was mixed and vortex mixed with 0.1 mL lysozyme solution. After incubation for 30 minutes at 37 °C and two hours at room temperature, the concentration of protein was determined by measuring the absorbance at 562 nm and using a linear calibration curve.

Rheological Characterization. ATS controlled stress rheometer equipped with a CC25 concentric cylinder cell (Rheologica Stress Tech HR) was used to measure the dynamic viscosity and elastic modulus. Solutions made with different concentrations of MGuar and lysozyme were loaded into the cup. All experiments were performed at 25°C controlled within ± 0.1 °C using circulation of temperature controlled water-bath. Details of the experiment have been explained in Chapter 4.

Friction Measurements. Friction testing used a procedure and the instrument recently employed in the studies of Zhang *et al*.(*17*). The PDMS prepolymer which contains a mixture of the curing agent and the elastomer base in a 1:10 ratio was initially degassed in a vacuum chamber. PDMS substrate was prepared by casting prepolymer mixture over a microscopic slide and cured at 90 °C for 120 minutes. Elastomer tips were first shaped using a Teflon hemispherical mold and pre-cured at 90 °C for 15 minutes. To produce a smooth surface, tips were coated by a layer of PDMS mixture followed by thorough curing at 90 °C for 2 hours. The average radius of tips was about 3 mm. They then were cooled down and immersed in solution samples for 30 minutes prior to each test.

To perform the friction experiments, the hemispherical tip is loaded against the PDMS substrate with the normal force of 0.1g, 0.5g, 0.8g, 1g, 1.5g and 2g and moved with the

sliding speed of 60 μm/s. Three reciprocating lateral movement cycles were carried and averaged to define the friction force.

Quartz Crystal Microbalance with Dissipation (QCM-D) Monitoring. Polystyrene QCM-D sensors (Q-Sense AB, Gothenburg, Sweden) were cleaned by immersing them in a 1% solution of Deconex in milliQ water for 30 minutes at 30°C followed by thorough rinse of milliQ water and 99% ethanol. They were then dried with nitrogen gas. Measurements were performed with an E4 QCM-D (Q-Sense AB, Gothenburg, Sweden) and monitored using Qsoft401 software version 2.5.2.

For each measurement, a solution of 10 mM HEPES buffer and 150 mM NaCl was injected at a constant flow rate of 150 μL/min followed by injection of guar, 12C8-2400 or 12C8-2400+0.3 wt% lysozyme. With keeping the flow rate constant, injection was continued until reaching a plateau. Afterwards, the sensors were rinsed with the same buffer at 150 μL/min. Processed data from the fifth overtone using Qtools software version 3.0.7 are shown and the changes in resonance frequency, **Δ**f, values have been normalized by the fifth overtone.

5.4 Results

We have previously examined the ability of hydrophobically modified guar to form complexes with HSA (Chapter 4). Formation of these complexes effectively raised the viscosity of MGuar solutions. The interaction, however, only occurs at elevated levels of HSA corresponding to its high concentration in diseased tear due to inflammation. To broaden the range of application for other types of dry eye syndrome, we propose methods to enable the interaction with lysozyme.

Hydrophobically modified guars (MGuars) were synthesized in a two-step process: A series of hydroxypropyl guars including hydrolysed samples with lower molecular weights were first oxidized through TEMPO mediated oxidation. The oxidization resulted in partial carboxylation of C6 hydroxyls (*18*). Alkyl amines were then conjugated to the carboxyl groups. Hydrophobic degree of substitution was measured based on the difference between carboxyl contents before and after alkylation. Table 1 summarizes major properties for various MGuars. Overlap concentration, C*, is calculated from the slope change of the viscosity-concentration curves, while a double logarithmic plot of viscosity against concentration is presented. An example of deriving C* is shown in chapter 2.

Table 1: Properties of MGuars employed for the experiments. MGuars are shown as xCy-z, where x is degree of substitution, y is the length of alkyl chain and z is polymer molecular weight. C* represents the overlap concentration of unmodified HPG. DS value is calculated based on two titrations, bearing the accumulated uncertainties.

Name of Sample	MW(kDa)	Overlap Concentration (C*) %	Carboxyl Degree of Substitution		Degree of Substitution
			Before Alkylation	After Alkylation	
30C6-2400	2400	0.08	0.518	0.222	0.296
4C8-2400	2400	0.08	0.201	0.163	0.038
6C8-2400	2400	0.08	0.201	0.136	0.065
12C8-2400	2400	0.08	0.201	0.084	0.117
12C8-425	425	0.08	0.201	0.073	0.128
12C8-265	265	0.18	0.201	0.086	0.115
12C8-160	160	0.27	0.201	0.090	0.111
12C8-130	130	0.47	0.201	0.076	0.125
10C10-2400	2400	0.08	0.201	0.102	0.099

Lysozyme binding to MGuar. Figure 1 shows the effect of NaCl concentration on the binding strength of lysozyme to 30C6-2400. Lysozyme binds to MGuar at the whole range of salt concentrations from 0 mM to 150 mM. The extent of binding alters with ionic strength variation. Below 20 mM NaCl, over 60% of the total lysozyme binds to MGuar. With increasing the salt concentration and with screening the charged groups both on lysozyme and MGuar backbone, bound lysozyme drops to about 40%. A gradual increase in the binding from 34% to 41% in the range of 50 mM to 150 mM NaCl has been observed.

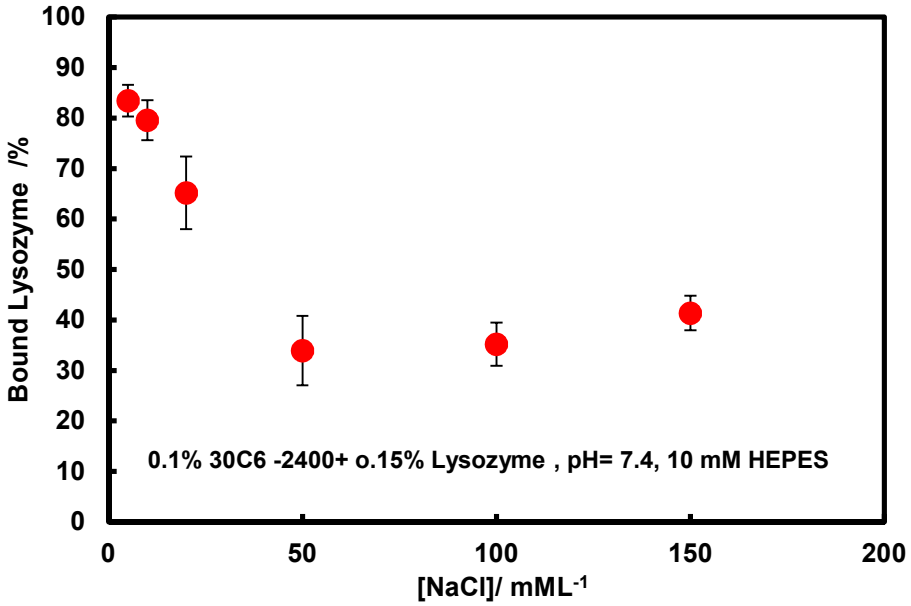

Figure 1: Variation of bound lysozyme to 30C6 as a function of salt concentration. The error bars are the standard deviation values based on 3 replicates.

Network Formation Due to Hydrophobic Interaction. To characterize MGuar/lysozyme complexes, Figure 2 reports the elastic modulus (G') as a function of lysozyme concentration for 12C8-2400 MGuar. The increasing trend of G' towards 0.15% of lysozyme concentration indicates the increase in the number of crosslinks, which leads to a stronger network with a more pronounced G'. We have not directly evaluated the degree of crosslinking. Formation of crosslinks is referred to the increase in viscosity or elastic modulus. Therefore, crosslinks might occur between a few number of polymer chains that only lead to chain extension and not an actual network formation. Saturation of the MGuar backbone due to the excessive concentration of lysozyme breaks the network and lowers the elastic modulus. Higher polymer concentration better shows the ascending and descending trends of complex formation and decomposition of the structure.

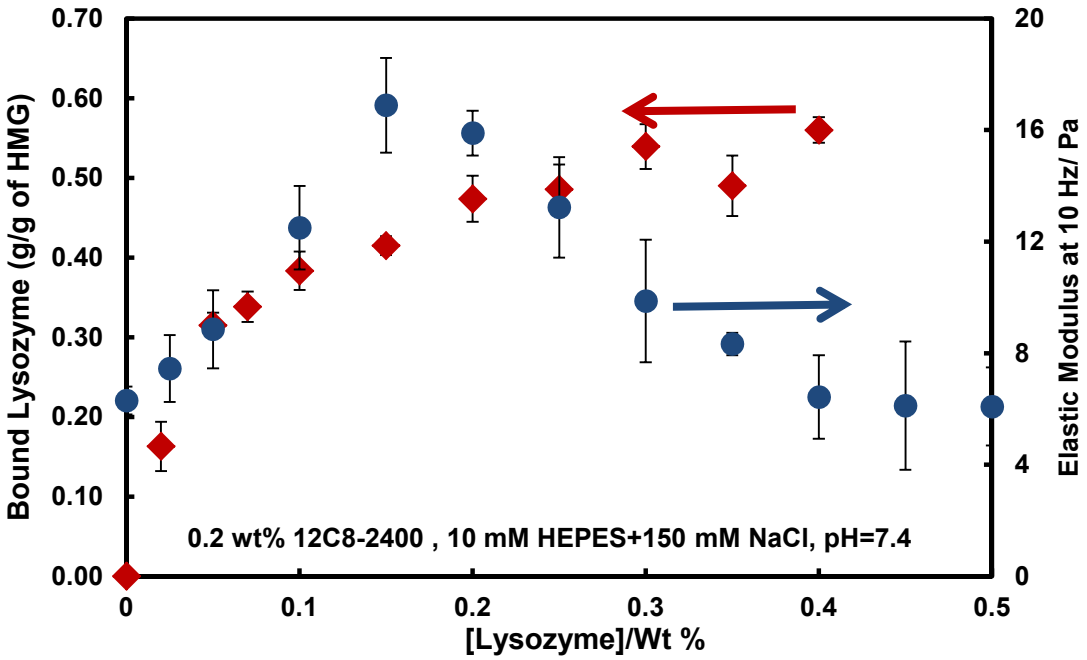

Figure 2: Variation of the elastic modulus (●) at 10 Hz for 12C8-2400-MGuar at 0.2 wt% concentration and the corresponding content of MGuar-bound lysozyme (♦) as functions of the total lysozyme concentration. The error bars are the standard deviation values based on 3 replicates.

Effect of Degree of Substitution. Zero shear viscosity has been estimated through extrapolation of the low shear rate viscosity region. A sample of zero shear rate viscosity derivation method for native guar in three different concentrations is shown in SI Figure 1. Variation of zero shear rate viscosity with lysozyme concentration has been evaluated for three types of C8-MGuars. Degrees of substitution of 4, 6 and 12 were compared. Figure 3 shows that the higher number of alkyl pendant groups leads to the interaction being effective at higher lysozyme concentration, close to the relevant range of ophthalmic concentration. Higher DS also produces a higher maximum viscosity, possibly due to the higher number of crosslinks. Oxidized hydroxypropyl guar has been compared with the C8-MGuars as a backbone reference without hydrophobes. No significant influence was observed on the oxidized guar with the addition of lysozyme. MGuars with 8 carbons in the pendant alkyl chain have the advantage of lower possibility of inter and intra molecular associations compared to C10 and C12, where higher DS is required to maintain the efficiency in raising viscosity.

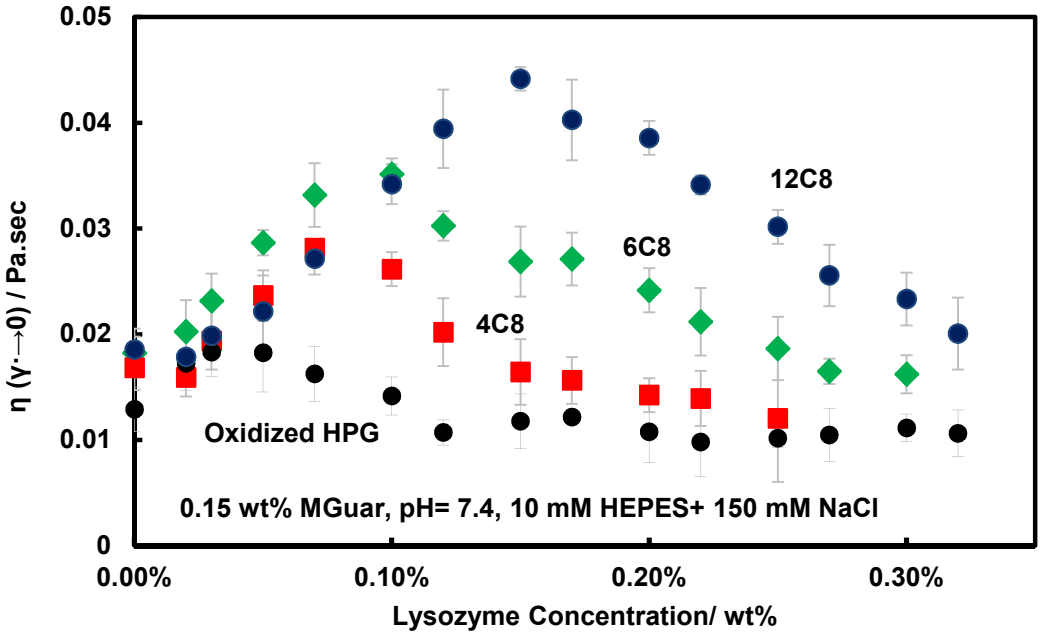

Figure 3: The influence of lysozyme concentration on zero shear viscosities of a series of modified guars. Viscosity measurements conducted in the shear rate range of 0.01 s^{-1} to 100 s^{-1} with delay and integration times of 1s. The error bars are the standard deviation values based on 3 replicates.

Effect of Molecular Weight. MGuars with various molecular weights have been made through acid hydrolysis of hydroxypropyl guar followed by oxidization and alkylation. Figure 4 compares the interaction of lysozyme with hydrolysed 12C8-MGuars at their overlap concentrations, which is the transition point between dilute and semi-dilute regimes. Solutions exhibit similar behavior prior to interaction with lysozyme. It is worth considering that solutions made with polymers of different molecular weights are not showing the same viscosity at similar mass concentrations. To reach similar viscosity, higher concentration of low molecular weight MGuar can be used.

Solubility limit and the critical flocculation concentration (CFC) of 12C8-MGuars with various molecular weights are summarized in Table 2. Emulsions are made using hexadecane as the oil phase and according to the procedure, which has been explained in Chapter 2. Emulsion droplets are stabilized by an anionic surfactant, phosphatidylcholine. The slope change in the average diameter- polymer concentration has been considered as the CFC as shown in SI Figure 2.

Table 2: The critical flocculation concentration (CFC) and solubility limit of 12C8-MGuars. Absorbance of 0.5 at 285 nm has been considered as the limit of solubility.

Molecular Weight (kDa)	130	265	425	2400
Solubility Limit (wt %)	0.7	0.65	0.65	0.5
CFC (wt %)	0.45	0.30	0.25	0.10

Polymer/protein complexes made with lower molecular weight MGuar resulted in the maximum viscosity with a greater value at higher protein concentrations. Higher number of polymer chains in the solution consumes larger fractions of lysozyme as the total number of hydrophobes is higher. Two solutions with 0.08 weight percent 12C8-2400 MGuar and 0.51 weight percent 12C8-130 were compared. They both exhibited similar zero shear viscosity of 6.9 mPa.s. The number of hydrophobes in the 12C8-130 solution is about 6.4 times higher than the MGuar with molecular weight of 2.4 MDa.

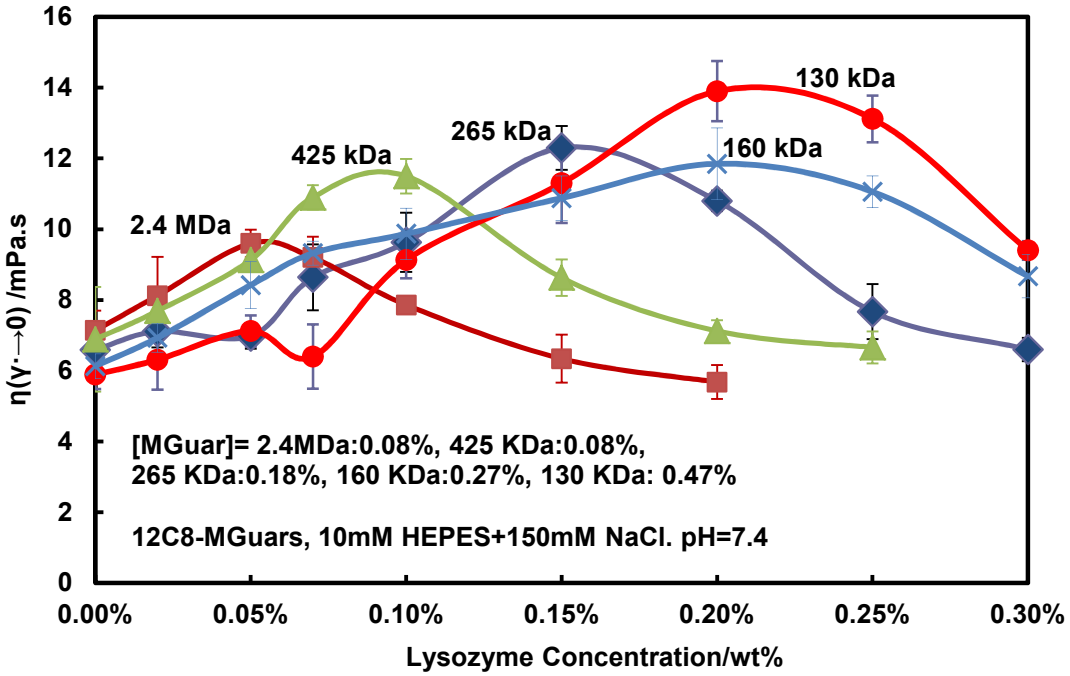

Figure 4: Molecular weight effect of 12C8-MGuars hydrolysed for different hours at their C* on the interaction with lysozyme. Viscosity measurements conducted in the shear rate range of 0.01 s^{-1} to 100 s^{-1} with delay time and integration time of 1s. The error bars are the standard deviation values based on 3 replicates.

To compare the shear thinning behavior of solutions made with different molecular weights, three different MGuar- lysozyme complexes with similar zero shear viscosity were prepared. Complex A contained 12C8-2400 MGuar, while we used hydrolysed MGuars with 425 kDa and 130 kDa for complexes B and C, respectively. Results are shown in Figure 5. At high shear rates (100.s^{-1}), the viscosity of complex C, which contains 12C8-130, is about 1.7mPa.s while 12C8-2400 reached the plateau at 5.7mPa.s. Therefore, complexes containing lower MW MGuars have less resistance against blinking, where a high shear rate of more than 4000 s^{-1} (*19*) is induced by eyelids.

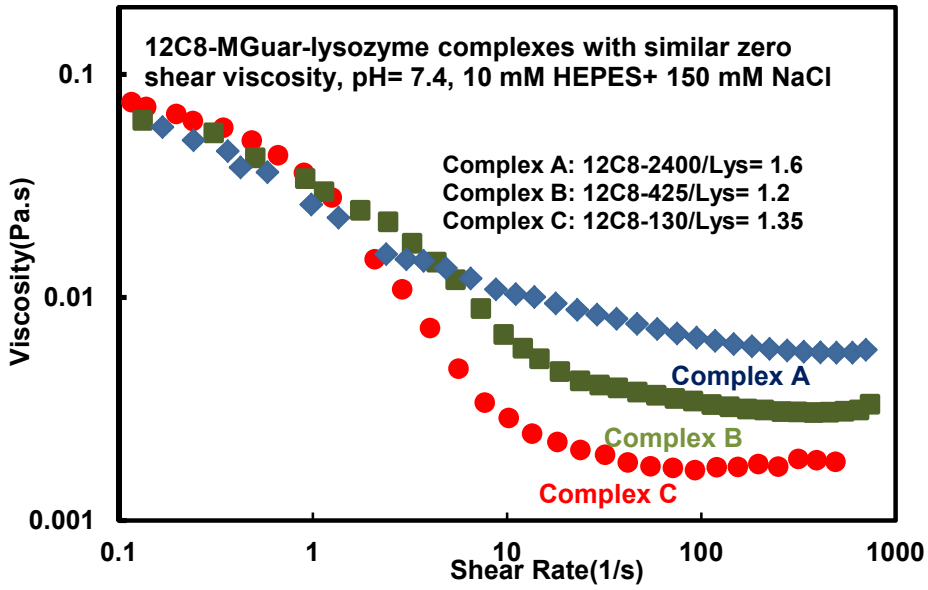

Figure 5: A log-log plot of viscosity vs shear rate showing the shear thinning behaviour of complexes of 12C8-MGuars and lysozyme with similar zero shear viscosities (12C8-2400, MGuar/lys.: 1.6; 12C8-425, MGuar/lys.: 1.2; 12C8-130, MGuar/lys.:1.35).

An important function of artificial tear solutions is to reduce the friction between the eyelid and the hydrophobic areas of the damaged cornea epithelium(*20*). Herein, we discuss the influence of guar modifications on lubrication. Various guar and modified guar samples were employed to measure the changes on friction between PDMS tip and substrate, as a model contact of the eyelid/eyeball. Both tip and substrate were immersed in polymer solution for an hour. First, we compared the adsorption of guar, MGuar and MGuar with added lysozyme on QCM-D sensors.

Adsorption on Hydrophobic Surfaces. Adsorption behaviors of guar, 12C8-2400 and 12C8-2400+ 0.3wt % lysozyme on PS sensor were compared and results are shown in Figure 6. This has been evaluated by QCM-D measurements on standard polystyrene (PS) sensors. PS sensors were selected to resemble the hydrophobic character of PDMS surfaces. Native guar does not adsorb on PS surface, while hydrophobically modified guar, 12C8-2400, adsorbed and caused 35 Hz decrease in frequency. This corresponds to 5.5 $mg.m^{-2}$ adsorbed polymer, which has been estimated by Sauerbrey equation. The effective thickness obtained from Voight viscoelastic model of QCM-D software is 75 nm. The radius of gyration of native guar with the molecular weight of 2.4 MDa has been previously reported to be about 200 nm(*21*). Hydrophobic modification enables MGuar molecules to adsorb onto hydrophobic surfaces. Saturation of hydrophobes on the backbone of 12C8-2400 with lysozyme molecules prevents the adsorption. No frequency

change has been observed for the 12C8-2400+ 0.3wt % lysozyme sample. According to the information given in SI Figure 4, the concentration of free lysozyme when 0.3 wt% lysozyme is exposed to 0.1 wt% 12C8-2400 MGuar is about 2.55 $g.L^{-1}$.

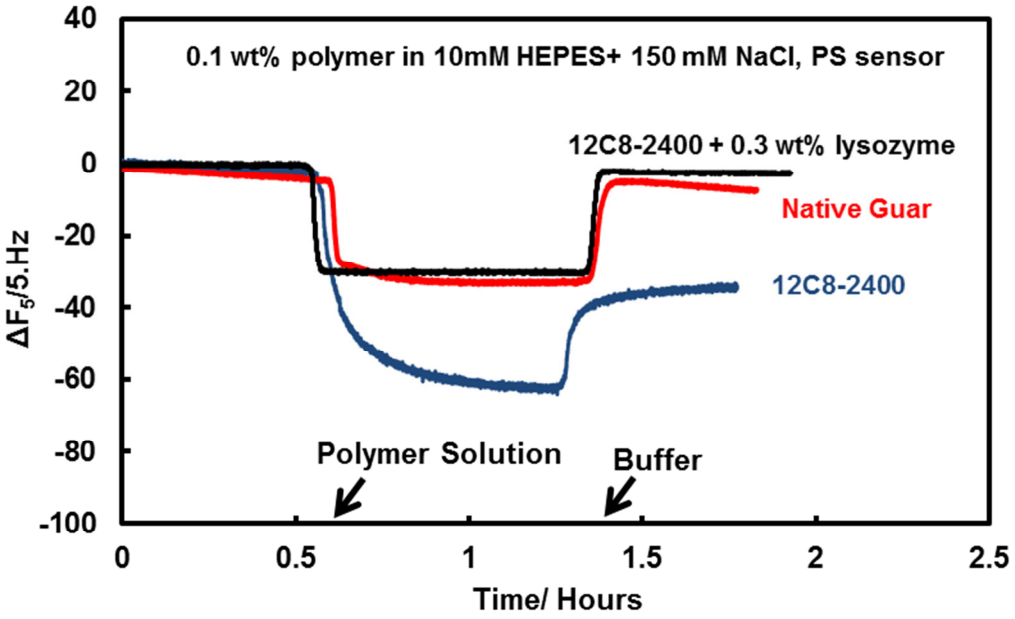

Figure 6: Comparing the adsorption of 12C8-2400 MGuar and Native Guar on standard polystyrene QCM-D sensor by the variation in frequency. The surface represents the hydrophobic surface.

Lubrication. Friction force was measured as a function of applied normal load and plots for different samples are presented in Figure 7. The average friction forces were calculated according to equation (1), which takes the average of F, lateral forces loops. A sample is shown in Figure 8 for 12C8-2400. Overlap of cycles shows that the friction force does not change with the progress of experiment.

$$F = \frac{\bar{F}_{forward} - \bar{F}_{reverese}}{2} \qquad (1)$$

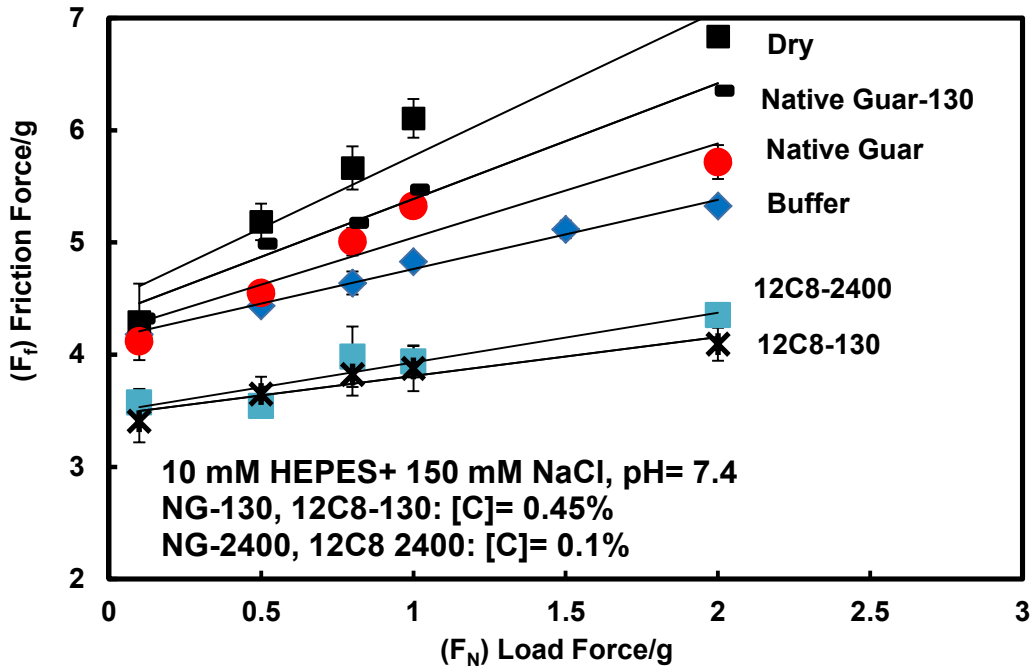

Figure 7: Plots of friction force versus applied load for various guar and MGuar solutions compared with wet and dry surfaces. Both tip and substrate were PDMS and entrainment speed was set to 60 µm/s. The error bars are the standard deviation values based on 3 replicates.

For smooth surfaces, the adhesion component due to molecular interaction cannot be ignored(*22*). Therefore, friction coefficients, which are summarized in Table 3, have been calculated based on the Bowden and Tabor theory (equation 2)(*23*). The intercept, σA, is the adhesion component and slope of each curve in Figure 7 shows the friction coefficient

$$F_f = \mu_B . F_N + \sigma A \qquad (2)$$

Table 3: Friction Coefficient (μ_B) between PDMS Tip and Substrate for various solutions. μ_B was calculated based on the Bowden and Tabor theory.

	Lubricant						
	Air	**Buffer**	**NG**	**NG-130**	**12C8-2400**	**12C8-130**	**12C8-2400+ 0.3 % Lysozyme**
Polymer Concentration (wt %)	_	**0**	**0.1**	**0.45**	**0.1**	**0.45**	**0.1**
MW of Polymer (kDa)	_	_	**2400**	**130**	**2400**	**130**	**2400**
Friction Coefficient (μ_B)	**1.29**	**0.62**	**0.84**	**1.03**	**0.44**	**0.35**	**0.79**
Zero Shear Viscosity (mPa.s)	–	**1** ±0.05	**2.89** ±0.17	**1.95** ± 0.11	**7.14** ±0.56	**5.89** ±0.41	**6.60** ±0.61

Native guar increases the friction coefficient from 0.62 (value of buffer) to 0.84. Employing low molecular weight guar (130 kDa) allows increasing the concentration of guar without a significant change in viscosity. However, the higher guar concentration further elevates the friction coefficient value to 1.03. Adsorption of MGuar to hydrophobic substrate, which caused about 30 Hz decrease in frequency, improved the lubrication as well and lowered friction coefficient to 0.44. The measurements show that the lowest friction coefficient was observed for 12C8-130 with the polymer concentration of 0.45%.

Friction coefficient of 12C8-2400, while it was saturated with lysozyme at 0.3 wt% is almost similar to native guar solution. This could be due to the blockage of hydrophobic sites that hinders MGuars to adsorb onto the PDMS surface. Zero frequency change in QCM-D measurement in Figure 6 corroborates this hypothesis.

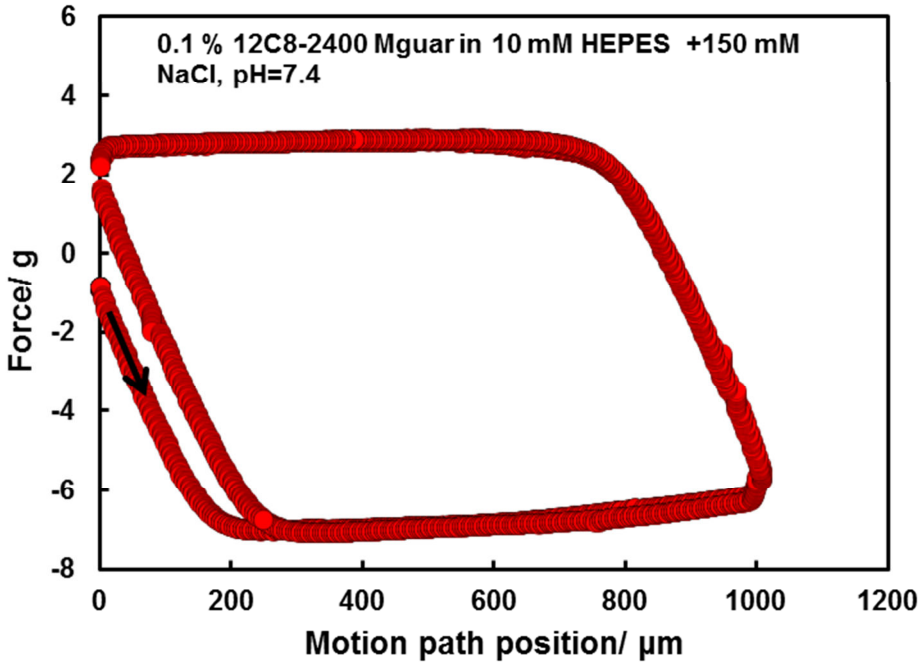

Figure 8: Friction force loops for a PDMS tip sliding over a PDMS substrate and immersed in a 0.1% solution of 12C8-2400 MGuar. Sliding speed=60 µm/s and normal force=0.5g.

5.5 Discussion

Water-soluble polymers are used in the formulation of artificial tear emulsions to provide lubricity and to increase the residence time. There is a concentration limit for incorporating polymers into the formulation. In bottle, concentration should be kept below the overlap concentration to avoid depletion flocculation(*1*). On the other hand, low initial viscosity causes better spreading of topically administrated eye drop over the surface of cornea. In the eye, chain extension of polymers through the formation of weak crosslinks helps rebuilding the lipid layer on the outer most layer of tear film and extends the residence time of the eye drop. Extending residence time through mild *in-situ* gelation produces viscoelastic hydrogels with shear thinning behavior where there is low resistance against blinking. Lysozyme, a protein with high concentration in tear film, has been found to be a potential connector that helps form a weak network through interactions with hydrophobically modified guar at physiologic conditions.

Depending on the salt concentration, electrostatic or hydrophobic interactions may govern the binding extent of lysozyme to MGuars. At low salt concentrations (below 20 mM)

and at physiologic pH, electrostatic interaction due to the presence of carboxylic acid groups in the backbone of MGuar dominates. Increasing the salt concentration towards the actual value of natural tear significantly reduces the bound lysozyme fraction as charged groups are screened. Hydrophobic interaction, which defines the binding extent over 50 mM salt concentration, has been improved towards 150 mM. This can be due to the stronger hydrophobic interaction at elevated salt concentration.

There are various methods that can effectively raise the viscosity in the concentration range of lysozyme in tear film. Increasing the degree of substitution is a method which moves the maximum viscosity to higher lysozyme concentrations. Although higher DS of hydrophobes on MGuar produces a more pronounced viscosity at the ophthalmic range, it has the disadvantage of improving the inter- and intra-molecular associations. As a result, solubility of MGuars becomes lower as the hydrophobic strength in the polymer backbone increases.

Molecular weight is the other controlling parameter, which defines the effective concentration range of protein for the interaction with MGuars. First, lowering the polymer molecular weight improves the accessibility of protein molecules to hydrophobic sites by raising the mobility of MGuar chains. Moreover, higher polymer volumes can be loaded into the formulation to reach the same initial viscosity. This moves the maximum viscosity to higher lysozyme concentrations due to the existence of a higher number of hydrophobic pendant groups in the backbone of total loaded polymer. Increased number of crosslinks in complexes containing lower molecular weight MGuars leads to formation of a network with higher number of crosslinks and consequently higher maximum viscosity as has been shown in Figure 4. Extending the hydrolysis intervals over 30 hours may result in polymers of low molecular weight (around 50 kDa), which may form a shell around protein molecules with a bigger size in a similar behavior that has been reported previously(*7*). Therefore, the protein molecules cannot be used as connectors between MGuar chains to raise the viscosity.

MGuar/lysozyme complexes are shear thinning and break easily with the high shear rate. Complexes with lower molecular weight polymers are more shear thinning. They exhibit lower viscosity at high shear rates when the structure is broken due to the applied shear rate and while the initial viscosity is similar. This effect improves the mixed and hydrodynamic lubrication.

Similar to the work of De Vicente *et al.* (*24*), while hydrophobic surfaces are sliding over each other at low speed, addition of even small amount of water-soluble polymer into water increases the friction compared to water. The increase of friction coefficient in the presence of non-adsorbing random coil polysaccharides such as guar gum supports

previous studies (*25, 26*). Non-adsorbing polysaccharides are excluded from the contact area of the tip and substrate as their greater hydrodynamic volume inhibits them to enter the inlet zone. Blocking the fluid to reach the contact zone causes a reduction in boundary lubrication(*24*). Even lowering the radius of gyration to about 40 nm for hydrolysed guar in comparison with the value of 250 nm for 2.4 MDa Guar is not sufficient enough to let the polymers enter the contact area. While neither native guar nor hydrolysed guar with lower molecular weight improve the boundary lubrication of PDMS sliding surfaces, hydrophobic modification of guar resulted in lowered friction coefficient. Increased affinity of MGuar to hydrophobic surface helps hydration of the hydrophobic surface and enables water retention in the contact area. The effect of polymer adsorption on tissue surface to improve lubrication has been previously stated by Meyer *et al.*(*27*). They emphasized in their conclusion that water retention by hydrophilic polymers is not sufficient to lower the friction. Saturation of hydrophobic sites with lysozyme molecules prevents the formation of a hydrophilic layer and reduces lubrication.

5.6 Conclusion

1. Using low molecular weight MGuars enables loading of high polymer concentration into the eye drop formulation without inducing depletion flocculation.
2. Formation of the MGuar/lysozyme complexes increased the viscosity of solution. Lowering the molecular weight and increasing the number of short hydrophobic pendant groups in the backbone of MGuar improved the viscosity enhancement. 12C8-130 formed the strongest, most shear thinning complex with lysozyme with the maximum viscosity occurred at the corresponding range of lysozyme concentration in tear. Compared to the MGuar with a higher molecular weight, 12C8-130/lysozyme complex contains higher number of lysozyme molecules. This causes saturation to occur at higher concentrations.
3. The ability of 12C8-130 MGuar to adsorb on hydrophobic surfaces increases lubrication, while hydrolysed guar with MW of 130 kDa failed to decrease the friction coefficient.
4. Saturation of MGuar backbone with lysozyme molecules abolished the efficiency of the MGuar to decrease the friction coefficient between hydrophobic surfaces.

References

1. Mafi, R., Gray, C., Pelton, R., Ketelson, H., and Davis, J. (2014) On formulating ophthalmic emulsions, *Colloids and Surfaces B: Biointerfaces 122*, 7-11.

2. Snibson, G., Greaves, J., Soper, N., Tiffany, J., Wilson, C., and Bron, A. (1992) Ocular surface residence times of artificial tear solutions, *Cornea 11*, 288-293.
3. Ding, S. (1998) Recent developments in ophthalmic drug delivery, *Pharmaceutical Science & Technology Today 1*, 328-335.
4. Borrega, R., Tribet, C., and Audebert, R. (1999) Reversible gelation in hydrophobic polyelectrolyte/protein mixtures: An example of cross-links between soft and hard colloids, *Macromolecules 32*, 7798-7806.
5. Petit, F., Audebert, R., and Iliopoulos, I. (1995) Interactions of hydrophobically modified poly (sodium acrylate) with globular proteins, *Colloid and Polymer Science 273*, 777-781.
6. Petit, F., Iliopoulos, I., Audebert, R., and Szönyi, S. (1997) Associating polyelectrolytes with perfluoroalkyl side chains: Aggregation in aqueous solution, association with surfactants, and comparison with hydrogenated analogues, *Langmuir 13*, 4229-4233.
7. Tribet, C., Porcar, I., Bonnefont, P., and Audebert, R. (1998) Association between hydrophobically modified polyanions and negatively charged bovine serum albumin, *The Journal of Physical Chemistry B 102*, 1327-1333.
8. Iliopoulos, I., Wang, T., and Audebert, R. (1991) Viscometric evidence of interactions between hydrophobically modified poly (sodium acrylate) and sodium dodecyl sulfate, *Langmuir 7*, 617-619.
9. Tong, L., Zhou, L., Beuerman, R. W., Zhao, S. Z., and Li, X. R. (2011) Association of tear proteins with Meibomian gland disease and dry eye symptoms, *British journal of ophthalmology 95*, 848-852.
10. Ohashi, Y., Dogru, M., and Tsubota, K. (2006) Laboratory findings in tear fluid analysis, *Clinica chimica acta 369*, 17-28.
11. McClements, D. (2000) Comments on viscosity enhancement and depletion flocculation by polysaccharides, *Food Hydrocolloids 14*, 173-177.
12. Ehlers, N. (1965) THE PRECORNEAL FILM. BIOMICROSCOPICAL, HISTOLOGICAL AND CHEMICAL INVESTIGATIONS, *Acta ophthalmologica. Supplementum*, SUPPL 81: 81.
13. Coles, J. M., Chang, D. P., and Zauscher, S. (2010) Molecular mechanisms of aqueous boundary lubrication by mucinous glycoproteins, *Current Opinion in Colloid & Interface Science 15*, 406-416.
14. Yakubov, G. E., McColl, J., Bongaerts, J. H., and Ramsden, J. J. (2009) Viscous boundary lubrication of hydrophobic surfaces by mucin, *Langmuir 25*, 2313-2321.
15. Bernal, D. L., and Ubels, J. L. (1993) Artificial Tear Composition and Promotion of Recovery of the Damaged Corneal Epithelium, *Cornea 12*, 115-120.
16. Stokes, J. R., Macakova, L., Chojnicka-Paszun, A., de Kruif, C. G., and de Jongh, H. H. (2011) Lubrication, adsorption, and rheology of aqueous polysaccharide solutions, *Langmuir 27*, 3474-3484.
17. Zhang, W., Yang, F. K., Han, Y., Gaikwad, R., Leonenko, Z., and Zhao, B. (2013) Surface and tribological behaviors of the bioinspired polydopamine thin films under dry and wet conditions, *Biomacromolecules 14*, 394-405.

18. Wu, X. Y., Ye, Y. Q., Chen, Y. N., Ding, B., Cui, J. J., and Jiang, B. (2010) Selective oxidation and determination of the substitution pattern of hydroxypropyl guar gum, *Carbohydr. Polym. 80*, 1178-1182.
19. Tiffany, J. M. (1991) The viscosity of human tears, *International Ophthalmology 15*, 371-376.
20. Petricek, I., Berta, A., Higazy, M. T., Németh, J., and Prost, M. E. (2008) Hydroxypropyl-guar gellable lubricant eye drops for dry eye treatment.
21. Tuinier, R., ten Grotenhuis, E., and de Kruif, C. G. (2000) The effect of depolymerised guar gum on the stability of skim milk, *Food Hydrocolloids 14*, 1-7.
22. Berman, A., Drummond, C., and Israelachvili, J. (1998) Amontons' law at the molecular level, *Tribology letters 4*, 95-101.
23. Bowden, F. P., and Tabor, D. (1939) The Area of Contact between Stationary and between Moving Surfaces, *Proceedings of the Royal Society of London. Series A, Mathematical and Physical Sciences 169*, 391-413.
24. De Vicente, J., Stokes, J., and Spikes, H. (2005) Lubrication properties of non-adsorbing polymer solutions in soft elastohydrodynamic (EHD) contacts, *Tribology International 38*, 515-526.
25. Garrec, D., and Norton, I. (2012) The influence of hydrocolloid hydrodynamics on lubrication, *Food Hydrocolloids 26*, 389-397.
26. Cassin, G., Heinrich, E., and Spikes, H. (2001) The influence of surface roughness on the lubrication properties of adsorbing and non-adsorbing biopolymers, *Tribology letters 11*, 95-102.
27. Meyer, A. E., Baier, R. E., Chen, H., and Chowhan, M. (2006) Tissue-on-tissue testing of dry eye formulations for reduction of bioadhesion, *The Journal of Adhesion 82*, 607-627.

Supplementary Information

SI Table 1: Titration data for MGuars before and after alkylation. MGuars are shown as xCy-z, where x is degree of substitution, y is the length of alkyl chain and z is polymer molecular weight. DS value is calculated based on two titrations, bearing the accumulated uncertainties.

MGuar Designation	MGuar Carboxyl Contents (meq/g)		Hydrophobe DS
	Before Alkylation	After Alkylation	
30C6-2400	2.72	1.339	0.296
4C8-2400	1.08	0.881	0.038
6C8-2400	1.08	0.744	0.065
12C8-2400	1.08	0.494	0.117
12C8-425	1.08	0.441	0.128
12C8-265	1.08	0.506	0.115
12C8-160	1.08	0.521	0.111
12C8-130	1.08	0.456	0.125
10C10-2400	1.08	0.587	0.099

- **Estimation of zero shear viscosity**

Dynamic viscometry measurements were done in the shear rate range of $0.1 s^{-1}$ to $1000 s^{-1}$. Shear rate was defined through the variation of applied stress in the range of 0.01 to 100 Pa. Both delay time and integration time was 1 second. Through the extrapolation of low shear rate region in viscosity-shear rate graphs, zero-shear viscosity values were obtained.

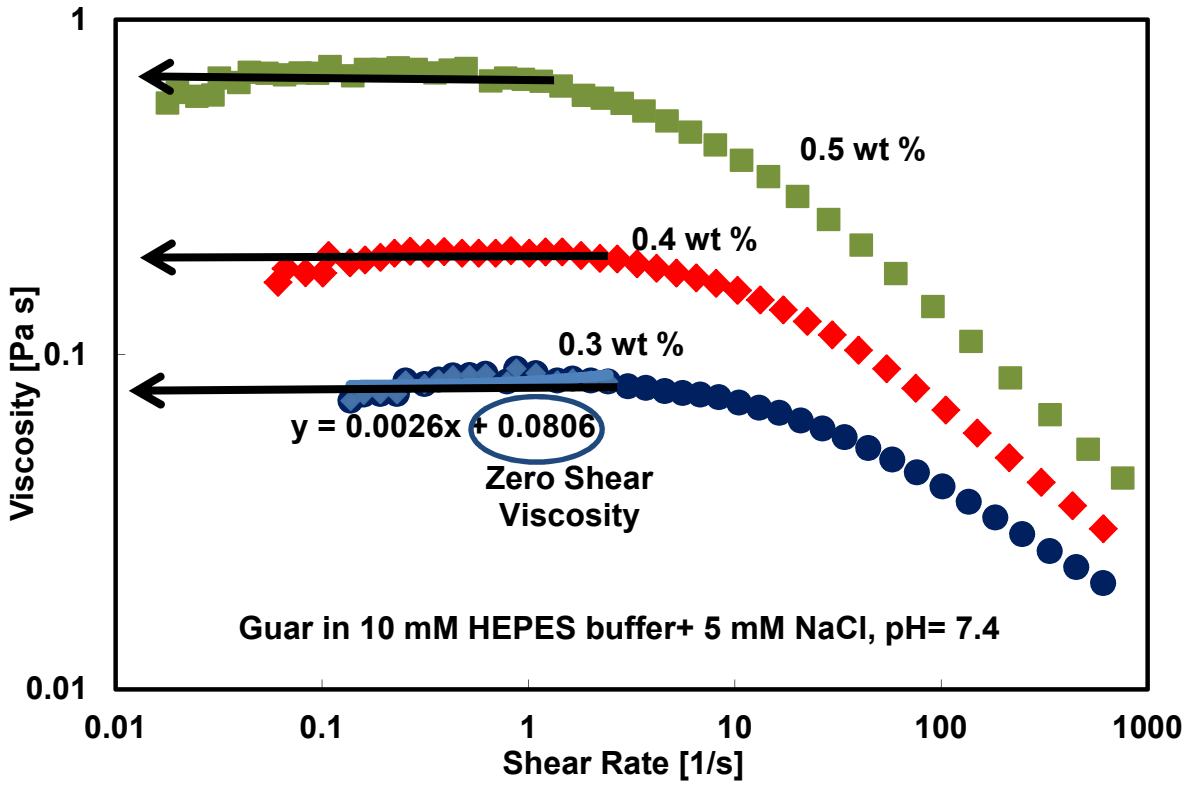

SI Figure 1: Estimation of zero shear viscosity through extrapolation of low shear rate viscosity region for native guar in three different concentrations.

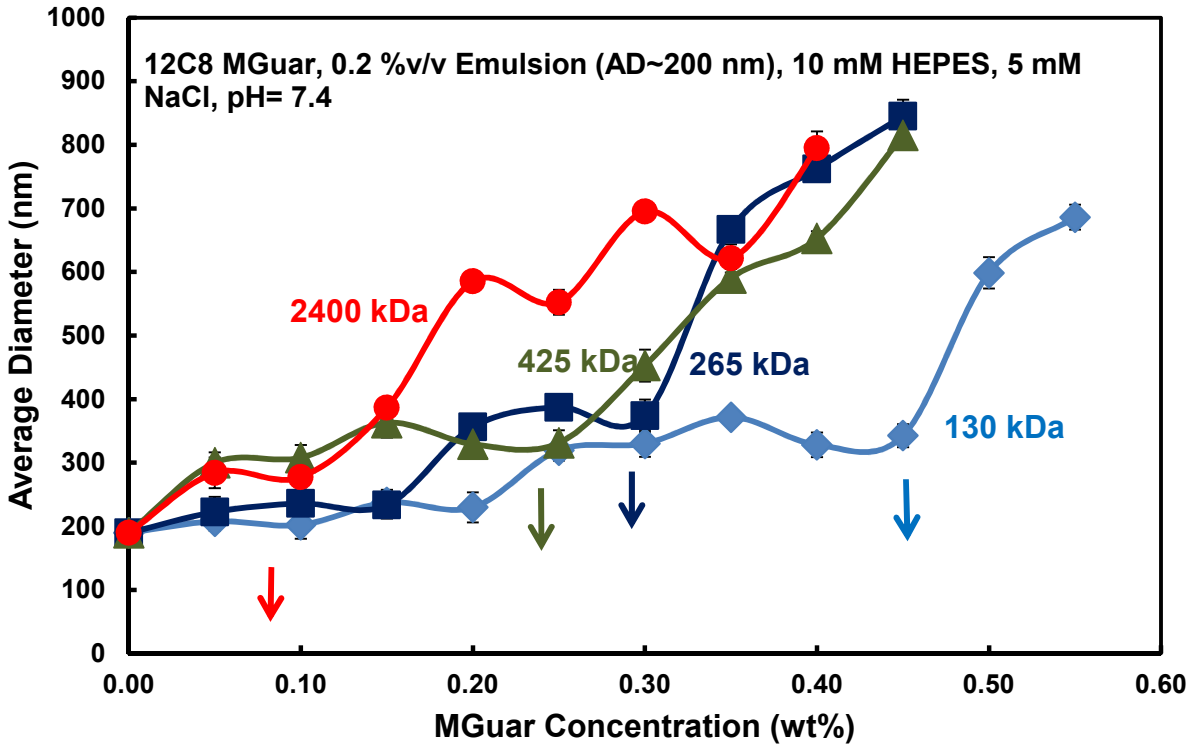

SI Figure 2: The influence of the concentration of MGuars with various molecular weights on the average emulsion diameter. The CFC has been defined as the slope change in the curves. Emulsions have the initial average diameter of about 200 nm.

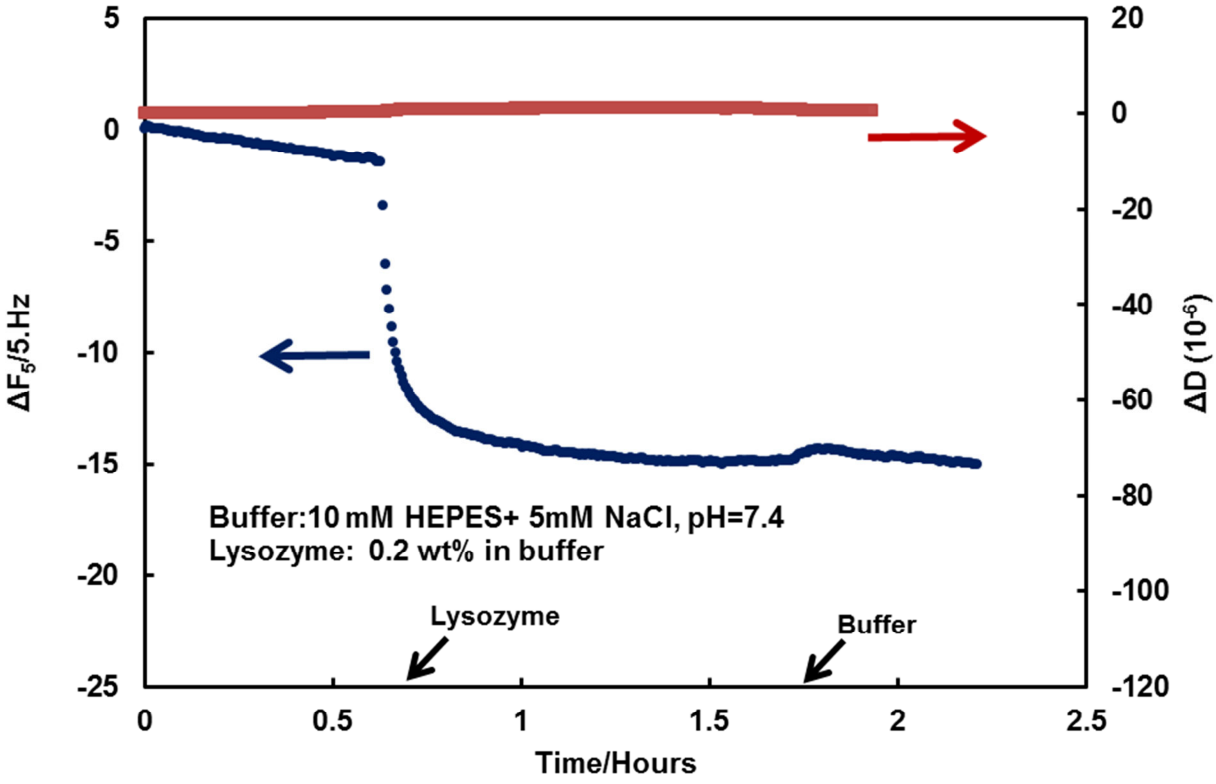

SI Figure 3: Adsorption of lysozyme on polystyrene QCM-D sensor at pH=7.4. The adsorbed mass of lysozyme on the substrate calculated based on Sauerbrey equation has been estimated to be 1.8 mg/m^2.

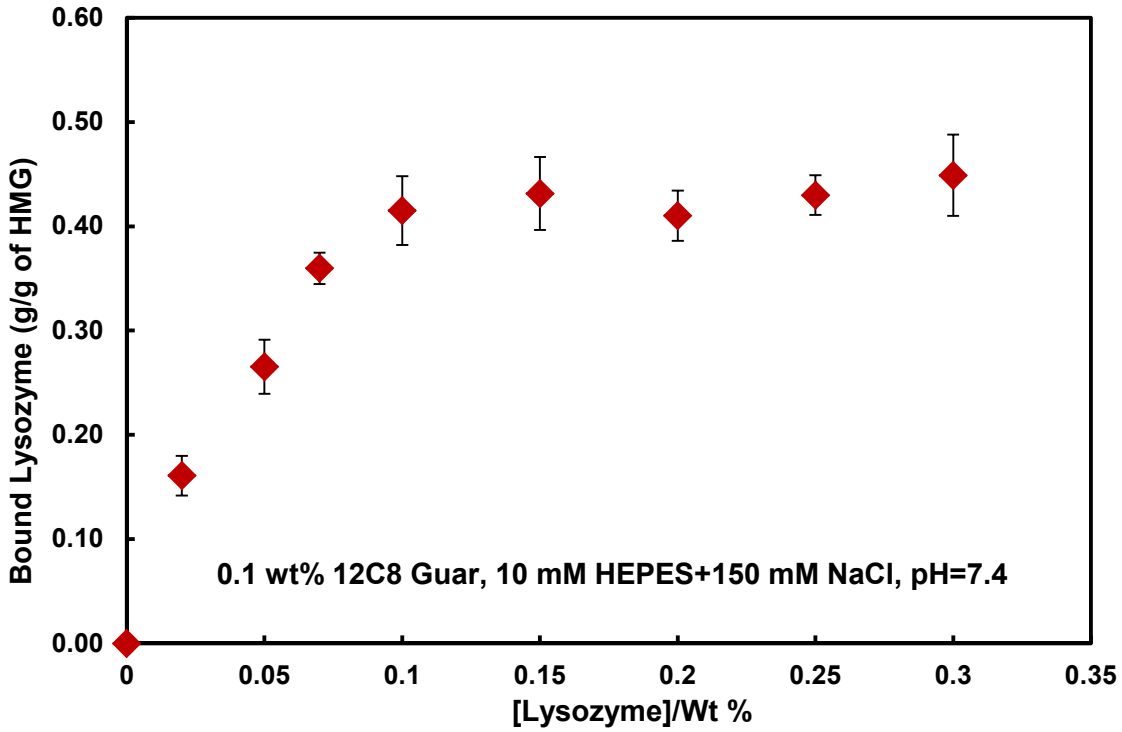

SI Figure 4: The corresponding content of MGuar-bound lysozyme as a function of the total lysozyme concentration.

Chapter 6. Concluding Remarks

In this work we have reported a simple method of weak gelation through interaction of modified guar (MGuar) and tear proteins. Various MGuars were prepared through grafting hydrophobic alkyl groups on oxidized guar. Guar derivatives with the ability to interact with HSA and lysozyme at their corresponding concentrations in tear film were developed. These derivatives are able to effectively increase the solution viscosity. The overall objectives stated in this work have been achieved.

6.1 Key Findings and Contributions

The specific conclusions arising from this research are summarized below.

1. The molecular weight and the concentration of the water-soluble polymer are the key formulation variables to control the stability of ophthalmic emulsions. Overlap concentration, C*, above which the lipid emulsions rapidly aggregate, is determined by these two properties. C* increases with decreasing molecular weight *(1)*. Therefore by lowering guar molecular weight, higher guar concentrations can be used in eye drop formulation without affecting the emulsion stability.

2. Through hydrophobic modification of guar, guar derivatives with the ability to interact with lysozyme and human serum albumin (HSA) were obtained. These modified guars (MGuars) can be used in eye drop formulation. MGuars help the formation of weak gels upon introduction of eye drop to the tear film.

3. Interaction of MGuar and HSA in model tear fluid results in a viscosity increase. Both longer alkyl group and higher degree of alkyl substitution result in higher viscosity values. This interaction may offer treatments for specific types of dry eye diseases, in which the HSA concentration in tear is elevated due to inflammation.

4. The MGuar with molecular weight of 2.4 MDa containing carboxyl (DS = 0.07) and decylamide groups (DS = 0.05) produced the largest viscosity increase in the concentration range of HSA in a diseased tear medium.

5. Shear thinning complexes of MGuar-HSA are weak enough to break down in a blink. These complexes are reproducible and can rebuild their structure upon removal of the shear.

6. MGuar-lysozyme complex formation also increases the viscosity of model tear fluid. Both lowering the molecular weight and increasing the number of short hydrophobic pendant groups in the backbone of MGuar were the techniques employed to improve the viscosity enhancement. MGuar with molecular weight of 130 kDa containing carboxyl (DS = 0.076) and octylamide groups (DS = 0.125) formed the strongest and the most

shear thinning complex with lysozyme, with the maximum viscosity obtained at the corresponding range of lysozyme concentration in tear.

7. Adsorption of MGuar on hydrophobic surfaces improves lubrication. However, saturation of MGuar backbone with proteins, which have hydrophobic characteristics, may diminish the efficiency of MGuar to decrease the friction coefficient between hydrophobic surfaces.

8. Whereas conventional QCM-D measurements monitors the deposition of emulsion droplets onto surfaces, measurements made with an inverted QCM-D cell without flow gives insight into the gravity-induced build-up of a concentrated emulsion layer (consolidation layer) near the sensor surface.

9. Some emulsions only show deposition with no evidence of a consolidation layer – these tend to be dilute, small and colloidally stable. By contrast, larger and less stable emulsions display rich behaviours in both frequency shifts and dissipation over the period of hours as consolidation layers build up next to the QCM-D sensor surface.

10. Voigt-based viscoelastic modelling fits to inverted QCM-D data gives insight into the evolution of the properties of the consolidation layers with time.

11. Of the many excellent techniques available for measuring emulsion properties, inverted QCM-D measurements are unique in terms of characterizing the first 100 nm of the consolidation layer next to a solid surface.

6.2 Future Work

6.2.1 Improvements on MGuar-Protein Complex Formation

In order to confirm the suitability of MGuar derivatives to be used in eye drop formulation, further experimental study should be carried out. This work should include *in vitro* or *in vivo* tests to evaluate irritation and clarity of the developed MGuar containing formulations. The effect of co-presence of other tear proteins on the polymer-protein complex formation must be evaluated as well.

5C10- MGuar was found to be the most suitable modified guar to form MGuar- HSA complexes with the ability to raise the viscosity in the concentration range of HSA in tear film. In this work, I was not able to produce water soluble MGuars with longer alkyl chain length, i.e.12 or 18 with degree of substitution higher than 5 for dodecyl and 1 for

octadecyl chains. Further improvements are required in order to keep the water solubility and obtain MGuars with long alkyl chain length and high degree of substitutions. The challenge would be having a complex with a more evident thickening effect, but does not precipitate. A more accurate method to assess degree of substitution should also be developed to avoid the interruptions of solubility in titration measurements or high viscosity in NMR experiments.

6.2.2 Lubrication of hydrophobic surfaces

MGuars are able to adsorb on hydrophobic surfaces. I have shown that MGuar adsorption lowered the friction coefficient of sample hydrophobic pairs. However, friction experiments have been done at the speed of about 60 μm/s, which is significantly lower than the blinking speed. The friction experiments can be designed to be done at higher entrained speeds and in mixed lubrication region. The results of friction coefficient can be then compared with previously reported values of commercial artificial tear solutions.

6.2.3 An Approach for Hydrogel Formation Using ss-DNA

The ability of DNA modified guar derivatives to form hydrogels has been evaluated in the early stages of my research. The ability of single strand DNA (ss-DNA) to act as a crosslinker was examined through two different methods. First, free ss-DNA, which contains complementary section with grafted ss-DNA, acted as the crosslinker DNA. Amine terminated DNA strands are the side chains, which are grafted to the guar backbone. In the second strategy, two different grafted DNA strands with complementary sections form the crosslink. The sol-gel transition occurs upon this binding. For the formation of target responsive DNA-guar hydrogel in tear film environment, lysozyme binding aptamer can be incorporated according to the strategy, which is shown in Figure 1. Due to the blocking of the complementary sections of crosslinker DNA strand by the lysozyme binding aptamer, hybridisation of crosslinker DNA with grafted ss-DNAs would be inhibited. This enables the production of a one component solution, which includes all active reagents as long as the aptamer blocked the crosslinker DNA strand. By introducing the solution into the eye environment, the aptamer will bind to lysozyme due to their higher affinity to this protein. Therefore, the crosslinker DNA strand will be

freed and activated to hybridize the complementary sections of ss-DNAs thus forming the hydrogel.

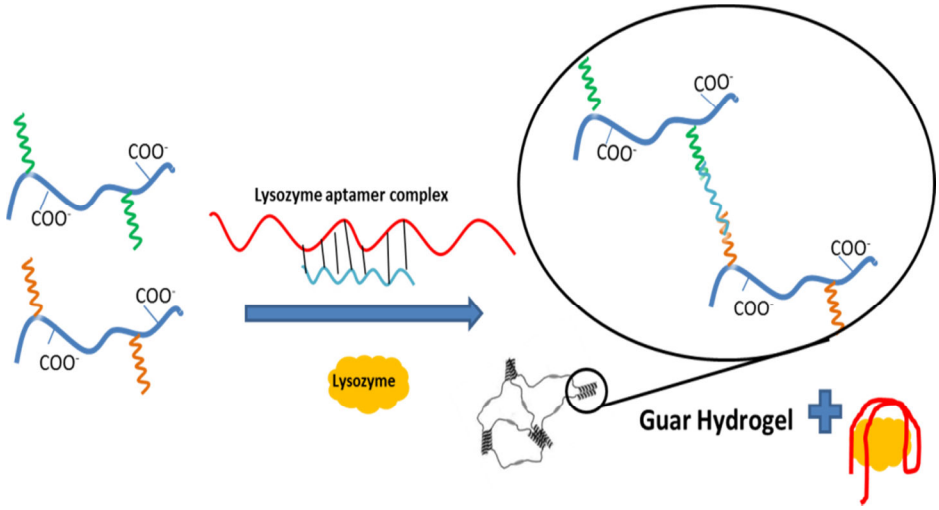

Figure 1: Mechanism of hydrogel formation by employing the lysozyme binding aptamer duplex with a short complementary oligonucleotide. Blue sequence is for bridging guar molecules through the hybridization of DNA strands. The aptamer (red sequence) binds to tear lysozyme, frees the crosslinker DNA strand.

1. Mafi, R., Gray, C., Pelton, R., Ketelson, H., and Davis, J. (2014) On formulating ophthalmic emulsions, *Colloids and Surfaces B: Biointerfaces 122*, 7-11.